Ph.D. Thesis

Crosstalk between FGF23- and Angiotensin II-mediated Ca^{2+} signaling in pathological cardiac hypertrophy.

submitted by

Ketaki Nitin Mhatre

for the academic degree of

Doctor of Philosophy

at the

Medical University of Graz
Department of Cardiology
Graz, Austria

under the Supervision of

Prof. Dr. Frank R. Heinzel

2018

Declaration

I hereby declare that this thesis is my own original work and that I have fully acknowledged by name all of those individuals and organizations that have contributed to the research for this thesis. Due acknowledgment has been made in the text to all other materials used. I have obtained all the permissions for reproduction from publications from their respective copyright holders wherever applied. Throughout this thesis and in the related publication, I have followed the “Standards of Good Scientific Practice and Ombuds Committee” at Medical University of Graz, Austria.

Ketaki Mhatre

05.08.2018

Disclosures

Part of this thesis has been published in

Mhatre, K.N., Wakula, P., Klein, O., Bisping, E., Völkl, J., Pieske, B., and Heinzel, F.R., 2018. Crosstalk between FGF23- and angiotensin II-mediated Ca2+ signaling in pathological cardiac hypertrophy. *Cellular and Molecular Life Sciences*, (0123456789).

The above publication is available at http://link.springer.com/10.1007/s00018-018-2885-x.

Statement of authors on the publication

The following people and institutions contributed to the publication of work undertaken as part of this thesis:

Ketaki N. Mhatre[1,2], Paulina Wakula[1], Egbert Bisping[2], Oliver Klein[1], Jakob Völkl[1], Burkert Pieske[1,3,4], Frank R. Heinzel[1,2,4]

[1]Department of Internal Medicine and Cardiology, Charité University Medicine, Campus Virchow-Klinikum, 13353 Berlin, Germany.

[2]Department of Cardiology, Medical University Graz, Auenbruggerplatz 15, 8036 Graz, Austria.

[3]German Center for Cardiovascular Research (DZHK), Partner Site Berlin, Germany

[4]Department of Internal Medicine and Cardiology, German Heart Center, 13353 Berlin, Germany

We agree with the use of the data from the above published peer-reviewed manuscript contributing to this thesis.

08.08.2018

Ketaki N. Mhatre, Paulina Wakula, Egbert Bisping,

Oliver Klein, Jakob Völkl, Burkert Pieske, Frank R. Heinzel.

Author's contribution

K.N.M. and F.R.H. designed the research; K.N.M. and E.B. developed methods for isolation and culture of cardiomyocytes; K.N.M. performed Ca^{2+} imaging, molecular biology, immunocytochemistry, western blot, ELISA experiments and sample preparation for mass spectrometry study; O.K. conducted mass spectrometry analysis of the samples; K.N.M., P.W., J.V., analyzed the data; and K.N.M., F.R.H. and B.P. wrote the paper.

Acknowledgments

The work for my Ph.D. thesis was partially carried out at the Department of Cardiology at the Medical University of Graz and at Charite' Medical University, Berlin, under the supervision of Prof. Dr. Frank Heinzel. Primary financial support was provided by Ph.D. program Molecular Medicine at the Medical University of Graz.

First and foremost, I would like to express my sincere gratitude to my advisor, Prof. Frank Heinzel, for not only introducing me to the field of cardiology but also for providing me tireless guidance and support throughout the course of this thesis. I could not be more grateful for the opportunities I have been afforded during my time in his lab and the experience of four of the most challenging, rewarding and enjoyable years of my career to date. I hope he agrees that he has managed to help bring out something of a scientist out of what was probably a somewhat naïve biology student. I am highly appreciative to him for giving me intellectual independence and for all the scientific discussions, which has further reinforced my curiosity in the field of cardiology.

I would like to thank Dr. Paulina Wakula, for her supervision throughout this project, the support and her meticulous attention to detail. I also want to express my immense gratitude Prof. Burkert Pieske, who not only is a source of unparalleled, scientific knowledge, but also whose generosity made it possible for me to complete my study.

I have had the fortune to enjoy the company of some great friends and colleagues over the course of my thesis. I owe a lot to Klaus Groschner, Egbert Bisping, Simon Sedej, Karin Hammer, Senka Ljubojević, Felix Hohendanner, Uwe Primessnig, Jakob Völkl, Oliver Klein, brilliant scientists and colleagues to the last who have all contributed to this thesis through their advice and discussion and moral support. I would like to thank all past and present members of the Department of Cardiology in Graz and Berlin for the support and good times throughout these years and hopefully, more to come.

My biggest thank goes to my parents for their constant support since birth and especially during my postgraduate studies. My sister who always reminds me of the good things in life. My special thanks go to Naresh Hanchate, who saved my soul a thousand times. You are my rock.

Last but not the least, great friends from all around the world who were responsible to keep up my body and spirits high. I wish I could name them all personally but instead will have to make use of the phrase “You know who you are”.

Thank you!

To my family,

and those who I have the fortune to count as friends,

and last but not the least coffee,

without any of whom this thesis would not have been possible.

Table of Contents

1.1. List of Tables

1.2. List of Figures

1.3. List of abbreviations

2APB	2-aminoethoxydiphenyl borate
ACE1	Angiotensin-converting enzyme 1
AGT	Angiotensinogen
ARVMs	Adult rat ventricular cardiomyocytes
AT1R	Angiotensin II Type 1 receptor
ATII	Angiotensin II
BDM	Butanedione Monoxime
Ca^{2+}	Calcium
$[Ca^{2+}]$	Calcium concentration
CaM	Calmodulin
CaMKII	Ca^{2+}/calmodulin-dependent protein kinase II
CaN	Calcineurin
CaT	$[Ca^{2+}]$ transient
CICR	Calcium-induced-calcium-release
CKD	Chronic Kidney Disease
CM	Cardiomyocyte
CRU	Ca^{2+} release unit
DAG	Diacylglycerols
DMSO	Dimethyl sulfoxide
ECC	Excitation-Contraction Coupling

ECC	Excitation-Contraction Coupling
ET-1	Endothelin-1
ETC	Excitation-transcription coupling
FGF23	Fibroblast Growth Factor 23
GPCRs	G protein-coupled receptors
HDAC	Histone-deacetylase
HF	Heart Failure
HFpEF	Heart failure with preserved left ventricular ejection fraction
HFrEF	Heart failure with reduced left ventricular ejection fraction
IICR	Inositol -1,4,5-trisphosphate -induced Ca^{2+} release
IP3	Inositol -1,4,5-trisphosphate
IP3R	Inositol -1,4,5-trisphosphate receptors
LTCC	L-type Ca^{2+} channels
LV	Left ventricular
MEF	Myocyte Enhancer Factor
NCX	Na^{+}/Ca^{2+} exchanger
NE	Nuclear Envelope
NFAT	Nuclear factor of activated T cells
NRVM	Neonatal rat ventricular cardiomyocytes
NT	Normal Tyrode solution
NXT	Nephrectomy
PBS	Phosphate Buffered Saline

PKA	Protein kinase A
PKC	Protein kinase C
PKD	Protein kinase D
PLB	Phospholamban
PLC	Phospholipase C
RAAS	Renin-Angiotensin-Aldosterone system
RTKs	Receptor Tyrosine Kinases
RV	Right ventricular
RyRs	Ryanodine receptors
SERCA	Sarco/endoplasmic reticulum Ca^{2+}-ATPase
SR	Sarcoplasmic reticulum
SOP	Sham Operated

1.4. Abstract

Heart failure (HF) manifestation and development are determined by systemic stimulation of neuroendocrine signaling cascades, like the renin-angiotensin-aldosterone system (RAAS). Fibroblast growth factor 23 (FGF23), an endocrine hormone secreted by osteocytes, is associated with chronic kidney disease which is a prominent co-morbidity in HF. FGF23 is also shown to facilitate left ventricular hypertrophy (LVH). High levels of circulating FGF23 are correlated with an altered systemic RAAS response *in vivo*. FGF23 is proposed to trigger pathological cellular signaling mediated by Ca^{2+}-regulated transcriptional pathways in cardiomyocytes (CMs).In this thesis, we studied Ca^{2+}-dependent hypertrophic signaling induced by FGF23 and its connection with angiotensin II (ATII) in CMs.

Both the triggers, ATII and FGF23, induced a rise in the cell area and hypertrophic gene expression, indicating hypertrophy in neonatal rat ventricular myocytes (NRVMs). In addition to a global increase in cytoplasmic Ca^{2+}, FGF23, like ATII, triggered inositol 1, 4, 5-triphosphate (IP3)-dependent Ca^{2+} release (IICR) from the nucleoplasmic Ca^{2+} store. This local nuclear Ca^{2+} release is associated with transcriptional upregulation of hypertrophic genes via activation of Ca^{2+}-calmodulin(CaM)- calcium/calmodulin-dependent protein kinase II (CaMKII) – histone-deacetylases 4 (HDAC4) pathway. FGF23 treatment indeed induced nuclear Ca^{2+}-regulated CaMKII – HDAC4 hypertrophic pathway, as is observed for ATII treatment. Strikingly, ATII receptor antagonist, losartan significantly attenuated FGF23-induced alterations in Ca^{2+} homeostasis and induction of cellular hypertrophy suggesting an involvement of ATII receptor-mediated signaling on FGF23 induction. Additionally, application of FGF23 increased intracellular expression of ATII peptide and its secretion in CMs, confirming the involvement of ATII in FGF23 signaling.

In this study, our data suggest that FGF23 acutely increases IP3-dependent intracellular nuclear calcium and ATII levels and further its secretion in CMs. These factors may be pivotal for cellular hypertrophy observed with persistent stimulation by FGF23. These findings indicate a pathophysiological role of the intracellular cardiac angiotensin system in FGF23-induced hypertrophy in ventricular CMs(Mhatre *et al.* 2018).

1.5. Zusammenfassung

Die Manifestation und Entwicklung von Herzinsuffizienz (HF) wird durch systemische Aktivierung von neuroendokrinen Signalkaskaden, wie dem Renin-Angiotensin-Aldosterone-System (RAAS), vorangetrieben. Fibroblast growth factor 23 (FGF23), ein endokrines Hormon, ist bei chronischer Nierenerkrankung, einer häufigen Komorbidität bei HF, erhöht. FGF23 führt auch zu linksventrikulärer Hypertrophie (LVH). Hohe zirkulierende Spiegel von FGF23 sind mit einer veränderten systemischen RAAS-Antwort assoziiert. Wir überprüften die Hypohese, dass FGF23 pathologische Signale auslöst, die durch Ca^{2+} -regulierte Transkriptionswege vermittelt werden. In der vorliegenden Arbeit untersuchten wir die Ca^{2+} -abhängige Signaltransduktion von FGF23 und dessen Verbindung mit Angiotensin II (ATII) in Kardiomyozyten (CM).

In neonatalen Rattenventrikelmyocyten (NRVMs) induzierten sowohl ATII als auch FGF23 Hypertrophie, erkennbar durch einen Anstieg der Zellfläche und hypertrophe Genexpression. Zusätzlich zu einem globalen Anstieg von cytoplasmatischem Ca^{2+} induzierte FGF23, wie ATII, Inositol-1,4,5-triphosphate (IP3) -induzierte Ca^{2+}-Freisetzung (IICR) aus dem nukleoplasmatischen Ca^{2+} -Speicher. Diese lokale nukleare Ca^{2+}-Freisetzung war mit zellulärer Hypertrophie über die Aktivierung des Ca^{2+} -Calmodulin (CaM) - Calcium / Calmodulin-abhängigen Proteinkinase II (CaMKII) - Histon-Deacetylase-4 (HDAC4) -Wegs assoziiert. Der ATII-Rezeptorantagonist Lorsartan verringerte die FGF23-induzierten Veränderungen der Ca^{2+} -Homöostase und die Induktion zellulärer Hypertrophie signifikant, was auf eine Beteiligung von ATII-Rezeptor-vermittelten Signalen hindeutet. Zusätzlich erhöhte die Anwendung von FGF23 die intrazelluläre Expression von ATII und dessen Sekretion durch CMs.

Unsere Ergebniss legen nahe, dass FGF23 akut zu einer Produktion und Sekretion von ATII in Kardiomyozyten führt und dass die FGF23-vermittelten Effekte auf das nukleäre Ca2+ und die Hypertrophie durch ATII vermittelt sind. Diese Mechanismen können auch

für eine zelluläre Hypertrophie entscheidend sein, die bei anhaltender Stimulation durch FGF23 beobachtet wird. Diese Befunde weisen auf eine pathophysiologische Rolle des zellulären Angiotensin-Systems bei FGF23-induzierter Hypertrophie bei ventrikulären CMs hin(Mhatre *et al.* 2018).

2. Introduction

2.1. Heart failure

2.1.1. Description and etiology

By definition, Heart Failure (HF) is the inability of the heart to efficiently pump blood throughout the cardiovascular system to fulfill the individual's metabolic demands and is the consequence of various and complex causes(Mudd and Kass 2008). The patients show a typical symptom of shortness of breath at rest or during exertion, and/or fatigue; accompanied by signs of fluid retention; and objective evidence of an abnormality of the cardiac structure and/or function in a clinical syndrome.

HF manifest itself as structural and functional cardiac abnormalities, neurohormonal activation and increased venous pressure. Based on the measurement of the Left ventricular ejection fraction (LVEF), HF patients are categorized into three groups according to 2016 ESC Guidelines (Ponikowski *et al.* 2016). Patients with normal LVEF (typically considered as ≥50%) are grouped as HF with preserved EF (HFpEF) while those with reduced LVEF (typically considered as, 40%) are considered as HF with reduced EF (HFrEF). Patients with an LVEF in the range of 40–49% represent a 'grey area', which are now defined as HFmrEF. In HFrEF or systolic heart failure, there is a reduction in cardiac contractility leading to an inadequate systemic perfusion, whereas, in HFpEF or diastolic heart failure, there is predominantly impaired cardiac relaxation and abnormal ventricular filling (Segovia Cubero *et al.* 2004).

The diseases or conditions that can lead to HF are very different and their detection is of utmost importance, as this can modify the diagnostic, therapeutic and preventive approach, as well as determine prognosis.

In most cases of HF, the clinical symptoms are due to impairment of the left ventricle and can be diverse. Left Ventricular (LV) systolic dysfunction is typically the outcome of coronary artery disease and other causes include valvular heart disease, hypertension,

congenital heart disease, inflammation and chemotherapeutic drugs or other toxic agents. Right Ventricular (RV) systolic dysfunction is commonly a consequence of LV systolic dysfunction(Segovia Cubero *et al.* 2004).

While LV diastolic dysfunction is relatively uncommon in younger patients, it increases in importance in the elderly. It mostly occurs in patients with chronic hypertension, diabetes mellitus, and/or aging. This proportion of HF patient's exhibit impaired ventricular filling but normal systole, characteristic of HFpEF. These patients carry a substantial risk of the subsequent development of heart failure and reduced survival, even when it is asymptomatic or preclinical, making this group of patients difficult to diagnose and treat (Gaasch and Little 2007).

2.1.2. Epidemiology and prognosis of HFpEF

The increase in HF incidence throughout the developed and developing regions of the world poses enormous challenges for caregivers, researchers, and policymakers. Heart failure is more common than most cancers with a prevalence of ~1-2% in the overall population and >10% in people older than 75 years (Schocken *et al.* 2008). It is the only major cardiovascular disease (CVD) whose prevalence and incidence are increasing, partly because of the burgeoning growth in the elderly population and a lack of curative therapies due to the complexity of its many causes and pathophysiological origins(Bobenko *et al.* 2018).

Because of the permanent increase in the prevalence of HFpEF during the past decades, HFpEF now accounts for up to 50% of the total HF population. In contrast to HFrEF, outcomes in HFpEF remained unchanged over the last years. In a recent meta-analysis, the mortality rate in HFpEF was alarming 121 deaths per 1000 patient-years, which is emphasizing the need for effective therapies in this highly relevant condition(Edelmann 2015).

As the heart's ability to efficiently pump blood decreases, HFpEF patients often times suffer from dyspnea and fatigue, which heavily affects or even inhibits the patient's tolerance to exercise. The kidneys compensate for the reduction in the blood flow by retaining more fluid and salt. Consequently, the patient may experience pulmonary congestion and or peripheral edema(Dunlay *et al.* 2014). Barring exceptions such as physically induced heart arrest or stress-induced cardiomyopathies, HFpEF has been recognized as a progressive disorder, which at first is asymptomatic before escalating into a symptomatic disease in a time-dependent manner.

The risk factors and symptoms require differential treatment depending on the stage of disease progression(Dickstein *et al.* 2008). The long-term prognosis associated with HFpEF is uniformly poor despite recent improvements in diagnosis and therapeutic treatment. Novel treatments for HF can slow, but not halt the progression of the disease. Despite the numerous advantages of modern treatment approaches, quality of life for patients surviving HFpEF-related hospitalizations is low and distress is often worse compared to many other chronic diseases(Bobenko *et al.* 2018). HFpEF is, therefore, an important area for further research.

2.1.3. Pathophysiology of HFpEF

HF triggers such as coronary artery disease, ischemia, hypertension, inflammation or toxic agents can cause myocardial tissue damage. Several compensatory mechanisms are activated as a response to such conditions to maintain cardiac output and proper organ perfusion by increasing muscle contractility and circulating blood volume and eventually heart functioning.

Compensatory mechanisms include activation of neurohormonal pathways such as the renin-angiotensin, adrenergic and endothelin system. This compensatory regulation may maintain cardiovascular homeostasis during acute cardiac stress, and the patient may remain asymptomatic over a variably long period. However, in this early, "compensated",

stage of HF a process called “cardiac remodeling” takes place as summarized in Figure 2.1(Heinzel *et al.* 2015).

There are two types of hypertrophy eccentric and concentric hypertrophy depending on the physiology of the hypertrophic LV.

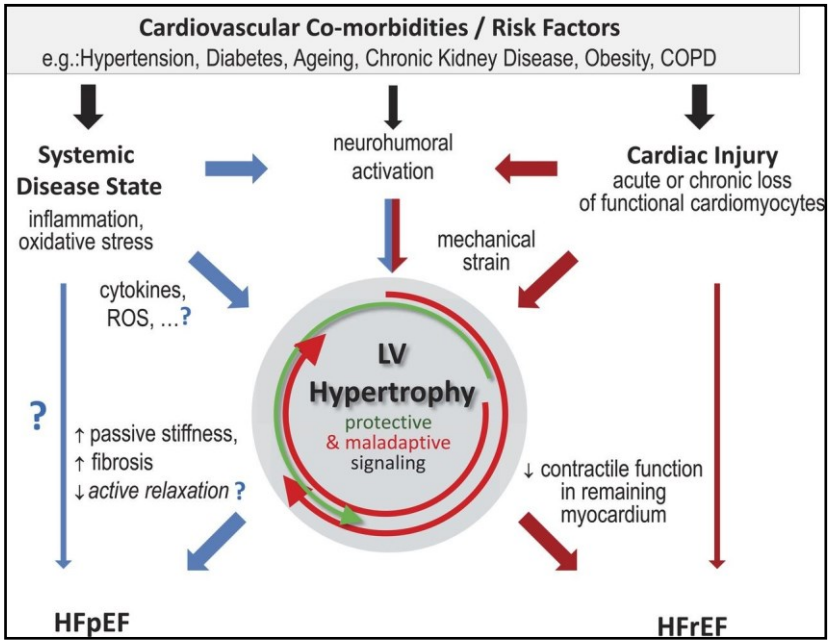

Figure 2.1 Pathophysiology of left ventricular (LV) hypertrophy in heart failure.

HFpEF and HFrEF are driven by different pathomechanisms Although both share some degree of neurohumoral activation Systemic inflammation and oxidative stress are more important mediators of HFpEF, whereas cardiomyocyte injury is vital in HFrEF. LV hypertrophic remodeling is a common the cellular phenotype in HF. (COPD, chronic obstructive pulmonary disease; ROS, reactive oxygen species).

The type of hypertrophic remodeling depends on the nature of the trigger and associated progression of contractile dysfunction. Elevated afterload due to valve stenosis, hypertensive heart disease lead to concentric hypertrophy. On the other hand, eccentric hypertrophy is commonly triggered in conditions of LV volume overload (e.g. valve

regurgitation or shunt) or after myocardial infarction. Thus, the nature of the trigger and not its temporal pattern (intermittent or continuous), determines the type of hypertrophy(Bisping *et al.* 2014).

Cardiac remodeling or hypertrophy can be characterized at the cellular and molecular level and includes myocyte cellular hypertrophy reflected in cell size increase, as well as changes in gene expression pattern in the direction of a “fetal gene program” reactivation (Shah and Mann 2011). In a fetus, before birth, the major energy source of the cardiac metabolism consists of carbohydrates. However, post birth, fatty acids becomes man energy source of the cardiac metabolism (Lopaschuk *et al.* 1992). Nevertheless, in failing heart muscle, to induce cardiac hypertrophy, it returns to expressing fetal genes. In this switch to “the fetal gene program”, there is an upregulation of expression of different isoforms of metabolic enzymes and other proteins with the purpose of helping the heart to adapt to an increased workload. The specific features include increased expression of natriuretic peptides (ANP, BNP), TGF-β, isoform switches in sarcomeric proteins (relative increase of α-actins, myosin heavy chains 7 (*MYH7*))(Lopaschuk *et al.* 1992).

Chronic, continuous neurohormonal stimulation (e.g. Renin-Angiotensin-Aldosterone System –RAAS, Adrenergic system) leads to further cardiac enlargement, fibrosis and a progressive decline in contractile function, increase in wall stiffness and mechanical strain eventually resulting in “decompensated” HF with its signs and symptoms(Bisping *et al.* 2014). In addition to neurohormonal stimuli, there is an activation of the systemic pro-inflammatory state by the release of cytokines and other inflammatory mediators. This systemic response to a local cardiac dysfunction leads to progressive systemic phenotypic alterations, including the vasculature, kidneys, skeletal muscle and other organs. These global changes in combination with cardiac dysfunction eventually result in the syndrome of HF.

As HFpEF is highly heterogeneous and may not represent a single condition, the underlying pathophysiology is difficult to understand. Patients with HFpEF frequently have co-morbidities such as hypertension, obesity, Type II diabetes, hyperlipidemia and renal

disease (Chronic kidney disease) as stated above in Figure 2.1. However, not all patients have all co-morbidities, the random interplay between diverse comorbidities is likely to result in multiple HFpEF phenotypes, and hence the disease is difficult to treat.

2.2. Calcium-mediated cellular and molecular pathomechanisms in Heart Failure

It is apparent that HF is highly complex, involving not only multiple stressors but also many activations of different signaling pathways and adaptations on the cellular level (Figure 2.2)(Bisping *et al.* 2014). Cardiomyocyte (CM) maladaptation such as electrical remodeling, and changes in Ca^{2+} handling, contractility, energy metabolism and cell viability leads to LV hypertrophy (Shah and Mann 2011).

It is well established that a crucial subcellular mediator for adaptation factors is Ca^{2+} and its regulation via different Ca^{2+} handling proteins within cardiomyocyte. Ca^{2+} regulates most of the signaling pathways involved in maladaptive hypertrophy. While some of these mechanisms are helpful in improving the cardiac output in the short term, they are a major contributor to the pathological development and further leading to mortality.

Although a lot is known about the cellular mechanism in the failing heart in HFpEF, the exact initiatory mechanisms of cardiac remodeling are still not clear. Current HF treatment focuses on inhibiting systemic maladaptive responses, but they fail to address and prevent pathology on the CM level. Thus, it is necessary to study the Ca^{2+} mediated early hypertrophic signaling that will further bolster novel drug target possibility against pathophysiology of LVH.

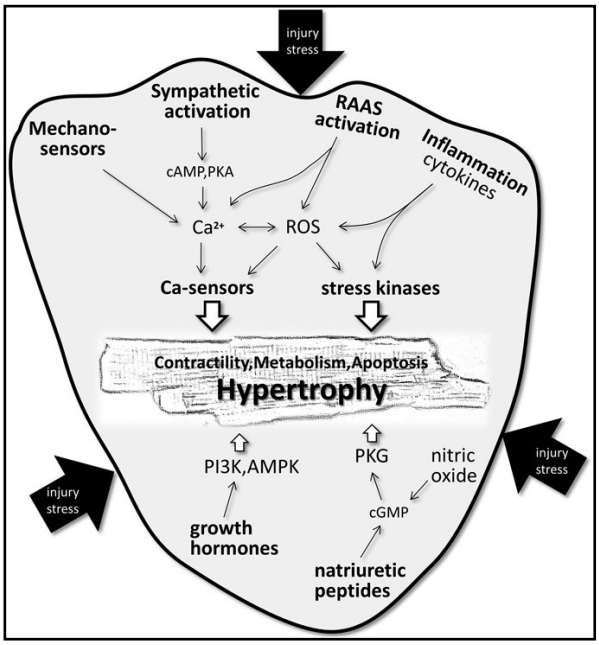

Figure 2.2 Patho-mechanisms of left ventricular (LV) hypertrophy in heart failure.

Important triggers and stressor and common signaling pathways of cardiomyocyte remodeling. (PKA, protein kinase A; PKG, protein kinase G; PI3K, phosphatidylinositol-4,5-bisphosphate 3-kinase; AMPK, 5′ AMP-activated protein kinase).

The figure is reproduced from "Bisping, E., Wakula, P., Poteser, M., and Heinzel, F.R., 2014. Targeting Cardiac Hypertrophy : Toward a Causal Heart Failure Therapy. *Journal of Cardiovascular Pharmacology,* 64 (4), 293–305". Copyright 2014 Wolters Kluwer Health, Inc. Reprinted with permission.

2.2.1. Calcium dynamics in Heart

For all its complexity, the heart has a simple task is to pump blood efficiently. In order to achieve this, the heart must be excited in a regular and ordered manner, must contract with sufficient force, and its structural dimensions must be balanced in order to maintain optimal wall strain.

Ca^{2+} plays an essential role in all of these demands(Bers 2008). As a charged ion moving across the cellular membrane, it is involved in excitation. In both, sino-atrial cells where it is responsible for the upstroke, as well as in ventricular myocytes where its charge is one of the important factors leading to plateau phase of the action potential. Ca^{2+} induces

contraction by binding to troponin and thereby allows the myofilaments in CM to exert a contractile force during the plateau phase(Figure 2.3).

In fact, the sporadic increase in intracellular calcium concentrations [Ca^{2+}]i during every heart beat is the key component of excitation-contraction coupling (ECC). In addition, Ca^{2+} plays an important role in gene and structural regulation in cardiomyocyte. Ca^{2+}-sensitive signaling proteins, like Calcineurin (CaN) and Ca^{2+}/calmodulin-dependent protein kinase (CaMKII), translate changes in Ca^{2+} concentration to altered gene expression patterns in CMs(Bers 2000). This constitutes excitation-transcription coupling (ETC).

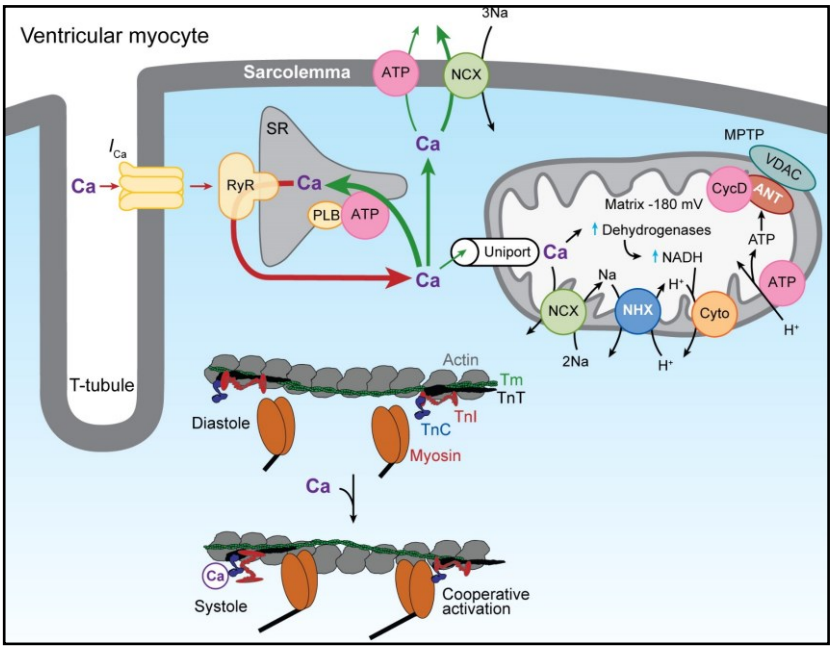

Figure 2.3 Ca^{2+} dynamics in ventricular cardiomyocyte.

Sarcoplasmic reticulum (SR), troponin C (TnC), troponin I (TnI), tropomyosin (Tm) troponin T(TnT), Na/Ca exchanger (NCX), Na/H exchange (NHX), mitochondrial permeability transition pore (MPTP), voltage-dependent anion channel (VDAC), adenine nucleotide translocator (ANT), and cyclophilin D (CycD). PLB, phospholamban; RyR, ryanodine receptor.

2.2.2. Calcium cycling and Excitation-Contraction Coupling

Ca^{2+} is a ubiquitous secondary messenger and important connection between electrical excitation and mechanical contraction. In the ventricular cardiomyocyte, excitation starts when neighboring cells transfer positive ions through gap junctions. The rise in membrane potential leads to opening of sodium channels and a consequent influx of positive sodium ions resulting in rapid depolarization.

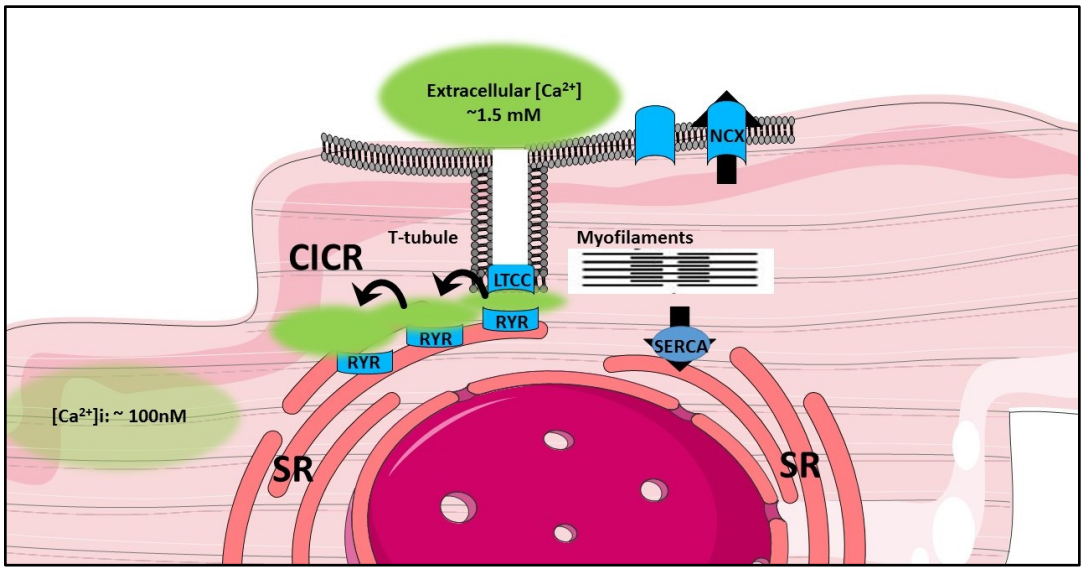

Figure 2.4 Excitation-contraction coupling.

T-tubule, transverse tubule; LTCC, L type Calcium channels; SR, sarcoplasmic reticulum; RYR, ryanodine receptor; NCX, Na/Ca exchanger; SERCA, Sarco/endoplasmic reticulum Ca^{2+}-ATPase; CICR, Calcium induced calcium release. The arrows indicate paths of ion translocation and Ca2+ release are highlighted in green cloud.

Upon this membrane depolarization, Ca^{2+} enters the cell via the opening of voltage-dependent L-type Ca^{2+} channels (LTCC) as inward Ca^{2+} current (Ica) and contributes to the plateau phase of the action potential (AP). LTCCs are predominantly located at sarcolemmal-SR junctions and they are in close proximity to ryanodine receptors (RyRs) that are Ca^{2+} sensitive Ca^{2+} channels of the SR. In a process called calcium-induced-

calcium-release (CICR), Ca^{2+} influx through L-type Ca^{2+} channels triggers the opening of RyR channels on the SR that in turn give rise to a massive increase in the intracellular calcium concentration $[Ca^{2+}]i$(Bers 2014). This free Ca^{2+} binds to troponin C activates the contractile apparatus leading to contraction.

For the cardiomyocyte to relax again, it is necessary that Ca^{2+} detaches from Troponin C and is removed out from the cytosol. This happens gradually by decreasing the Ca^{2+} concentration via two main pathways involved in Ca^{2+} reuptake, which are pumping of Ca^{2+} back into the sarcoplasmic reticulum (SR) via the SERCA and out of the cell via the Na^{2+}/Ca^{2+} exchanger (NCX) (Figure 2.4). Depending on the species these two pathways contribute to different extend to the Ca^{2+} elimination (Bers 2002).

2.2.3. Altered Ca^{2+} homeostasis in the pathophysiology of Heart failure

Given the central role of Ca^{2+} in the heart, it not surprising that disturbances in Ca^{2+} handling can have catastrophic effects on the heart like ventricular arrhythmias, HFpEF, and dilated cardiomyopathy. Ca^{2+} also serves as a second messenger in CMs (Gorski *et al.* 2015). This functionality is dependent on sustaining a balanced homeostasis across the sarcolemma, cytosol, and SR set by Ca^{2+} channels, ATP dependent transporters, and ion exchangers working in synergy with Ca^{2+} handling proteins (Figure 2.5).

SERCA, Sarco/endoplasmic reticulum Ca^{2+}-ATPase, involved in relaxation, is the most abundant protein in the SR membrane and the second largest ATP consumer after myosin ATPase in a cardiomyocyte. SERCA2a is regulated by phospholamban (PLB), which inhibits SERCA2a activity of Ca^{2+} removal from the cytosol, however, it is in turn inhibited by PKA dependent phosphorylation(MacLennan and Kranias 2003). Activators of PKA, like adrenergic stimulation, thus affects SERCA2a promoting faster relaxation and contraction (Simmerman and Jones 1998). However, in pathophysiological conditions, higher phosphorylated levels of PLB are prone to be proarrhythmic (Bers 2001). In heart failure, there is reduced expression and activity of the SERCA2 pump and an increased leak of Ca^{2+} through the RyR channel(Hasenfuss *et al.* 1994; Periasamy

and Kalyanasundaram 2008). This, in turn, leads to a reduced Ca^{2+} release from the SR in diastole and contractile dysfunction which characteristic of heart failure (Anger *et al.* 1998; Schmitt *et al.* 2003)

Another feature of the impaired Ca^{2+} handling in heart failure is the prolongation of the Ca^{2+} transient. Studies have shown that an increased phosphorylation of the LTCC leads to an increased influx of Ca^{2+} through the LTCC which further aggravates pathological Ca^{2+} handling(Correll *et al.* 2017).

$Na+/Ca^{2+}$ exchanger (NCX) is, besides SERCA, the second major transporting protein involved in Ca^{2+} extrusion(Hilgemann *et al.* 1991; Blaustein and Lederer 1999; Hasenfuss *et al.* 1999). However, under the pathological condition, higher $[Na+]_i$ shifts the reversal potential of NCX, consequentially reducing Ca^{2+} efflux via the NCX over the time course of an AP. These changes to the AP are denoted to as early afterdepolarizations (EADs) and delayed afterdepolarizations (DADs) and are observed often in pathophysiological conditions, in which excitation-contraction is altered (ventricular remodeling)(Sipido *et al.* 2007; Antoons *et al.* 2012). NCX1 protein expression is also increased during heart failure and is proposed to compensate for the reduced SR Ca^{2+} uptake and enhances diastolic Ca^{2+} concentration(Hobai and Rourke 2000).

Next, to excitation and contraction, Ca^{2+} is also involved in intracellular signaling as a secondary messenger. It is capable of activating the signaling proteins such as Ca^{2+}/calmodulin-dependent protein kinase II (CaMKII) and Calcineurin (CaN). Both are heavily involved in changes in gene expression related to pathological hypertrophy, characterized by dilation, reduced fractional shortening, and pro-arrhythmic changes like deposition of fibrosis and reduced intercellular coupling (Backs *et al.* 2009; Lu *et al.* 2011). CaMKII is identified to influence the calcium handling on multiple levels. It can directly phosphorylate the LTCC and RyR, both causing a gain-of-function and in that way induce afterdepolarizations(Kirchhof *et al.* 2004). It is also capable of phosphorylating PLB, which in effect diminishes the inhibitory effect of PLB, leading to more SERCA activity

(comparable to the effects of PKA-dependent phosphorylation). Consequently, this results in a higher SR calcium load, higher calcium fluxes and increased contraction(Hoch *et al.* 1999). Whereas CaN is activated by prolonged increased diastolic Ca^{2+} concentrations, CaMKII has been shown to be activated by increased frequency and longer action potentials(Lu *et al.* 2006). During heart failure, increased sarcolemmal Ca^{2+}

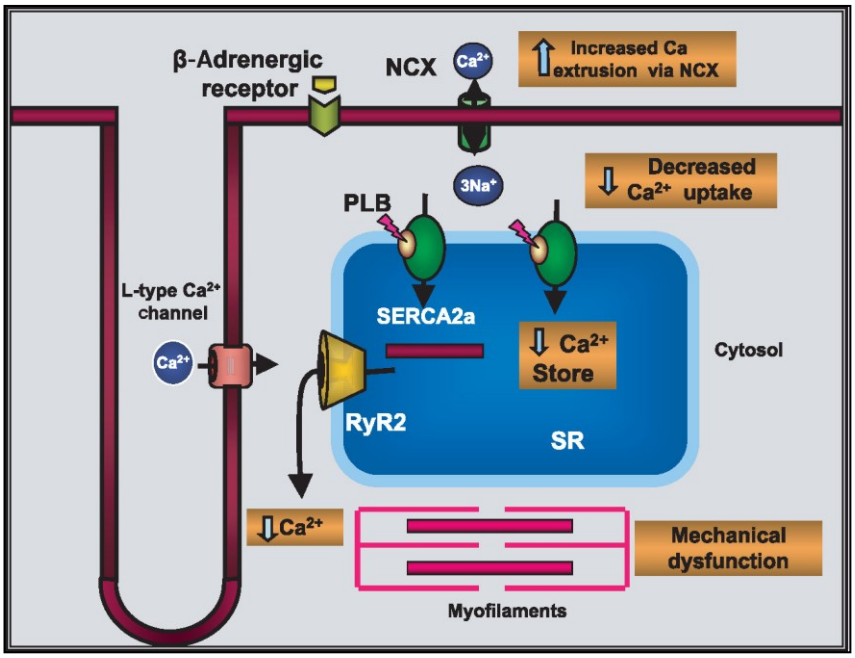

Figure 2.5 Altered Ca^{2+} transport in heart failure

SERCA, Sarco/endoplasmic reticulum Ca^{2+}-ATPase; NCX, sodium-calcium exchanger; PLB, phospholamban; RyR2, ryanodine receptor; SR, sarcoplasmic reticulum.

flux, increased the inflow of Ca^{2+} through the LTCC, spontaneous RyR2 opening and the inward current generated by increased NCX1 mediated Ca^{2+} efflux result in arrhythmias and sudden cardiac death(Pogwizd *et al.* 2001).

Ca^{2+}, therefore, does not only link excitation to contraction, but also regulates long-term structural changes (ventricular remodeling) via excitation-transcription coupling (ETC). Thus, it is pivotal to study these early cellular Ca^{2+} mediated signaling in LVH.

2.2.4. The function of microdomain in Ca^{2+} signaling

Several groups have shown that signaling regulated by spatially restricted Ca^{2+} signaling pathways could be accountable for hypertrophy in cardiac myocytes (Wu *et al.* 2006; Escobar *et al.* 2011) Microdomains are subcellular spatially restricted signaling regions facilitated by a large number of Ca^{2+} interacting proteins and the unique cellular architecture of a CM.

Dyadic Ca^{2+} release unit (CRU) is a prototypical microdomain in a CM where sarcolemmal invaginations studded with LTCC, referred to as t-tubules, juxtapose an expanded SR terminal cisterna expressing the RyR2 protein (Figure 2.6). This creates a unique environment whereby a small amount of trigger Ca^{2+} from the LTCC directly bathes the adjacent RyR2 to promote a much larger release of Ca^{2+}, promoting CICR. Thus, it acts as a critical Ca^{2+} regulatory microdomain with tight spatial and geometric constraints to ensure proper RyR2 control and Ca^{2+} release. In a brief period, a local elevation of the Ca^{2+} concentrations at the site of release (i.e. near the RyR2 or the LTCC) exceeds the Ca^{2+} concentrations in the bulk cytoplasm of the cell by several orders of magnitude (Rizzuto and Pozzan 2006). These Ca^{2+} peaks at these 'hot spots' are limited spatially and temporarily away from large subcellular Ca^{2+} gradients found in rest of the cytosol, where Ca^{2+} binds to myofilaments to induce contraction.

There is an emerging model of Ca^{2+} microdomains where it likely helps CMs to have functional Ca^{2+} domains independent of total fluxing contractile Ca^{2+}. One of the examples is the expression of LTCC in caveolae, highly specialized membrane regions enriched in cholesterol and sphingolipids that contain the scaffolding protein caveolin(Galbiati *et al.* 2001). A certain percentage of LTCCs are localized to sarcolemmal caveolae providing a local pool of Ca^{2+} in non-junctional membrane regions to initiate hypertrophic signaling

via Ca^{2+} handling protein calcineurin downstream to hypertrophic signaling receptors and effectors(Balijepalli *et al.* 2006; Houser and Molkentin 2008).

The most important Ca^{2+} microdomain that likely regulates the cardiac hypertrophic response is the nuclear envelope (NE). The NE comprises a complex involving the IP3R, CaMKII, and class II histone deacetylases (e.g. HDAC4,5). There are two complex Ca^{2+} mediated signaling cascades working in beating CMs.

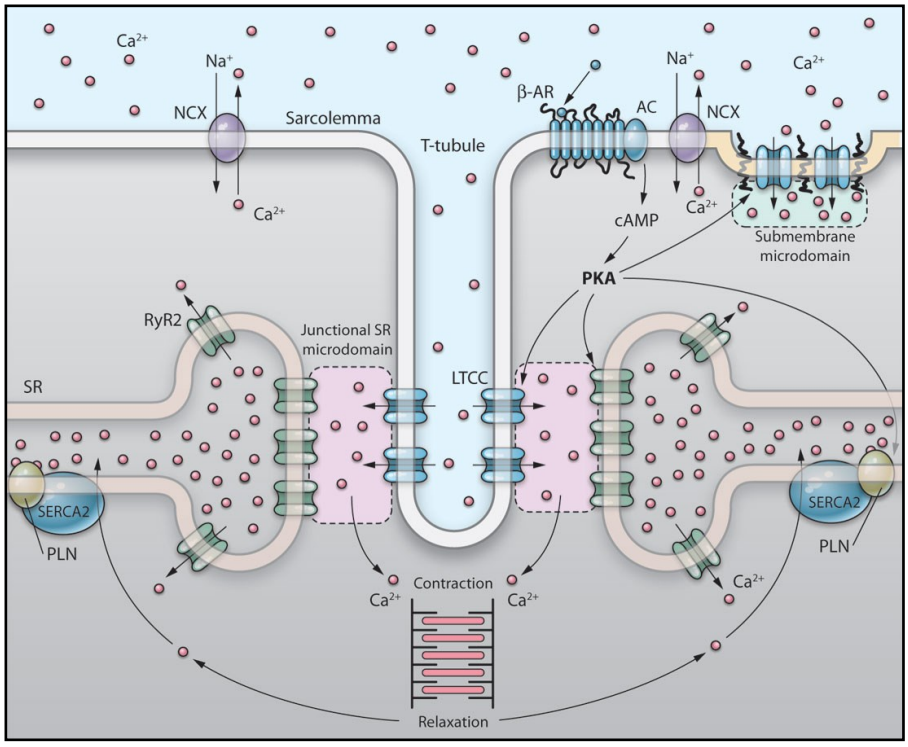

Figure 2.6 Cytosolic Ca^{2+} microdomain in ventricular cardiomyocytes

β-AR β-Adrenergic receptor, SERCA, Sarco/endoplasmic reticulum Ca2+-ATPase; NCX, sodium-calcium exchanger; PLB, phospholamban; RyR2, ryanodine receptor; SR, sarcoplasmic reticulum, PKA Protein kinase A. The Ca2+ microdomains within the cardiomyocytes are highlighted in dotted boxes.

One is mediated via large amounts of Ca^{2+}-induced Ca^{2+} release (CICR) during ECC which also flows through the nucleus and second, local nuclear Inositol 1,3,5 triphosphate (IP3) induced Ca^{2+} signaling (IICR) via nuclear IP3 receptor (IP3R) during ETC leading to hypertrophic remodeling(Ljubojević and Bers 2015). There is sufficient evidence supporting the existence of IP3Rs in the inner nuclear membrane of cardiomyocyte suggesting a functional releasable Ca^{2+} source and store in the nucleus (NE) in response IP3 released by the action of extracellular stimuli like Endothelin-1 (ET-1), Angiotensin II (ATII) on their specific G-protein coupled receptors(Higazi *et al.* 2009; Ljubojević *et al.* 2014). Thus, the nucleus provides a local environment lead to confined Ca^{2+} signaling independent of the global Ca^{2+} changes. This local Ca^{2+} signaling has deemed to be important for early hypertrophic maladaptation in CMs(Ljubojević *et al.* 2014).

Nuclear CaMKII had been established as a critical player in regulating cardiac hypertrophy, where it phosphorylates class II histone deacetylases (e.g.HDAC4) leading to cardiac hypertrophy(Dewenter *et al.* 2017). While overexpression of IP3R in the nucleus of CMs can enhance cardiac hypertrophy to select stress stimuli like neurohumoral activations(Garcia *et al.* 2016). This microdomain involves Ca^{2+} release through IP3R2 within the nuclear envelope to generate a local pool of Ca^{2+} that then directly activates CaMKII, which in turn phosphorylates HDAC4 leading to its nuclear export to permit expression of hypertrophic genes (Figure 2.7).

A similar paradigm was also shown to be responsible for CaN–NFAT activation in and around the nucleus through IP3R activity and local Ca^{2+} release to induce hypertrophy(Wu *et al.* 2006).

Thus, the nucleus is an important microdomain in cardiomyocyte with respect to maladaptive hypertrophic signaling regulated by Ca^{2+}.

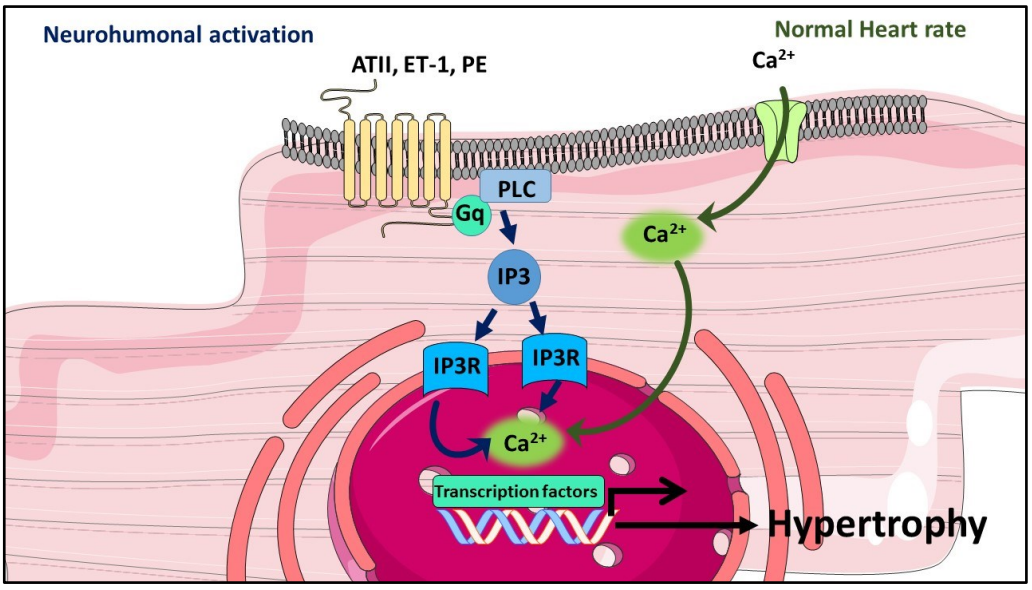

Figure 2.7 Nuclear Ca^{2+} microdomain and signaling in ventricular cardiomyocytes

ET-1 , Endothelin-1; ATII, Angiotensin II; PE, Phenylephrine; ECM, Extracellular matrix; PLC, Phopholipase C; IP3, Inositol 1,3,5 triphosphate; IP3R, Inositol 1,3,5 triphosphate receptor. The Ca2+ release are highlighted in green cloud. The nuclear area within cardiomyocyte is denoted as dark pink.

2.3. Excitation-Transcription Coupling and pathological hypertrophic signaling

In the presence of a chronic demand for an increased cardiac output, the heart attempts to increase the cardiac mass and contractile fibers in a process known as cardiac hypertrophy. As discussed earlier, cardiac hypertrophy is a complex process that involves multiple signaling pathways and is yet to be fully understood(Berridge *et al.* 2003). From starting signals at the CM membrane, a host of signal transduction events occurs in a complex and integrated manner to arouse adaptive or maladaptive responses. Several signaling pathways have been identified and are linked to the development of cardiac hypertrophy. Research has emphasized multiple signaling networks that receive

converging inputs from several upstream molecules to effect on hypertrophy and the maintenance of cardiac function. Surprisingly, however, the hypertrophic response in highly trained athletes or pregnant mothers and in patients with pathologic cardiac disease seems to differ in several key ways(Bisping *et al.* 2014; Thienpont *et al.* 2017). While neither comprehensive nor inclusive, here I have highlighted Ca^{2+}-mediated signaling in pathologic cardiac hypertrophy (Figure 2.8).

Within distinct microdomains (Figure 2.7), Ca^{2+} act as a potent signal transduction molecule and lead to modulation of key Ca^{2+} mediated pathways, termed as ETC. Increased intracellular Ca^{2+} concentration $[Ca^{2+}]i$ in the cardiomyocyte, can activate two major Ca^{2+}-dependent hypertrophic signaling pathways: Ca^{2+}-calmodulin (CaM)- CaMKII-histone-deacetylase (HDAC) and Ca^{2+}-CaM- Calcineurin(CaN)-nuclear factor of activated T cells (NFAT) pathways (Figure 2.8)(Bers 2008).

ETC is coordinated by the multifunction calcium sensor, calmodulin (CaM). CaM is a universal second messenger that carry Ca^{2+} signals. Upon binding of Ca^{2+} ions, CaM undergoes conformational changes and further leads to interaction of Ca^{2+}-CaM complex with different target proteins, initiating downstream signaling pathways. It is shown that transgenic overexpression of CaM causes hypertrophy(Gruver *et al.* 1993), while CaM inhibition can block myocyte hypertrophy(McDonough and Glembotski 1992), thus emphasizing its importance.

CaM on binding with Ca^{2+} stimulate CaMKII that binds Ca^{2+} via its EF-hands. CAMKII is a serine/threonine protein kinase that can phosphorylate and activate several downstream targets proteins in the cell as mentioned earlier. CaMKII consists of 4 different isoforms which have distinct expression patterns (Tombes *et al.* 2003). However, cardiomyocyte expresses mainly CaMKII isoform: CaMKIIδ (Maier 2005).

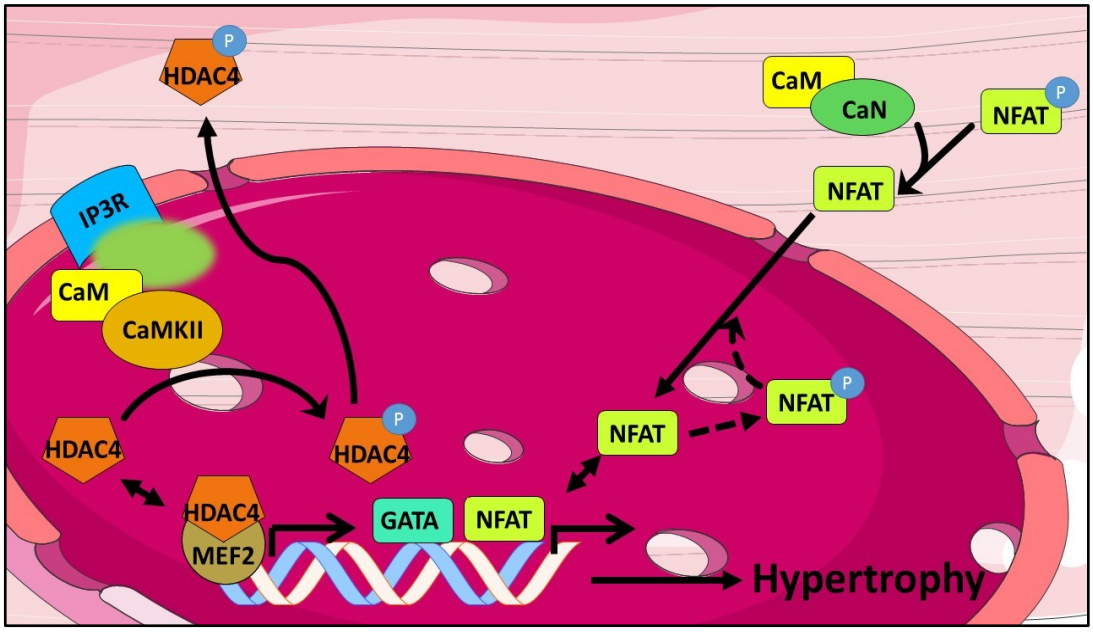

Figure 2.8 Ca^{2+}-dependent excitation-transcriptional coupling in cardiomyocytes

IP3R, Inositol 1,3,5 triphosphate receptor; CaN, Calcineurin ; NFAT, Nuclear factor of activated T-cells; CAMKII, Ca^{2+}/calmodulin-dependent protein kinase II; p/HDAC-4, phosphorylated /Histone deacetylase-4. Local [Ca] elevation is indicated as green cloud. The nuclear area within cardiomyocyte is denoted as dark pink. GATA and MEF2 are the transcription factors involved.

Overexpression of this isoform in mice leads to an early onset of hypertrophy whilst ablation leads to protection from hypertrophy and fibrosis(Backs *et al.* 2009). There are two splice variants of CaMKIIδ (1) CaMKIIδB, which comprises a nuclear localization sequence (NLS) and therefore localizes in the nucleus and (2) CaMKIIδC with no NLS, which compartmentalizes in the cytoplasm(Mishra *et al.* 2011). Activation of CaMKIIδC mostly affects ECC through modulation of Ca^{2+} handling proteins such as PLB, RyR, and L-type Ca^{2+} channel. However, CaMKIIδB phosphorylates proteins responsible for the regulation of gene transcription like transcription factors and proteins of the epigenetic machinery, e.g. HDACs class II(Anderson *et al.* 2011).

Cellular hypertrophy inducing Ca^{2+}-calmodulin(CaM)-calcium/calmodulin-dependent protein kinase II (CaMKII) – histone-deacetylases 4 (HDAC4) pathway is shown to be regulated by nuclear Ca^{2+} release events(Ljubojević *et al.* 2014). In this pathway, CAMKII

specifically phosphorylates Serine 632 site of anti-hypertrophic transcription repressor histone deacetylase 4 (HDAC-4)(Backs *et al.* 2006). As a result, HDAC4 is exported from the nucleus to cytoplasm, where it no longer serve anti-hypertrophic functions against transcription factors like MEF2 and SRF resulting in activation of hypertrophic gene programs that are controlled by these transcription factors(Passier *et al.* 2000). HDAC4 and MEF2 signaling are important in the development of cardiac hypertrophy as is evident by enhanced responsiveness to transverse aortic constriction (TAC) induced hypertrophy in mice in which class II HDACs are mutated or genetically deleted (Zhang *et al.* 2002).

One arm of CaM signaling is via its interactions with calcineurin, (CaN), a serine/threonine protein phosphatase. CaN has a much higher affinity for Ca^{2+}/CaM complex than CaMKII. Thus, whereas CaMKII may react to high-amplitude Ca^{2+} spikes, CaN can be better at sensing smaller, sustained Ca^{2+} elevations (Bers 2008).

The activation of CaN by a sustained increase in Ca^{2+} levels (Dolmetsch *et al.* 1997) leads to dephosphorylation of NFAT, which is predominantly located in the cytoplasm. This allows the transport of NFAT to the nucleus which activates hypertrophic gene transcription with the transcription factor GATA4 (Frey *et al.* 2000; Molkentin 2004). There are four Ca^{2+} sensitive NFAT isoforms expresses in mammalian hearts (NFATc1 to NFATc4) which are activated by CaN(Kehlenbach *et al.* 1998). NFATc4 isoform is held to be most associated with remodeling in adult ventricular CMs(Rinne *et al.* 2010). Indeed, NFAT transcription factors have been shown in genetic mouse models to mediate cardiac hypertrophy while deficiency of CaN decreases the reaction to hypertrophy agonists(Wilkins and Molkentin 2002). Transgenic mice which overexpressed CaN and NFATc4 lead to robust hypertrophy that rapidly progressed to dilated heart failure within 2-3months(Molkentin *et al.* 1998; Saito *et al.* 2003). In HF patients, the increase in CaN activity and expression were associated with failing or hypertrophic hearts(Lim and Molkentin 1999). However, few studies have also suggested a role for peri-nuclear CaMKII in activation of CaN-NFAT signaling in cardiac hypertrophy(Passier *et al.* 2000).

Indeed, impaired Ca^{2+} signaling especially nuclear Ca^{2+} signaling is the main contributor to diminished ventricular contractile function, the occurrence of arrhythmias and hypertrophy in HF.

2.3.1. Regulation of nuclear Ca^{2+} in healthy and diseased cardiomyocyte

It is apparent that Ca^{2+} signaling is paramount to cardiomyocyte function as a rise in intracellular Ca^{2+} can initiate both cardiomyocyte contraction and Ca^{2+} triggered signal transduction pathways. Considering the highly organized architecture of cardiac myocytes, spatial regulation by microdomains is a particular requirement for Ca^{2+} signaling efficacy (Peskoff and Langer 1998) as discussed earlier (2.2.4 above). The nucleus is one such microdomain important for localized signaling activation. Subcellular nuclear Ca^{2+} transients have shown to regulate important cellular processes such as gene expression, apoptosis, assembly of the nuclear envelope and nucleo-cytoplasmic transport(Sullivan and Wilson 1994, Stehno-bittel *et al.* 1995; Zhang *et al.* 2009).

In CMs, with each heartbeat, there is a transient rise in the cytoplasmic free Ca^{2+} concentration. Each cytoplasmic [Ca^{2+}] transient (CaT) elicits a nucleoplasmic CaT subsequently(Kockskämper *et al.* 2008b). However, studies have shown that nucleoplasmic [Ca^{2+}] transients (CaT) follow a considerably slower kinetics as compared to the kinetics of cytoplasmic CaTs, with slower and delayed upstroke, a lower peak, and a prolonged return back to baseline(Genka *et al.* 1999; Ljubojević *et al.* 2011; Hohendanner *et al.* 2014). It is mainly due to restricted diffusion to the nucleus from the surrounding cytoplasm through the nuclear envelope (NE). The NE provides nuclear structural integrity and controls bidirectional transport of ions (including Ca^{2+}) and macromolecular cargo (Malhas *et al.* 2011). It is shown to also acts as a functional Ca^{2+} store to regulate nucleoplasmic Ca^{2+} concentration [Ca^{2+}] and gene expression and has important functions in downstream signaling (Ljubojević and Bers 2015).

NE consists of the inner and outer nuclear membrane and has intermittent nuclear pore complexes (NPC) connecting the nucleoplasm and the cytoplasm. These NPCs allow the

passive diffusion of small molecules and ions including Ca^{2+} between these two compartments.

However, it was found that NE also gives out invaginations or tubular structures that reach deep into the nucleoplasm in CM(Genka *et al.* 1999; Malhas *et al.* 2011). NE can function deep within the nucleus in regions that are otherwise remote from the nuclear surface due to the presence of a network of invaginations(Malhas *et al.* 2011; Ljubojević *et al.* 2014). These invaginations might help decrease the diffusion delay and increase membrane surface area thus facilitating the intranuclear regulations of ions and transcription factors that cross the cytoplasm and nucleus. This might be critical for the regulation of gene transcription. In addition, T-tubules from sarcolemma are found to reaching deep into the cytosol in close proximity to the nuclear envelope, constituting microdomain for Ca^{2+} cycling and signal responsiveness(Dewenter *et al.* 2017).

The presence of SERCA pumps on the invaginations facing the cytoplasmic side enables removal of Ca^{2+} from deep within the nucleus, thus important in shaping the nucleoplasmic CaT kinetics (Ljubojević *et al.* 2014). Interestingly, however numbers of primary active pumps for Ca^{2+} reuptake found on the inner nuclear membrane are inconsiderable (Humbert *et al.* 1996). Therefore, it seems like Ca^{2+} mostly diffuses out of the nucleus via NPCs. This extruded Ca^{2+} then taken up by SERCA on the outer nuclear membrane and the junctional SR, by nearby mitochondria or is pumped out by NCX on T-tubules in proximity to the nuclear envelope (Jaconi *et al.* 2000; Escobar *et al.* 2011). Thus, the decay of nuclear Ca^{2+} transients is slower compared with cytoplasmic Ca^{2+} transients; consequently, the Ca^{2+} strikingly builds up within the nucleus when diastole is shortened. This explains why the nuclear diastolic baseline [Ca^{2+}] increases with higher beating frequencies (Ljubojević *et al.* 2014).

The NE has found to be an extension of the SR. Thus, outer nuclear membrane show the same characteristics on their composition, and the perinuclear space, which is in between the outer nuclear membrane and the inner nuclear membrane, resembles the SR in ion and protein content(Fricker *et al.* 1997) and thus can possibly act as an intracellular Ca^{2+}

store(Wu and Bers 2006; Bootman *et al.* 2009). There are two components of nuclear CaTs: a) passive diffusion of cytoplasmic CaTs to the nucleus through nuclear pore complexes b) Active Ca^{2+} release from NE in a specific and regulated manner upon different stimuli. The nuclear envelope expresses the whole Ca^{2+}-regulating proteins apparatus including the SERCA, Ca^{2+} release channels, and Ca^{2+}-buffering proteins which support the notion of NE as a Ca^{2+}store(Gerasimenko and Gerasimenko 2004; Bootman *et al.* 2009). As stated earlier (2.2.4 above), IP3R- mediated Ca^{2+} release (IICR) is important for the localized nuclear Ca^{2+} triggered signaling. There is a preferential expression of type 2 IP3Rs as compared to ryanodine receptors on NE (Hohendanner *et al.* 2014). Lipp *et al.* have shown that small perinuclear Ca^{2+} release events, Ca^{2+} sparks or puffs within 3μm of the nuclear envelope can contribute to an increase in nuclear Ca^{2+} while not affecting the rest of the cytosol(Lipp *et al.* 1997). NE has shown to have an entire PIP2-PLC-IP3 cascade, along with GPCRs and IP3Rs(Tadevosyan *et al.* 2010). Thus, the nuclear GPCRs in combination with nuclear IP3R-mediated IICR and Ca^{2+} removal constitute a putative distinct signaling domain that regulates nuclear Ca^{2+} dynamics. This clearly confirms that many features beyond the whole-cell Ca^{2+} oscillation influence nuclear Ca^{2+} regulation.

Remarkably, early changes of CM nuclei regarding increased nuclear size and less frequent intrusions of NE are observed during cardiac remodeling. In addition, these early changes induce functional consequences like reduced NPC and SERCA within the nuclear core(Ljubojević *et al.* 2014). Also, there are few studies showing an increase in expression of IP3R in hypertrophied CMs(Harzheim *et al.* 2009). Further, leading to an enhancement of nuclear CaTs, slow extrusion, elevated nuclear diastolic Ca^{2+} ultimately instigating altered nuclear Ca^{2+} signaling which implicated in hypertrophic gene program activation leading to HF(Ljubojević *et al.* 2014).

2.3.2. Role of IP3R in the regulation of nuclear Ca^{2+}

In addition to RyR, interestingly, a higher density of IP3R is found preferentially but not exclusively found in the nuclear and perinuclear region in CMs, suggesting a prominent

role for IP3R in nuclear Ca^{2+} signaling(Lipp *et al.* 2000; Bare *et al.* 2005). The most predominant subtype in CMs is IP3 receptor type 2 (IP3R2) (Zima *et al.* 2007). Due to various factors as discussed earlier (2.3.1 above), IP3R-mediated Ca^{2+} release elevates local nuclear Ca^{2+} independent from cytoplasmic Ca^{2+} changes(Wu *et al.* 2006). This localized Ca^{2+} increase constitutes IP3-induced Ca^{2+} release (IICR).

G-protein coupled receptors (α-adrenergic, ET-1, and ATII receptor) activating phospholipase C (PLC), has a potential to modulate nuclear Ca^{2+} through IICR from the nuclear envelope. Thus any event which either leads to increase in cytoplasmic [Ca^{2+}] via mechanical stretch, increased heart rate or non-excitatory stimulation or active stimulation of IP3R on NE (i.e. neurohormonal activation), will also lead to an increase in nucleoplasmic [Ca^{2+}]. Such mechanism offers myocyte a means to regulate nuclear Ca^{2+} independently from the AP-induced cytoplasmic CaT during ECC and would constitute the basis of ETC(Wu and Bers 2006; Kockskämper *et al.* 2008a). Furthermore, elevated levels of nuclear Ca^{2+} have shown to enhance the IP3 sensitive of IP3Rs(Taylor and Tovey 2010) which might be one explanation for this phenomenon. There is the development of cardiac hypertrophy in IP3R2 TG mice in response to chronic isoproterenol infusion, Gαq overexpression, and exercise stimulation(Nakayama *et al.* 2010). Strikingly, a set of G protein-coupled receptors (GPCRs), including receptors for ET-1, and ATII, and the entire machinery for IP3 signaling is been located in the nucleoplasm, possibly aiding IP3R-mediated Ca^{2+} release from the nuclear envelope(Tadevosyan *et al.* 2010; Merlen *et al.* 2013). Furthermore, in hypertrophy and HF, an increase in IP3R expression and higher diastolic nuclear Ca^{2+} versus cytoplasmic Ca^{2+} is observed, thus reemphasizing the role of IP3-IP3R signaling(Ai *et al.* 2005; Harzheim *et al.* 2009; Ljubojević *et al.* 2014)

The rise in nucleoplasmic [Ca^{2+}] has shown to be able to activate transcription factors thus modulating the gene expression which is associated in the development of cardiac hypertrophy (Dolmetsch *et al.* 1998; Zhang and Brown 2004; Backs and Olson 2006). As specified earlier (2.3), the CAMKII is an important regulator of hypertrophy especially

CaMKIIδB which is specifically localized in the nucleus. Moreover, α-adrenergic receptor activation selectively increased nuclear CaMKIIδ phosphorylation via Ca^{2+} mobilized through nuclear IP3-sensitive stores (Remus *et al.* 2006). ET-1 induces local nuclear envelope Ca^{2+} release via IP3 receptors and activates CAMKII/HDAC4/MEF2 axis (Wu *et al.* 2006).

Similarly, NFAT, a key player in cardiac remodeling, have shown to be accumulated locally in the nucleus possibly making is easy for shuttling in and out of the nucleus when local [Ca^{2+}] is elevated(Bodi *et al.* 2005). This is speculated to be regulated by nuclear IICR(Rinne *et al.* 2010). This assumption is supported by studies where nuclear CaN is increased in human HF heart, also it is required for full transcriptional effects of NFAT(Kaye *et al.* 1995; Engelhardt *et al.* 1999). In addition, the development of cardiac hypertrophy in IP3R2 TG mice is sensitive to blocking via genetic CaN deletion (Nakayama *et al.* 2010).

Thus, nuclear IICR plays an important role in ETC via CAMKII and CaN.

Overall, nuclear accumulation of IP3Rs, neurohumoral activation mediated release of IP3 CMs enhanced NFAT and CaMKII signaling and activation of a hypertrophic gene program characterize cardiomyocyte of failing hearts. The increased cytoplasmic and nucleoplasmic [Ca^{2+}] has been shown to be vital for initiation and progression of heart failure (Berridge *et al.* 2003) while altered Ca^{2+} homeostasis has been a trademark for hypertrophic and failing human hearts(Hasenfuss and Pieske 2002, Bers 2006). Thus, in order to treat and prevent the underlying causes of heart disease, it is necessary to understand the basic regulators of cardiac physiology and their role in the pathophysiology of the cardiac disease. Thus, the study of subcellular Ca^{2+} changes in the nucleus is of vital importance for understanding the pathological processes in the heart(Gwathmey *et al.* 1987).

2.3.3. Hypertrophic transcription factors and activation of fetal response genes

In a fetus, before birth, energy supply of the cardiac metabolism primarily consists of carbohydrates. After birth, the cardiac metabolism switches to the use of oxidation of fatty acids. A feature of the failing heart muscle, such as cardiac hypertrophy, is the return to fetal heart physiology expressing fetal genes. This switch to “the fetal gene program” is accompanied by the expression of different isoforms of metabolic enzymes and other proteins with the purpose of helping the heart to adapt to an increased workload. Activation of the fetal gene program allows synchronized synthesis of the proteins needed to bring about enlarged cardiac myocyte size and compensation for the altered energy demands of these larger cells. These genes trigger structural, functional, and electrical remodeling of the heart. Thus, in both eccentric and concentric hypertrophy, there is re-induction of the fetal gene program along with inflammatory genes, whereas this induction is not observed in physiological hypertrophy(Thum *et al.* 2007).

Specific features include, increased expression of natriuretic peptides (ANP, BNP), fibrosis-related (TGF-β), Immediate early genes (ERK), isoform switches of many other proteins including metabolic enzymes and sarcomeric proteins (relative increase of myosin heavy chains 7 (MYH7) compared to myosin heavy chains 6 (MYH6), and α-actins). Since each isoform of myosin heavy chains (MHC) has a distinct enzymatic activity, their relative ratios greatly influence cardiac function, thus an increase in β-MHC coded by MYH-7 decreases the myosin ATPase enzyme velocity, which in turn slows the myocyte contraction rate, a key adaptation to altered workload. Atrial natriuretic peptide (ANP; also known as Nppa) and brain natriuretic peptide (BNP; also known as Nppb), correlates well and are used as a marker for the clinical severity and prognosis of HF(Barry *et al.* 2008). Gene for the regulator of calcineurin (RCAN-1) have shown to be upregulated and acts in a feed-forward mechanism with respect to CaN-NFAT hypertrophic signaling pathway in HF(Kreusser *et al.* 2014).

In adult cardiac myocytes, activation of the MEF2 transcription factor in response to stress signaling activates a pro-hypertrophic gene expression profile. Stress signaling due to

triggers like stretch, neurohumoral activation stimulates MEF2 by causing the nuclear export of class II HDACs (HDAC-4) (as stated in 2.3 above), possibly regulated through protein kinase C/D(Vega *et al.* 2004), which in normal condition would associate with MEF2 and suppress its transcription activity(Lu *et al.* 2000). On the other hand, acetylation of the GATA-4 transcription factor by CBP/p300 results in eccentric left ventricular hypertrophy(Lu *et al.* 2000). Activation of p300/CBP in response to stressor phenylephrine (PE) via its specific β-adrenergic receptor occurs through the downstream protein kinase pathways, downstream of Gq, specifically ERK, p38, MSK1, and PKA. However, strikingly, different stressors that induce different post-translational modifications in GATA-4 trigger distinct cardiac remodeling. For e.g., in contrast to the above, activation of the MEK-ERK pathway by hypertrophic stimuli leads to phosphorylation of GATA-4 at serine 105 and the development of concentric hypertrophy(Lu *et al.* 2000).

Thus, the type of hypertrophic remodeling depends on the trigger and associated progression of contractile dysfunction (afterload, LV volume overload, Myocardial Infarction)(Kuo *et al.* 2012). Furthermore, based on previous experimental findings, the distinct patterns of concentric and eccentric hypertrophy depends on differential and etiology-specific activation of hypertrophic signaling pathways(Toischer *et al.* 2010; Kehat *et al.* 2011).

2.4. Neurohumoral activation in heart failure

Cardiac remodeling is the response of the body to myocardial injury. It acutely aims at restoring and maintaining the cardiac output. Short-term neurohumoral adaptation helps maintain the arterial pressure during inadequate blood flow by vasoconstriction and by increasing myocardial contractility and heart rate. This restores cardiac output and redistribution of the flow to vital organs (Middlekauf and Mark 1998). The important neurohumoral mediators are angiotensin II (ATII), which is part of the Renin-Angiotensin-Aldosterone system (RAAS) and endothelin (ET) and catecholamines (Figure 2.2).

Endothelin is a strong vasoconstrictor primarily expressed in the endothelium. Out of the three isoforms, ET-1 has a potent inotropic activity and is expressed in cardiac myocytes(Maccarthy *et al.* 2000). ET-1 exerts its function by binding to Gq protein-coupled receptors endothelin-A and endothelin-B receptors (ETARs and ETBRs)(Archer *et al.* 2017). Activation of these receptors leads to the release of diacylglycerol (DAG) and inositol-1,4,5-trisphosphate (IP3)(Kockskämper *et al.* 2008b; Bootman *et al.* 2009). There is strong evidence that ET-1 causes cellular hypertrophy by activating IP3-mediated Ca^{2+} release from IP3Rs located at the NE (Wu *et al.* 2006; Kockskämper *et al.* 2008a). IP3 as discussed earlier (2.3.2 above), lead to sustained nuclear Ca^{2+} release and activate the fetal gene response. Numerous studies have demonstrated that plasma ET levels are elevated in patients with HF and in animal models of HF(Löffler *et al.* 1993; Pieske *et al.* 1999).

While, DAG activates numerous isoforms of protein kinase, PKC, and PKD, which regulate myocyte contractility and are also involved in hypertrophic signaling cascades (Viero *et al.* 2016). Catecholaminergic mediators like epinephrine and norepinephrine are shown to modulate CMs via action on their specific adrenergic receptors (AR). Depending on the subtype of the AR, its activation leads to either stimulation of PLC/IP_3/IP_3R pathway or trigger cAMP-dependent PKA, which phosphorylates and controls SR Ca^{2+} regulation via LTCC, RyR, and PLB. These effects regulate the inotropic and chronotropic functions of the healthy heart, however, chronic activation of adrenergic receptors leads to substantial alterations of Ca^{2+} homeostasis further leading to HF(Engelhardt *et al.* 1999; Bodi *et al.* 2005). It is quite evident in transgenic mice with overexpression of human β1ARs where various negative effects were observed on the heart. The chronic triggering of the sympathetic nervous system in patients with HF contributes to the poor prognosis associated with severe HF(Kaye *et al.* 1995; Engelhardt *et al.* 1999).

2.4.1. Angiotensin II

The renin-angiotensin-aldosterone system (RAAS) plays a crucial role in the compensatory neurohumoral response to myocardial injury. Angiotensin II (ATII), major

RAAS hormone, is an active vasoconstrictor peptide composed of eight amino acids (Asp-Arg-Val-Tyr-Ile-His-Pro-Phe)(Chow and Allen 2016). It has seminal effects on the cardiovascular system causing vasoconstriction, increased blood pressure, and release of aldosterone from the adrenal cortex. In the simplest form, the RAAS contains sequential proteolytic conversion of AGT (angiotensinogen) to Angiotensin I (AT I) by renin produced by the kidneys. Angiotensin I is further acted upon by angiotensin-converting enzyme (ACE) into ATII (Barry *et al.* 2008). ATII has a very short half-life and is rapidly degraded to ATIII and AT (1–7) by the angiotensin-converting enzyme 2 (ACE2)(Keidar *et al.* 2007) (Figure 2.9). ATIII has similar actions to those of ATII but AT (1–7) seems to have opposite effect. It acts as an indigenous inhibitor of ATII by exerting hypotensive action via synthesis and release of vasodilator prostaglandins, an increase of the metabolic actions of bradykinin and augmenting the release of endothelial nitric oxide(Ferrario *et al.* 2005).

The bioactive form, ATII, has both physiological and pathological effects. ATII peptide stimulates vascular smooth muscle, contraction, aldosterone release, and production of extracellular matrix proteins. Its effects are dependent on the time course of exposure - acute or chronic. Pathological effects appear when the balance of RAAS go haywire and the exposure to elevated ATII lasts longer than normal.

ATII signals primarily via the Gq-coupled ATII receptor type 1 (AT1) that is coupled to the Gq protein and induces myocardial hypertrophy, fibrosis, and CM apoptosis. Both ATII and angiotensin-converting enzyme (ACE) are found to be at high levels after myocardial infarction and during cardiac hypertrophy (Schunkert *et al.* 1993; Studer *et al.* 1994). Mice with overexpression of AT1Rs in the heart have induced hypertrophy and fibrosis in otherwise healthy mice. These mice also exhibited enhanced hypertrophic responses to pressure overload and premature death in response to heart failure (Paradis *et al.* 2000). While mice with a gain of function mutant AT1 subtype A receptor displayed cardiac fibrosis and diastolic dysfunction in otherwise healthy mice (Keidar *et al.* 2007).

On binding to ATII, an AT-1 receptor on CMs has shown to induce cascades of intracellular signaling pathways (e.g. MAPK) with increased PLCβ activity (Miyata and Haneda 1994, Sadoshima *et al.* 1995; Rajapurohitam *et al.* 2006). As discussed previously in the sections earlier (2.3 above), PLCβ signaling pathway and IP3-mediated Ca^{2+} release are strongly associated with pathological hypertrophy. When the AT-1 receptor is activated by ATII, it activates PLCβ, which hydrolyzes phosphatidylinositol 4, 5 bisphosphate (PIP2), into IP3 which mediates an increase in cytosolic and nuclear [Ca^{2+}], and diacylglycerols (DAG).

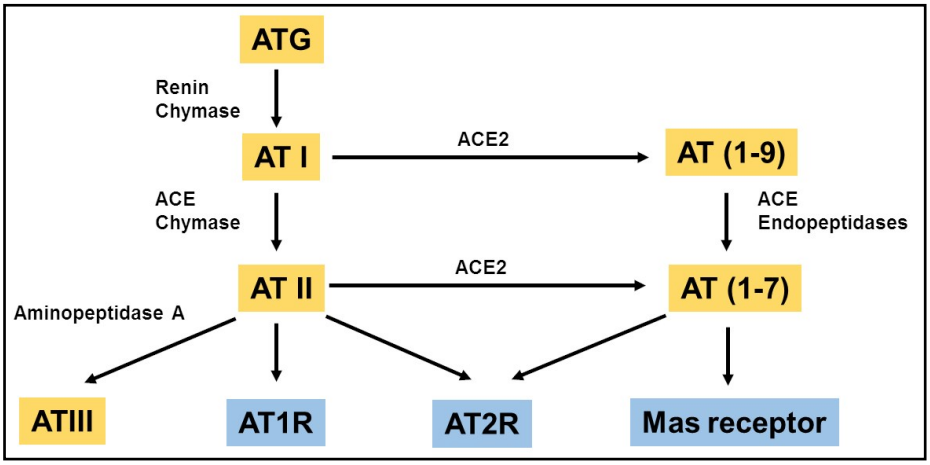

Figure 2.9 Angiotensin II biosynthesis

Schematic diagram of the enzymatic events involved in the formation of Angiotensin II and its peptides. Angiotensinogen, ATG; Angiotensin, Ang; Angiotensin-converting enzyme (ACE); AT receptor, Angiotensin receptor.

DAG activates several serine-threonine isoforms of protein kinase C (PKC). PKC signaling is important for myocyte apoptosis, necrosis, and for triggering pro-hypertrophic gene transcription in CMs. However protein kinase D, a downstream effector of PKC, directly phosphorylates HDAC4/5 and stimulates its nuclear export, thus is also involved in activation of hypertrophic genes(Harrison *et al.* 2006). The four most functionally significant PKC isoforms in CMs are PKCα, β, δ, and ε. PKCα is the most predominant isoform in the human heart and is primarily a regulator of contractility via modulation of

PLB and SERCA activity in CMs. While, PKCβ is vital for the transduction of cardiac hypertrophy, contractility, and regulation of neonatal cardiac growth (Salazar *et al.* 2007).

The other second messenger of PLCβ, IP3, binds several IP3 receptors on the SR and NE to induce the release of calcium stores into the cytoplasm and in the nucleus. As stated earlier (2.3.2 above), unlike the short bursts of contraction and relaxation induced by CICR, IP3-mediated Ca^{2+} signaling (IICR) results in a sustained Ca^{2+} release especially in the nucleus that allows for the activation of hypertrophic response genes (Figure 2.7 and Figure 2.8). A sustained increase in intracellular [Ca^{2+}] activates CaN and its target, the NFAT family of transcription factors, which are critical mediators of pathologic hypertrophy (Dorn II *et al.* 2005; Rinne *et al.* 2010). Similarly, in ventricular myocytes, ATII selectively increased specifically nuclear CaMKIIδ phosphorylation and translocation of HDAC-4 via Ca^{2+} mobilized through nuclear IP3-sensitive stores(Backs *et al.* 2009). These secondary messenger cascades also cause the activation of the angiotensinogen gene and thereby induce intracellular production of ATII and activation of RAAS (Sadoshima and Izumo 1993; Wagner *et al.* 1999). Thus, ATII is indeed a strong and established driver of cardiac hypertrophy and HF.

The anti-neuroendocrine therapy is the foundation for modern treatment of HF. However, the treatment strategies to slow HF progression depends on the symptoms of the individual patients. The strong indication for the long-term deleterious effect of ATII specific neurohumoral overstimulation is evident in the increase in patient survival associated with the usage of ACE inhibitors, AT1R blockers (Losartan), and aldosterone antagonists (Pitt *et al.* 2000; Rossignol *et al.* 2011). In both humans and animal models, targeting the renin-angiotensin-aldosterone system can reduce cardiac hypertrophy and/or negative remodeling of the ventricles back to pre-disease states independent of effects on blood pressure, though blood pressure management is an additional protective aspect of these antagonists. However, in some cases, additional pharmacologic agents are needed, as some patients are refractory to the beneficial effects of ACE inhibitors and

AT1R blockers. Furthermore, the overall efficacy is limited for these agents, as cardiovascular disease still progresses even in responsive patients(van Berlo *et al.* 2013).

There is an increasing evidence of local production of ATII in heart tissue other than classically synthesized ATII in circulating blood. All components of the renin-angiotensin system (RAS) and ATII receptors (AT1R and AT2R) have been identified in cardiac tissue (Paul *et al.* 2006). However, a number of questions remain to be answered regarding cell types that produce RAS components and the sites and regulation of ATII production in the heart. *In vivo*, metabolism and function of cardiac RAS components at the cellular level in normal and diseased states also remain to be determined.

Thus, even though, neurohormonal pathways like RAAS are initially compensatory and beneficial, chronic activation leads to a number of maladaptive consequences eventually leading to the development of hypertrophy and its progression into HF. However, investigation of novel local RAS is of utmost importance to study the exact cellular mechanism of the initiation and maintenance of process of ATII-mediated cardiac hypertrophy and remodeling to unravel the possible targets for HF therapy.

2.5. Chronic Kidney Disease, a co-morbidity of HF

Co-morbidities like hypertension, diabetes and renal failure are of great importance in HF and its treatment. These co-morbidities promote the manifestation and progression of HF. Due to various reasons; the drugs used to treat co-morbidities may cause worsening of HF. Hence, the diagnosis and management of co-morbidities is a key component of the treatment patients with HF. HFpEF has a higher prevalence of co-morbidities compared with HFrEF, and many of these may be involved in the progression of this syndrome(Ponikowski *et al.* 2016).

HF and Chronic kidney disease (CKD) frequently coexist and share many risk factors (diabetes, hypertension, and hyperlipidemia) that interact to worsen prognosis. CKD is a heterogeneous disorder affecting kidney structure and function over a period of more than

3 months. The presence of CKD is accompanied by a drop in glomerular filtration rate, an increase in the occurrence of systemic diseases (heart failure) and pathological anatomic outcomes within the kidney(Levin and Stevens 2014). CKD progression is promoted by other risk factors such as hypertension, diabetes mellitus type 2, obesity, inherited kidney disorders, and cardiovascular disease(Jha *et al.* 2013).

Stepwise changes in bone and mineral homeostasis characterize the course of CKD leading to decrease of renal function. This may be demonstrated through either or all of the following; abnormalities of calcium, phosphate, PTH, and vitamin D metabolism, abnormalities in bone turnover, mineralization, volume, linear growth or strength, vascular calcification or other soft tissue calcification(Pavik *et al.* 2013).

Fibroblast growth factor 23 (FGF23) is a phosphaturic hormone and is secreted by osteocytes in response to various stimuli to increase renal phosphate excretion. FGF23 also suppresses parathyroid hormone expression and secretion and inhibits the renal formation of vitamin D (Silver and Naveh-Many 2009). In CKD, an increase in circulating FGF23 levels is observed in contrast to decline in glomerular filtration rate (GFR) and the renal capacity for phosphate excretion (Gutierrez *et al.* 2005) (Figure 2.10). A CKD animal model, Col4a3$^{-/-}$ KO mouse, exhibits an early increase in FGF23 in the course of CKD (Stubbs *et al.* 2012). In end-stage renal disease (ESRD), FGF23 reaches levels that can be 1000-fold above the normal range(Viaene *et al.* 2012). Furthermore, elevated FGF23 levels have been associated with mortality in CKD patients before and after renal transplantation, thus making FGF23 important prognostic marker of CKD (Isakova *et al.* 2011). Interestingly, *in vivo*, FGF23 is proposed to have a direct stimulatory effect on the RAAS via suppression of ACE2 enzyme in CKD mice model(Kovesdy and Quarles 2016).

2.6. Fibroblast Growth Factor 23

The seminal function of FGF23 involves regulation of phosphate homeostasis, intestinal uptake of calcium and Vitamin D3 metabolism (Angelin *et al.* 2012). In pathological conditions, however, FGF23 rises even at early stages of CKD. It has shown to be linked

even with cardiovascular disease and all causes mortality in end-stage renal disease (Itoh and Ohta 2013).

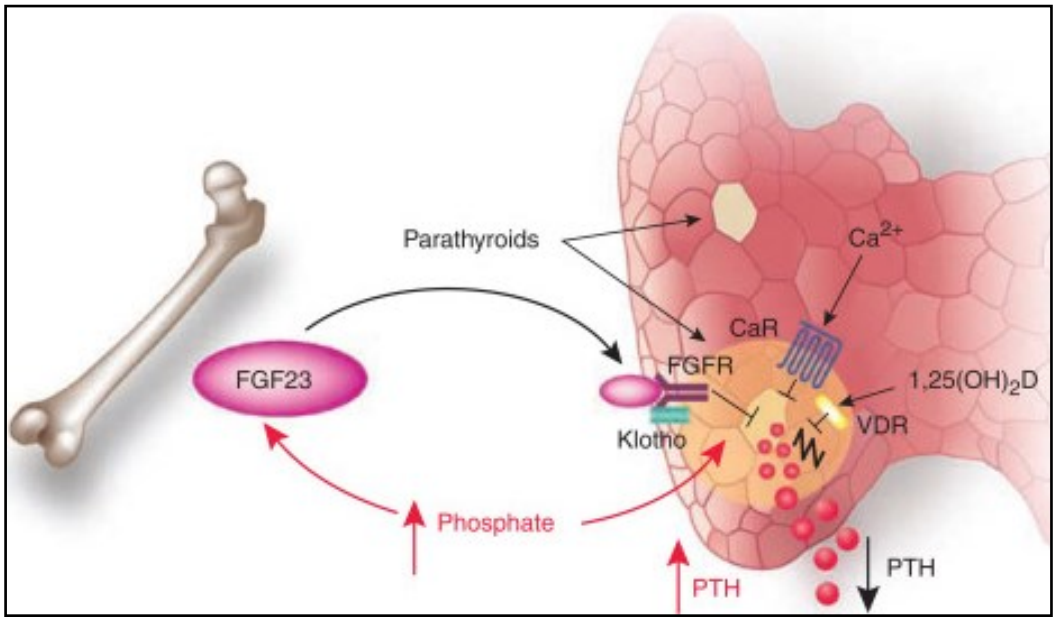

Figure 2.10 Pathophysiology of FGF23

FGF23, fibroblast growth factor 23; FGFR, fibroblast growth factor receptor; CaR, calcium receptor; PTH, parathyroid hormone; VDR, vitamin D receptor. The pink mass in right is the kidney. The red arrows indicate stimulatory pathological pathways.

The figure is reproduced from “Silver, J. and Naveh-Many, T., 2009. Phosphate and the parathyroid. *Kidney International*, 75 (9), 898–905”. Copyright 2009 by Elsevier. Reprinted with permission.

FGF23 along with FGF2 belongs to basic FGF family and mediates its biological actions via specific FGFR-dependent manner. FGF23 exerts its physiological function via FGFRs with α-klotho as a co-factor present on its classic target organs of the kidney and the parathyroid glands. Klotho is an endocrine hormone primarily produced in the kidney and functions as co-receptor for FGF23, whereby it increases the binding affinity of FGF23 to its FGF receptors (FGFRs). In the kidney, FGF23 proficiently binds to FGFR1c with αKlotho, and activate FGF23-MAPK signaling to regulate renal phosphate and 1,25D metabolism (Hu *et al.* 2013) (Figure 2.10).

2.7. Fibroblast Growth Factor 23 and Heart Failure

LVH is one of the key cardiovascular complications in patients with CKD that contributes to aggravate cardiac dysfunction leading to diastolic dysfunction, congestive heart failure, arrhythmias and death(Eckardt *et al.* 2013). CKD progression often accompanied by LVH, is associated with raised serum levels of FGF23(Gutiérrez *et al.* 2009). Greater left ventricular mass and increased incidence and prevalence of LVH independently correlates with elevated FGF23 levels(Faul *et al.* 2011). It is highly likely that elevated serum levels of FGF23 directly contributes to the high rates of LVH and cardiac death in CKD.

Fibroblast growth factors (FGFs) and their receptors are part of a large family of highly conserved signaling molecules that have been implicated in cardiac remodeling. However, αKlotho is not expressed in the heart, so it was assumed that FGF23 could not act directly on the heart to induce injury. Nevertheless, in 2011, Faul and colleagues presented for the first time that FGF23 induced hypertrophy in cultured CMs expressing FGFRs, but not αKlotho(Faul *et al.* 2011). In addition, *in vivo*, there was the development of LVH on direct injection of FGF23 into the left ventricular myocardium in mice, in an FGFR-dependent but α-klotho-independent manner. These results proposed an αKlotho-independent FGF23 signaling in CMs(Touchberry *et al.* 2013)

Downstream FGF23-klotho binding to FGFR leading to auto-phosphorylation signal transduction can proceed via three major pathways—Ras/MAP kinase pathway, phospholipase Cγ (PLCγ)/Ca^{2+} pathway, or PI3 kinase/Akt pathway(Eswarakumar *et al.* 2005) (Figure 2.11). In classic target cells of the kidney and parathyroid glands, FGF23 signaling requires FGFR and the co-receptor klotho.

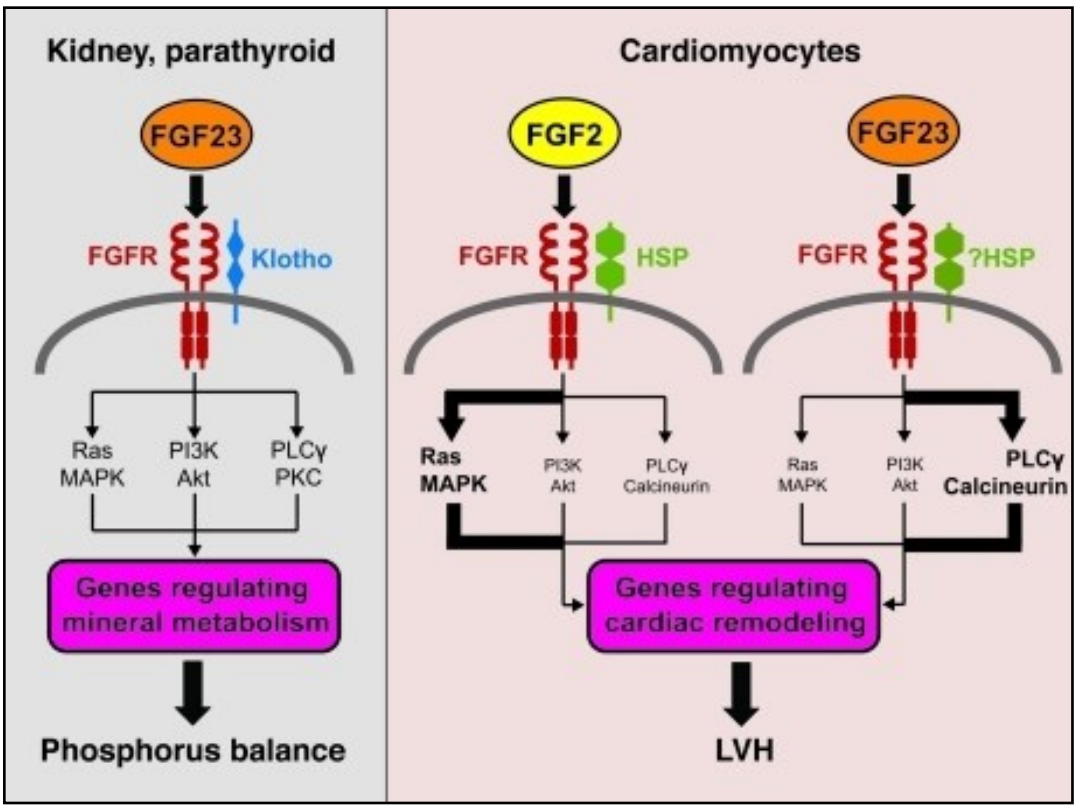

Figure 2.11 FGF23-FGFR mediated signaling in classic target cells and cardiomyocytes.

FGF23, fibroblast growth factor 23; FGF2, fibroblast growth factor 2; FGFR, fibroblast growth factor receptor; PLC γ, phospholipase C γ; CaN, Calcineurin; HSP, heat shock protein; RAS, Rat sarcoma protein, MAPK, Mitogen-activated protein kinase; PKC, Protein kinase C;PI3K, Phosphatidylinositol 3-kinase; Akt, AKT serine/threonine kinase. The highlighted black arrows indicate stimulatory pathological pathways.

The figure is reproduced from Faul, C., Amaral, A.P., Oskouei, B., Hu, M., Sloan, A., Isakova, T., Gutiérrez, O.M., Aguillon-prada, R., Lincoln, J., Hare, J.M., Mundel, P., Morales, A., Scialla, J., Fischer, M., Soliman, E.Z., Feldman, H.I., St, M., Sutton, J., Ojo, A., Gadegbeku, C., Seno, G., Marco, D., Reuter, S., Kentrup, D., Tiemann, K., Brand, M., Hill, J. A., Moe, O.W., Kuro-o, M., Kusek, J.W., Keane, M.G., and Wolf, M., 2011. FGF23 induces left ventricular hypertrophy. *Journal of Clinical Investigation*, 121 (11), 4393–4408. Copyright 2011 by American Society for Clinical Investigation. Reprinted with permission.

In contrast to FGF2, binding of FGF23 to FGFR on CMs stimulates auto-phosphorylation of the receptor tyrosine kinase independent of klotho, which is not expressed in CMs, and signals primarily through the PLCγ-CaN pathway(Faul *et al.* 2011). It is hypothesized that FGF23 activates Ca^{2+}-mediated hypertrophic signaling especially CaN/NFAT signaling in

cultured CMs. Interestingly, these effects are independent of blood pressure levels. Thus, in an endocrine manner, FGF23 trigger cardiac hypertrophy by having a direct effect on CMs (Faul *et al.* 2011; Faul 2012).

The tissue-specific alternative splicing of FGFRs, the mesenchymal splice form FGFR1c, was the major form identified in both the embryonic and adult heart(Pasumarthi *et al.* 1995). However, it has been reported that FGF23 exclusively activates FGFR4 found on CMs. This interaction stimulates PLCγ/CaN/NFAT signaling. Activation of FGFR4 is required for the FGF23-induced hypertrophy as FGFR4-specific blocking antibody prevents FGF23-induced cellular hypertrophy in NRVMs. In addition, attenuation of LVH in rats with CKD was observed with treatment of specific FGFR4-blocking antibody. These results are consistent with the *in vivo* studies demonstrating an absence of hypertrophy induced by FGF23 in $FGFR4^{-/-}$ mice(Grabner *et al.* 2015). Interestingly, FGF23 has also been implicated in age-related cardiac remodeling (Gutiérrez *et al.* 2009; Grabner *et al.* 2017). Older FGFR4 knock-out mice were protected from age-related cardiac remodeling notwithstanding high serum FGF23 levels when compared to wild-type littermates(Grabner *et al.* 2017). Thus, FGF23 indeed promotes LVH by activating FGFR4 on CMs.

Application of FGF23, *in vitro* on primary cultures of ventricular CMs, alters Ca^{2+} homeostasis by increasing Ca^{2+} influx via L–type Ca^{2+} channels(Touchberry *et al.* 2013). FGF23 has also shown to modulate SR Ca^{2+} pump (SERCA) activity and dysregulate electrophysiology of atrial cells. This lead to increases in SR Ca^{2+} content delayed afterdepolarizations and arrhythmogenicity (Kao *et al.* 2014). Moreover, FGF23 treatment induced increased intracellular Ca^{2+} levels in CMs and raised contractility in mouse ventricular muscle strips, *ex vivo,* possibly via FGFR4 activation(Touchberry *et al.* 2013). Thus, activation of cardiac FGFR4 might be required to induce early Ca^{2+} changes that progress to pathologic remodeling including cardiac hypertrophy and fibrosis.

FGF23-induced cardiac hypertrophy has been reported to be reversible *in vitro* and *in vivo* upon removal of the hypertrophic stimulus. A reversal of FGF23-mediated

hypertrophic growth of isolated cardiac myocytes was possible with isoform-specific FGFR4 blocking antibody treatment. FGFR4 inhibition reverses LVH in an animal model of CKD with high FGF23 levels, without any side effects on renal function, tissue calcification, serum phosphate levels, hypertension, and mortality(Grabner *et al.* 2017). This is in contrast with the other studies, where the earlier mentioned side effects were observed with the FGF23 neutralization and pan-FGFR inhibition interventions(Touchberry *et al.* 2013; Yanochko *et al.* 2013). These findings indicate that FGFR4 does not mediate all effects of FGF23, including its physiological actions on the kidney that are mainly mediated by FGFR1 and αKlotho(Liu *et al.* 2008; Gattineni *et al.* 2014).

Thus, studies until now have strongly implicated FGF23 as a causal mechanism for pathological hypertrophy and HF in relation with co-morbidities like CKD and aging. To date, however, no studies have shown that lowering FGF23 improves CVD outcomes in individuals with or without CKD. Whether cardiac FGF23 alone is sufficient to induce cardiac hypertrophy, must be investigated in further studies. The cellular mechanism of αKlotho-independent FGF23 signaling remains unclear. Undoubtedly, future mechanistic studies are required to elucidate the potential direct effects of FGF23 on isolated CMs with respect to Ca^{2+} homeostasis and signaling which are pivotal for LVH and HF.

3. Aims and description of the thesis project

HF is a syndrome of symptomatic cardiac dysfunction with high morbidity and mortality. Left ventricular hypertrophy (LVH) and remodeling is a pivotal adaptation of the heart to stress. Even though these adaptations can be beneficial in the short term, eventually, they activate maladaptive pathways that ultimately lead to HF(Bisping *et al.* 2014). Current HF treatment focuses on inhibiting systemic maladaptive responses, however, fail to target and prevent cellular pathology on the CM level. Although there has been huge research interest, the exact initiatory cellular mechanisms of cardiac remodeling still remain to be elucidated.

Cardiac hypertrophy is one of the important cardiovascular complications in HF patients with CKD. The accompanied LVH in these patients is associated with elevated serum levels of Fibroblast growth factor 23 (FGF23). FGF23 is an endocrine hormone primarily involved in calcium and phosphate metabolism. However, FGF23 also has an effect on CMs via specific receptor tyrosine kinase FGFR4, which mediates hypertrophy(Grabner *et al.* 2015). However, there is a lack of a systematic mechanistic study on how FGF23 induces pathological hypertrophy signaling in CMs.

Early Ca^{2+} homeostasis changes and signaling are important for inducing cellular hypertrophy. It is pivotal to study early Ca^{2+} mediated signaling in LVH. Nuclear Ca^{2+} homeostasis is claimed to be important with respect to maladaptive hypertrophic signaling in CMs(Ljubojević *et al.* 2014). Thus, it is necessary to study the Ca^{2+} mediated early hypertrophic signaling, especially in the nucleus. Not much is known about the FGF23 effect on Ca^{2+} homeostasis, particularly within the nucleus. As well as, potential alterations in hypertrophic cellular mechanisms mediated by FGF23 are still unknown.

Studies until now have strongly associated FGF23 as a causal mechanism for pathological hypertrophy and HF in relation with co-morbidities like CKD. Interestingly, the high circulating level of FGF23 is linked with an altered systemic renin-angiotensin-aldosterone system (RAAS) response, which one of the important systems activated

during LVH(Kovesdy and Quarles 2016). A mechanistic study is required to elucidate the potential direct effects of FGF23 on isolated CMs with respect to pathological Ca^{2+} signaling, which will further bolster novel drug target possibility against hypertrophy in these HF patients.

In this project, we investigate FGF23-mediated maladaptive hypertrophic Ca^{2+}-dependent signaling in ventricular CMs.

Therefore, the aim of my Ph.D. work was:

1. To establish an *in vitro* cell culture model of hypertrophy to study underlying molecular mechanisms.

2. Study the mechanistic effect of novel hypertrophic trigger FGF23 as compared to established hypertrophic triggers like angiotensin II (ATII) and phenylephrine (PE).

3. Study the mechanistic effect of FGF23 on Ca^{2+} homeostasis as compared to established hypertrophic triggers like ATII.

4. To investigate underlying hypertrophic signaling pathways activated by FGF23 in CMs.

The data obtained in this study is published as an original article:

Mhatre, K.N., Wakula, P., Klein, O., Bisping, E., Völkl, J., Pieske, B., and Heinzel, F.R., 2018. Crosstalk between FGF23- and angiotensin II-mediated Ca2+ signaling in pathological cardiac hypertrophy. *Cellular and Molecular Life Sciences*, (0123456789).

In neonatal rat ventricular myocytes (NRVMs) culture, both ATII and FGF23 triggered hypertrophy with respect to cell area and hypertrophic gene expression. FGF23 induced additional Ca^{2+} release from the nuclear envelope, a known mediator of hypertrophic gene activation. Furthermore, FGF23 activates nuclear Ca^{2+}-regulated CaMKII–HDAC4 pathway, similar to ATII. ATII receptor (AT1R) antagonist losartan significantly attenuated

FGF23-induced changes in Ca^{2+} homeostasis and cellular hypertrophy. Interestingly, FGF23 treatment increased intracellular expression and secretion of ATII peptide in NRVMs in a time-dependent manner (Mhatre *et al.* 2018).

Collectively, based on the results obtained in this study, we propose that ATII is one of the mediators of the FGF23 triggered hypertrophic responses. Our results suggest that the local cardiac renin-angiotensin system plays a pathophysiological role in FGF23 action on CMs. FGF23 not only stimulated intracellular ATII production, but also its secretion. Thus, ATII may act as an autocrine ligand able to trigger an IP3-mediated release of Ca^{2+} from perinuclear stores and regulate hypertrophic transcription observed on FGF23 stimulation.

4. Materials and Methods

The part of the Material and Methods section specified below is published as an original article:

Mhatre, K.N., Wakula, P., Klein, O., Bisping, E., Völkl, J., Pieske, B., and Heinzel, F.R., 2018. Crosstalk between FGF23- and angiotensin II-mediated Ca2+ signaling in pathological cardiac hypertrophy. *Cellular and Molecular Life Sciences*, (0123456789).

4.1. Cell culture preparation

The culture of isolated CMs are a vital tool in cardiovascular research but are challenging to prepare and culture. Adult and neonatal ventricular CMs can be isolated and cultured *in vitro* via sequential enzymatic digestion of heart tissue. Adult CMs can be maintained in culture depending on the animal species and culture conditions for about 24-48 hours; in contrast, neonatal ventricular CMs can be maintained in culture for up to two weeks(Pinz *et al.* 2011).

4.1.1. Isolation and culture of Adult rat ventricular cardiomyocytes (ARVMs)

All animal experiments were approved by the local authorities and performed in agreement with the Guidelines for the Care and Use of Laboratory Animals (National Institute of Health, U.S.A.). Ventricular CMs were isolated by a modification of a procedure described previously (Primessnig *et al.* 2016). Wistar rats (3–6 months) were weighed and anesthetized with isoflurane and placed in a polystyrene chamber. Loss of reflexes was verified prior to sacrifice of animal by gluten. The animal was turned on the back and needles were used to fix all extremities to the plate. The skin over the chest was removed while holding it with a pair of tweezers. In order to gain full access to the thorax, a subcostal cut was cranially extended to the left and right. The aorta was grabbed with a forceps and the visibly beating heart was cut out and quickly transferred to a beaker

glass containing an ice-cold Perfusion Solution. After excessive tissue was removed the heart was weighed, then the heart was placed in a Petri dish containing ice-cold Perfusion Solution along with 1mM Ca^{2+}. A syringe with a cannula with an appropriate width was used to cannulate the aorta. The heart was fixed with 5-0 surgical silk to the cannula and flushed with Perfusion Solution with 1mM Ca^{2+}, to remove blood from the myocardium. The needle with the attached heart was removed from the syringe and transferred to a Langendorff-system with a constant flow. It was ensured that no air bubbles had formed between the Langendorff-system and the cannula to avoid ischemia. The heart was perfused at 3ml/min for 4 min at 37°C with oxygenated Perfusion Solution and then followed by Enzyme Solution (Perfusion Solution with Liberase™ (80µg/ml) and Trypsin (0.1%; Life Technologies, Carlsbad, CA, USA) with 0.1 mmol/L $CaCl_2$ added) for 10 to 13 min, depending on the weight of the heart. The heart turns slightly pale, swollen and becomes flaccid due to enzymatic digestion. After the perfusion was stopped, the ventricles were separated from the atria and minced into small pieces with a scissor in perfusion solution containing 10% BSA (to inhibit further digestion) and 0.125mM Ca^{2+}. Mechanical separation of single CMs was carried out by pipetting the cell suspension up and down with three plastic Pasteur pipettes. The opening diameter was decreased from the first to the last pipette to ensure an effective dissociation. The suspension was filtered through a 200µm nylon mesh into a 50ml tube to remove undigested tissue. Viable cells, settled by gravity and formed a cell pellet on the bottom of the tube. After ten minutes, the supernatant was discarded and NT with 0.125mM Ca^{2+} solution was added. Cells were resuspended and given ten minutes to settle again. This procedure was repeated until a final Ca^{2+} concentration of 1.8mM was reached. The procedure yielded 80–90% rod-shaped, quiescent CMs, which were used within 6h after isolation. The ARVMs are cultured in culture medium consisting of M199 GlutaMAX Supplement (Thermo Scientific, Rockford, IL, USA) with 1% Insulin transferrin selenium (ITS-G) (100X), 1% penicillin/streptomycin (100units/ml) (Thermo Scientific, Rockford, IL, USA) and HEPES (10µM). CMs were seeded at a density of 1×10^6cells/ml on laminin-coated cell culture and imaging dishes.

4.1.2. Isolation and culture of neonatal rat ventricular cardiomyocytes (NRVMs)

Neonatal rat ventricular cardiomyocytes (NRVMs) were isolated from 1-3 days old rat pups and cultured for a period of a week as previously described (Bisping *et al.* 2006; Mhatre *et al.* 2018). In short, hearts were excised from neonatal rat pups and placed in ice-cold PBS. Unwanted blood and connective tissues were removed and ventricles were minced into small pieces. Cells were dissociated from the tissue by five rounds of digestion at 37°C for 10-12 min in digestion buffer containing Liberase^{TM} (80µg/ml), Trypsin (0.1%; Life Technologies, Carlsbad, CA, USA) and DNase I (20µg/ml) in 10 µM Ca^{2+}-1X HBSS-buffered solution with constant stirring. The dissociated cells of each round of digestion were treated with 10% horse serum (Life Technologies, Carlsbad, CA, USA) to eliminate fibroblast and further centrifuged. The cell pellets obtained were re-suspended in culture medium containing DMEM-F12 medium (Thermo Scientific, Rockford, IL, USA) with 10% fetal bovine serum (VWR International, PA, USA) to inhibit further digestion, along with 1% penicillin/streptomycin (100units/ml) and kept on ice. Pooled cells were passed through a cell strainer (100µm) and further pre-plated for 1h for CMs enrichment and to remove contaminating fibroblasts. CMs were counted and seeded at a density of 0.5-1×10^6cells/ml on 1% gelatinized cell culture and imaging dishes. CMs were cultured in the above-mentioned culture medium at 37°C in a humidified atmosphere containing 5% CO_2. After 24h, the culture medium was changed to serum-free medium containing 80% DMEM-F12 and 20% M199 GlutaMAX Supplement (Thermo Scientific, Rockford, IL, USA) with 1% penicillin/streptomycin (100units/ml). CMs were cultured under serum-free conditions at least 48h before experiments. The experiments and stimulation were started at day 4 post isolation.

4.2. Nephrectomy rat model

Subtotal (5/6) nephrectomy was carried out as described previously (Primessnig *et al.* 2016). Young male 8 weeks old Wistar rats (HsdRCCHan, Harlan, Italy) with a body weight between 250 and 275 grams underwent subtotal (5/6) nephrectomy (NXT) or sham operation (Sham). Animals were premedicated with the analgetic carprofen (5 mg/kg/BW)

and the antibiotic enrofloxacin (7.5 mg/kg/BW). Rats were anesthetized with 5 % isoflurane (Abbott, Germany) and 1.6 l/min oxygen in an induction chamber for 1-2 minutes and afterward placed on a heated table to maintain body temperature at 37.5°C (rectal probe). Anesthesia was maintained by injection of 400 µl/kg/BW ketamine/xylazine i.p. and reduction to 2 % isoflurane with same oxygen flow rate via an anesthetic mask (spontaneous breathing). Animals were monitored via tail pulse oximetry and regular control of their reflexes. Furthermore, Ringer‘s solution (10 ml/kg/h) was applied through a tail vein cannula and an eye cream (Oleovit, Bayer, Germany) to prevent eye dryness. The surgical procedure was performed in a one-time intervention (4, 5). In a primary step, the left kidney was exposed through a flank incision and decapsulated. Renal vessels were ligated and the kidney was carefully removed. Furthermore, the right kidney was exposed and the two poles and the cortex were quickly removed. In Sham animals, both kidneys were exposed for the same time but left intact. As post-operative analgesia animals received metamizole (40 mg/kg/BW) subcutaneously.

4.3. Real-time quantitative RT-PCR

To investigate upstream hypertrophic signaling pathways, we quantified classical marker genes for cardiac hypertrophy and fibrotic remodeling. ACTA-1 codes for α-actinin, MYH-7, which encodes β-myosin heavy chain, NppB codes for natriuretic peptide BNP and TGF-β as a marker for fibrosis, at an early time points following the hypertrophic triggers. We also measured the calcineurin reporter gene, RCAN-1, which is involved in Ca^{2+}-dependent cardiac hypertrophic signaling(Kreusser *et al.* 2014). After the stimulus, total RNA was isolated from the single wells of the 6-well plates at suitable time-point using the RNeasy Mini Kit (Qiagen, Hilden, Germany), including DNase treatment. Quality and quantity of RNA were assessed with a Nanodrop 1000 spectrophotometer (Thermo Fischer Scientific, Wilmington, DE, USA) and reverse transcription was performed with QuantiTect ReverseTranscription Kit (Qiagen, Hilden, Germany). qPCR was carried out using SYBR Green Mastermix (BIO-RAD) in 10µl total reaction volumes on a LightCycler® 480 Instrument II at optimized thermocycling settings. Relative gene

expression was calculated using the ddCt method, with expression normalized to GAPDH as a reference gene. Each sample was run in triplicates and fold changes were calculated in comparison with corresponding control (untreated ARVMs/NRVMs). Sequences of used primer-oligonucleotides are provided in Table 4.1(Mhatre *et al.* 2018).

4.3.1. GAPDH as an appropriate housekeeping gene

In order, to check the stability of GAPDH in our study setting, we compared the expression of GAPDH to RLP-4, which is commonly used as internal control gene in cardiac hypertrophy gene expression studies(Ruiz-Villalba *et al.* 2017).

Table 4.1 Primer sequences used for RT-PCR (SYBR green method)

Adapted from "Mhatre, K.N., Wakula, P., Klein, O., Bisping, E., Völkl, J., Pieske, B., and Heinzel, F.R., 2018. Crosstalk between FGF23- and angiotensin II-mediated Ca2+ signaling in pathological cardiac hypertrophy. *Cellular and Molecular Life Sciences*, (0123456789)". Copyright 2018 by Springer Nature. Reprinted with permission.

Gene	Forward (5'-3')	Reverse (5'-3')
GAPDH	GCA ACT CCC ATT CTT CCA CCT TT	TAT CCT TGC TGG GCT GGG TG
ACTA-1	AGA GTC AGA GCA GCA GAA ACT AGA	CAC GAT GGA TGG GAA CAC AGC
RCAN-1	AGT CGC TTG GGC TGT GAC GG	AAG AGC CGC AGG CAG AGT CA
TGF-β	GAG GCG GTG CTC GCT TTG T	ATT GCG TTG TTG CGG TCC AC
NppA	AGG GCT TCT TCC TCT TCC TGG	CTT CAT CGG TCT GCT CGC TCA
NppB	AGT CGC TTG GGC TGT GAC GG	AAG AGC CGC AGG CAG AGT CA
RPL-4	CGC CAG GCT AGG AAT CAC AAA	AGC CCC CTT CTC TGG AAC AA

4.4. Ca^{2+} transient measurements:

4.4.1. Ca^{2+} dye loading

Cultured CMs were washed with Normal Tyrode Solution (NT) (1.8mM CaCl2). Cells were loaded with the Ca^{2+} -sensitive fluorescent dye Fluo-4AM (20 μM) (fluo-4/AM; Molecular Probes, Eugene, OR, USA) with pluronic acid in NT and incubated for 30 min in dark at room temperature. After loading, cells were then washed twice with NT for 15mins for de-esterification and used for Ca^{2+} imaging.

4.4.2. Compartmental Ca^{2+} Imaging

Intracellular Ca^{2+} recordings in cytosol and nucleus were performed using a confocal laser scanning microscope (ZEISS LSM 800) that consisted of an inverted microscope equipped with a x40 oil-immersion objective lens (N.A. 1.3). Fluo-4AM was excited by the 488nm light from an argon-ion laser and fluorescence was collected at wavelengths >515 nm. The temporal resolution of the scanning was 0.58 or 0.8ms per line. The confocal line was set to the middle of the nuclei for the recording of the [Ca^{2+}] nucleus, thus ensuring that fluorescence originating only from the nucleoplasm was collected. Cells were field-stimulated via two platinum electrodes at 1 or 5Hz using 5ms pulse with a voltage of 24.2 amplitude. Steady-state CaT was recorded at room temperature(Mhatre *et al.* 2018).

4.4.3. Ca^{2+} transient analysis

4 to 5 consecutive transients in the line scan image were segmented and were averaged using custom-made algorithms coded in IDL (IDL 7.0, ITT Visual Information Solutions, Paris, France) as previously described(Heinzel *et al.* 2008). The amplitude of the [Ca^{2+}]i transient (ΔFpeak) was deduced by normalizing the peak of CaT (F) to F averaged during 30 ms before the onset of the Ca^{2+} transient (F0). Total cytosolic or nuclear Ca^{2+} load during a paced beat was calculated *as* Area under the curve (AUC) as the area under the CaT using Area (mV.ms) function in pCLAMP 10.2 (Molecular Devices, California, USA).

Hypertrophy stimuli, ATII (1 μM; Sigma-Aldrich) or FGF23 (25 ng/ml; R&D Systems) were added to the cells in NT solution. A subset of cardiomyocytes was treated 30 mins with 2-Aminoethoxydiphenyl borate (2-APB, 5-10μM; Sigma-Aldrich), Losartan potassium (1 μM; Sigma-Aldrich), Xestospongin.C. (10μM) or vehicle (DMSO) 30min prior to the agonist stimulation. Frequency and of Ca^{2+} sparks were measured using SparkMaster(Picht *et al.* 2008). The temporal profiles of CaT were then fitted to gamma function to analyze time to peak (TTP), and decrease time to half-maximum (D50) using pCLAMP 10.2.

4.5. Immunocytochemistry (ICC) analysis

4.5.1. Cardiomyocyte size measurements

NRVMs were fixed with methanol/acetone (ratio 1:1, at -20 °C), permeabilized for 5 min with in phosphate-buffered saline (PBS) containing 0.1% Triton X-100 and 0.1% Na-citrate, and blocked with PBS containing 5% Bovine serum albumin for 1 h. Cells were incubated with primary antibody for sarcomeric desmin (mouse monoclonal antibody, 1:50, Dako, catalog no. M0760) for overnight at 4°C in the same solution as blocking solution. Cells were washed three times with PBS, incubated with the secondary AlexaFluor® 488-conjugated antibody (rabbit anti-mouse IgG, dilution 1:1000, Invitrogen) and washed three times with PBS. Nuclei were stained with DAPI (Sigma-Aldrich, catalog no. F6057). NRVMs were visualized with an inverted fluorescence phase-contrast microscope (BZ-9000E, All-in-One fluorescence microscope, Keyence) at a ×20 and ×60 magnification, and images were captured using a digital camera CFI60 (Nikon). Open source Fiji software (ImageJ) (http:// fiji.sc/Fiji) was used to measure the cell. Cell surface area was calculated based on desmin–positive staining (ImageJ)(Mhatre *et al.* 2018).

4.5.2. Intracellular Angiotensin formation

Methanol/acetone fixed NRVMs were co-stained with the anti-desmin antibody (1:50, Dako, catalog no. M0760) and anti-Angiotensin II antibody (1:50, Angiotensin (N-10),

Santa Cruz Biotechnology, catalog no. sc-7419) as specified in protocol above. Along with FGF23 (25ng/ml), we used high glucose (25mM) as a positive control for induction of ATII formation in CMs. Rest of the conditions (Negative control, control, FGF23) were in 10mM glucose medium. Intracellular ATII formation in NRVMs was visualized using confocal laser scanning microscope (ZEISS LSM 800) with a x40 oil-immersion objective lens.

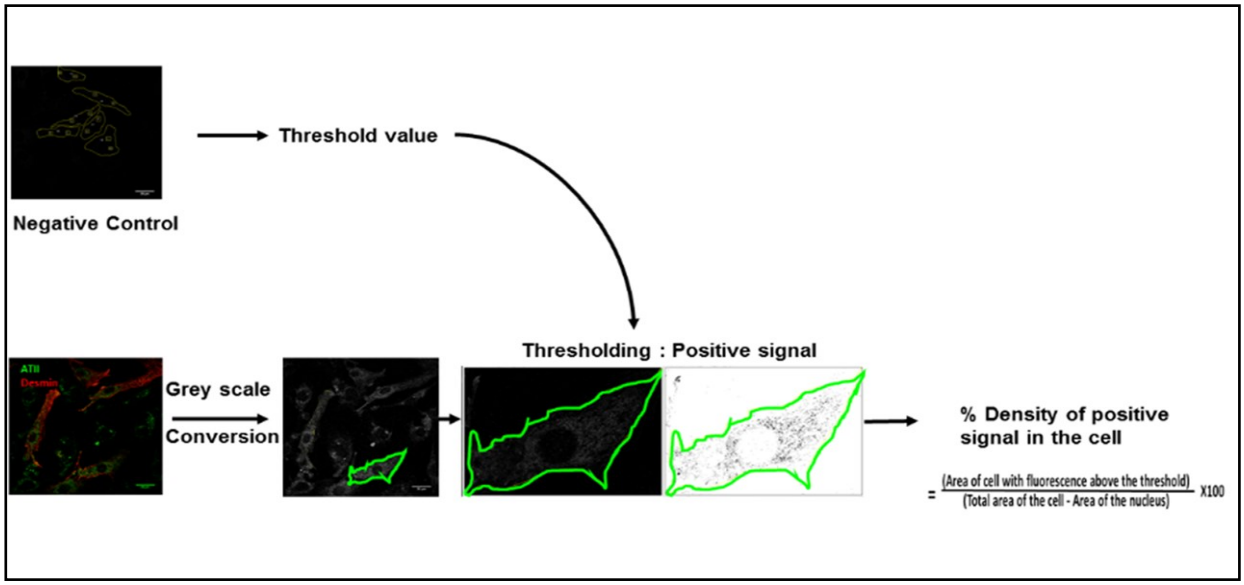

Figure 4.1 Schematic representation of ATII expression analysis in NRVMs.

A field of vision with 2-3 NRVM was chosen. Using confocal microscopy, a z-stack of five adjacent layers was recorded for each view to determine the optimal focus setting for the equatorial plane. Z-stack was recorded with a pixel volume of 0.078 µm in XY and 1.0 µm in Z-axis. Equatorial plane of each of the scanned cardiomyocyte for every condition with identical settings for excitation and detection were analyzed. Images were converted to binary by thresholding with a signal threshold defined as mean + 3 standard deviations of the intracellular intensity in negative controls (without primary antibody). The area with positive signal was normalized to the total area of the cell and corresponding nucleus. Thereby deriving % density of positive signal (Figure 4.1) that is directly proportional to

the cytoplasmic formation of ATII present as measured by the standard area function in the open source Fiji software (ImageJ) (http:// fiji.sc/Fiji).

4.6. Western Immunoblotting

For Western blot analysis, NRVMs from 6-well plate were homogenized at 4°C in 160µl of cell lysis buffer (with freshly added protease inhibitor (PMSF, leupeptin, aprotinin, pepstatin A). Lysates were run on 4–12% Bis-Tris polyacrylamide gels and transferred to nitrocellulose membranes for 2 h. Proteins on the membrane were stained with Ponceau S. The signal was detected with the Odyssey CLx System. The band intensities were determined by Image Studio software (LI-COR, Nebraska, USA).

4.6.1. PLC-γ phosphorylation

Non-specific binding was blocked with 5% powdered milk in Tris-buffered saline (pH 7.4) containing 0.1% Tween-20. Lysates were analyzed by immunoblotting using antibodies against phospho-PLC-γ (Tyr783) and total- PLC-γ (Cell Signaling Technologies, Massachusetts, USA). Respective secondary antibody Goat anti-rabbit IRDye 680RD (LI-COR, Nebraska, USA) was used. The fluorescence was detected using the LI-COR Odyssey® CLx Imaging System.

4.6.2. HDAC-4 phosphorylation

Non-specific binding was blocked with 3% Bovine serum albumin in Tris-buffered saline (pH 7.4) containing 0.1% Tween-20. Membranes were probed with anti-HDAC4 phosphoS632 and anti-HDAC4 (Abcam, Cambridge, USA) sequentially, overnight at 4 °C. Anti-rabbit IgG linked with IRDye 800CW (pHDACS632) and anti-rabbit linked with 680RD (HDAC-4) (LI-COR, Nebraska, USA) were used as a secondary antibody(Mhatre *et al.* 2018).

4.7. BNP ELISA

BNP ELISA was performed according to the manufacturer's protocol (KA0979, Abnova, Taiwan) with a 1:2 dilution of the samples.

4.8. Mass Spectrometry

4.8.1. Sample Preparation

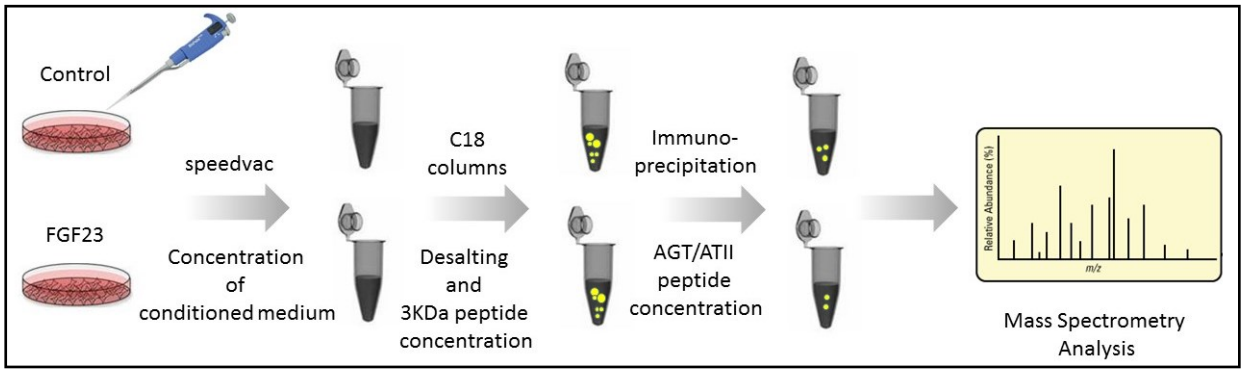

Figure 4.2 Work-flow of sample processing for Mass spectrometry analysis of ATII peptide in conditioned medium.

Proteins are indicated as yellow

Supernatants (12ml) were first dried in a speedvac (Eppendorf, Hamburg, Germany) and resuspended in 1 ml 0.1%TFA. Next, these 100µl sample solution was desalted and peptides concentrated by using ZipTip (C18) according to the standard manufacturer protocol (Merck Millipore, Billerica, MA, USA). Thus, samples got concentrated and desalted using 3kDa molecular weight cut-off spin-filter columns to remove the very abundant albumin and immunoglobulins, so that these proteins would not hinder analysis of less abundant protein of interest. Subsequently, the sample was concentrated if required specifically for ATII using immunoprecipitation using ATII antibody.

4.8.2. MALDI-TOF/TOF analysis

The resulting peptide mixtures were then spotted on one 384-anchor-containing MALDI AnchorChip targets (Bruker Daltonic, Bremen, Germany) and mixed with a 1µl matrix solution and analyzed. MALDI-IMS data acquisition was performed in positive ion reflector

mode on an Autoflex III MALDI-TOF/TOF using flexControl 3.0 software (Bruker Daltonic). Measurement settings were as follows: detection range of m/z 800–3000, 200 laser shots per spot, the sampling rate of 2.0GS/s(Mhatre *et al.* 2018).

4.9. Solutions and chemicals

All chemicals were obtained from Sigma-Aldrich (St. Louis, MO, USA) unless noted otherwise. Perfusion Solution in mmol/L: 130 NaCl, 5 KCl, 0.5 MgCl2, 0.33 NaH2PO4, 22 Glucose, 5 Glutamine, 25 HEPES; pH adjusted to 7.4 with NaOH. Normal Tyrode solution (NT) contained (in mM): 130 NaCl, 4 KCl, 1.8 CaCl2, 1 MgCl2, 10 D-glucose, 10 HEPES; pH 7.4 with NaOH. Cell lysis buffer (in mM): 20 Tris pH 7.5, 150 NaCl, 1 Na2EDTA pH8, 1 EGTA pH7, 1% Triton, 2.5 Na4P2O7, 1 Na3VO4, 1 β-glycerophosphate). Matrix solution contained: 1ml 7g/L a-cyano-4-hydroxycinnamic acid (Bruker Daltonic) in 50% acetonitrile (Fluka, St. Louis, USA) and 1% trifluoroacetic acid (spectroscopy purity, Merck, Darmstadt, Germany)(Mhatre *et al.* 2018).

4.10. Statistical analysis

Primary cell culture experiments were conducted on 3-5 independent cell culture isolates obtained on different days with technical replicates. The appropriate statistical analysis was performed using paired or unpaired t-test or Mann-Whitney U test (for 2 groups), ANOVA or Kruskal–Wallis followed by Bonferroni or Dunn's test for multiple comparisons (for 3 or more groups). Chi-square test was used to compare nuclear spark incidence between the treatment groups. Statistical tests were performed using SPSS (IBM SPSS Statistics for Windows, Version 23.0. Armonk, NY: IBM Corp, USA). Results are reported as a mean ± standard error of the mean (SEM) or Standard deviation (SD), and a P value <0.05 was considered significant. N is the number of independent isolations, and n is the number of individual cells analyzed(Mhatre *et al.* 2018).

5. Results

The part of the Result section specified below is published as an original article:

Mhatre, K.N., Wakula, P., Klein, O., Bisping, E., Völkl, J., Pieske, B., and Heinzel, F.R., 2018. Crosstalk between FGF23- and angiotensin II-mediated Ca2+ signaling in pathological cardiac hypertrophy. *Cellular and Molecular Life Sciences*, (0123456789).

5.1. Establishment of a hypertrophy *in vitro* cell culture model

We were successful in culturing freshly Isolated ARVMs from adult Wistar rats for 48h in our culture conditions. Percentage viability was measured at different timepoints Day0, Day1 (24h) and Day2 (48h). There was a considerable decrease in viability with an increase in the culture days (Figure 5.1A, B, C). Also, there was visible de-differentiation with respect to the cell morphology, rounding of the sarcolemma, loss of t-tubule etc.(Louch *et al.* 2015). As a marker for hypertrophy, we checked the cell size and fetal (hypertrophic) gene response in the ARVM cell culture model.

5.1.1. ATII and PE do not have any effect on cell size in ARVMs

We used standard hypertrophy triggers to induce hypertrophy in our cell culture. ATII, a neurohormone is a strong hypertrophy and hypertension stimulus (Ljubojević *et al.* 2014). β-adrenergic receptor agonist PE was used as a comparative stimulus which is known to trigger hypertrophy via PKC pathway(Schreckenberg *et al.* 2004).

PE (10μM) significantly decrease the viability at day 1 and day 2 as compared to ATII (250nM) and untreated cells (Figure 5.1B, C). This can be explained by the possible trigger of apoptosis by independent pathways induced by PE(Heger *et al.* 2009). We measured the cell size of the ARVMs after treatment with ATII (250nM) and PE (10μM) at different time points Day0, Day1 (24h) and Day2 (48h) as a read-out of hypertrophy.

As seen in Figure 5.1D, there was no significant difference between the groups at all the time points.

5.1.2. No significant effect of treatment of ATII and PE on hypertrophic gene expression in ARVMs

The gene expression for pro-hypertrophic marker genes was studied as a second hypertrophy read-out in ARVM cell culture. Gene expression was measured at 24h with

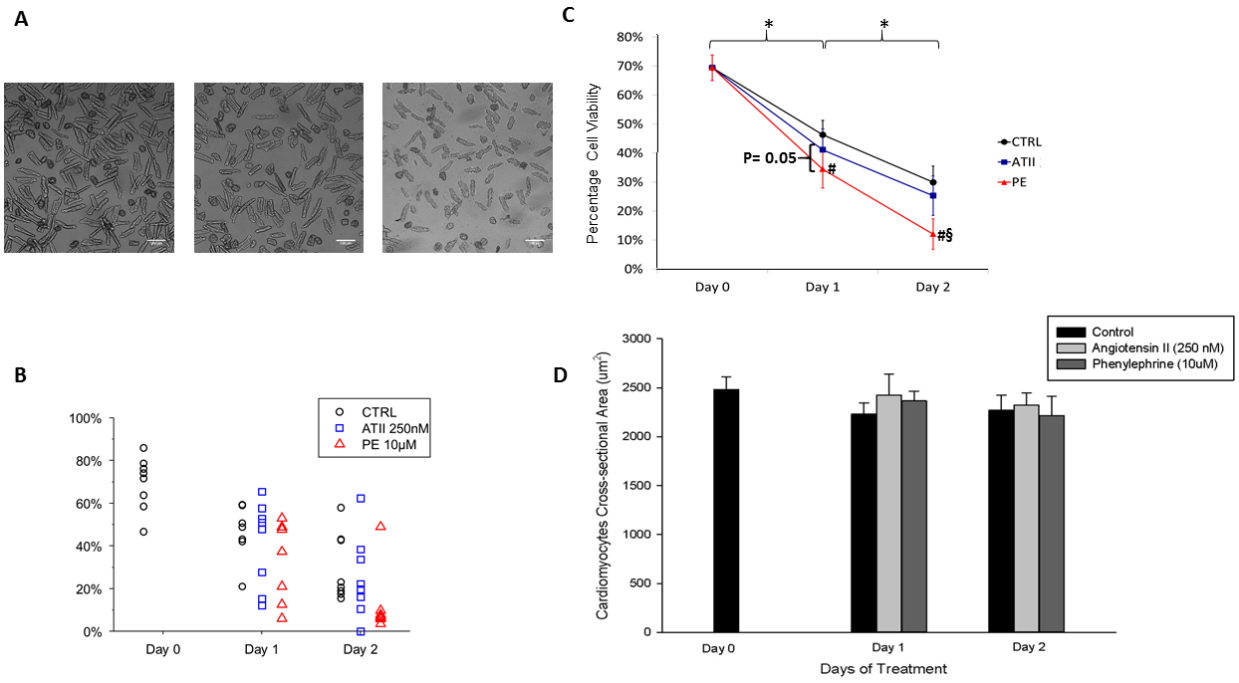

Figure 5.1 Effect of ATII (250nM) and PE (10µM) on cell size of ARVMs

A Bright field images of ARVMs at timepoint day 0 (right), day 1 (middle) and day 2 (left). The scale bar denotes 100µm. **B** Percentage cell viability at different timepoints of ARVMs after ATII (250nM, blue) and PE (10µM, red) treatment vs. (CTRL) vehicle-treated control cells. (mean±SEM; n>6 Isolations for each timepoint and treatment; *P<0.05, #§P=0.05; Kruskal-Wallis followed by Dunn's test). **C** Dot blot showing percentage cell viability of individual isolation at different timepoints of ARVMs after ATII (250nM, blue) and PE (10µM, red) treatment vs. (CTRL) vehicle-treated control cells. **D** The bar graph (below) represents cross sectional area of ARVMs in ATII (250nM, light grey) and PE (10µM, dark grey) treatment group at different timepoint compared to corresponding vehicle-treated control (black) group.

ATII (1μM) and PE (10μM) treatment. At 250nM, the concentration of ATII did not show any hypertrophic effect on ARVMs with cell size as readout (Figure 5.1D). Hence, a higher concentration of 1μM was used for the gene expression study. Only MYH-7 showed a significant increase in expression for 2-folds with ATII (1μM) and 2.3 folds with PE (10μM) treatment at 24h (Figure 5.2A, B). The remaining genes (ACTA-1, NPPB, RCAN-1) did not show any significant change in expression at 24h with both the treatments.

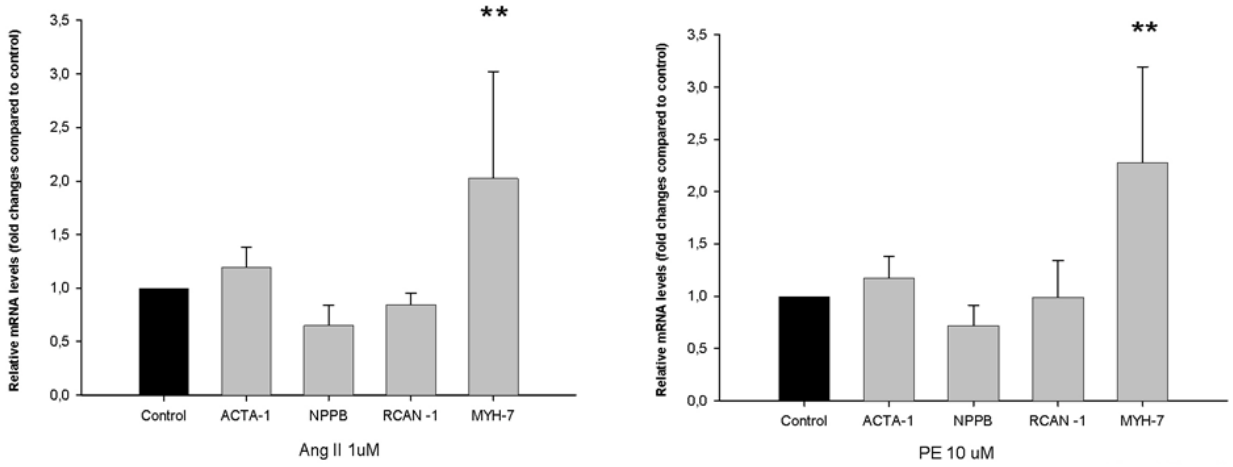

Figure 5.2 Effect of ATII (1μM) and PE (10μM) at 24h timepoint on hypertrophic gene expression in ARVMs

Compared to control cells (black), expression of genes ACTA-1, NPPB, RCAN-1 and MYH-7 at 24h of ATII treatment (bar graph in left) (grey). In bar graph on right**,** Compared to control cells (black), expression of genes ACTA-1, NPPB, RCAN-1 and MYH-7 at 24h of PE treatment (grey).(mean±SEM; N=3 independent isolations quantified by RT-PCR normalized to GAPDH gene expression; **P<0.01, compared with corresponding control; unpaired t-test or Mann-Whitney U test).

As the effect of these triggers on hypertrophy genes is transient, we measured the effect of ATII (1μM) on all the genes acutely at time points 20mins, 2h, and 6h. Only TGF-β showed a significant increase in the 2h treatment of ATII which returned to basal levels at 6h (Figure 5.3).

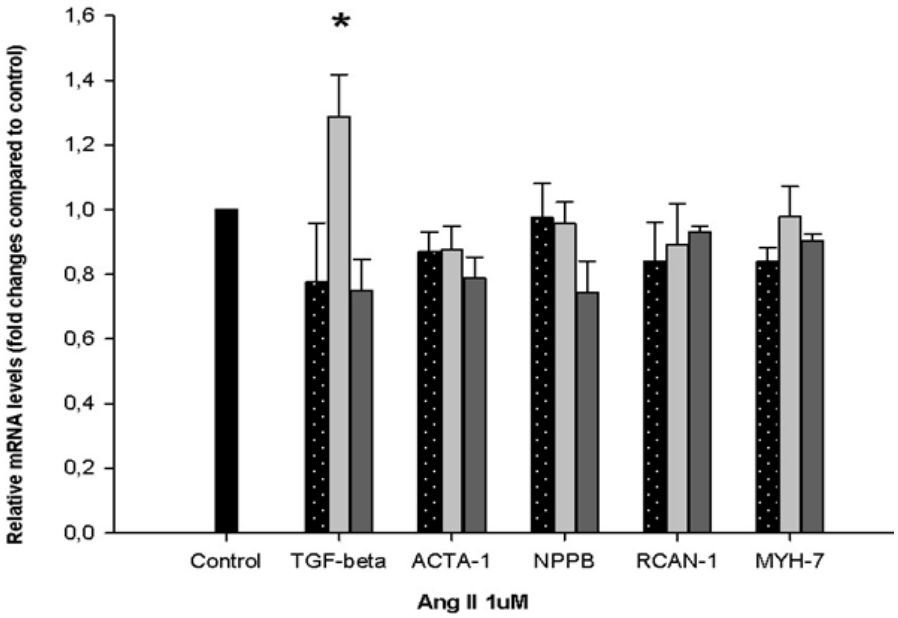

Figure 5.3 Effect of ATII (1μM) at 20mins, 2hrs, 6hrs timepoint on hypertrophic gene expression in ARVMs

Compared to control cells (black), expression of genes TGF-beta, ACTA-1, NPPB, RCAN-1 and MYH-7 at 20mins (patterned), 2hrs (light grey), 6hrs (dark grey) of ATII treatment.(mean±SEM; N=3 independent isolations quantified by RT-PCR normalized to GAPDH gene expression; *P<0.05, compared with corresponding control; unpaired t-test or Mann-Whitney U test).

5.1.3. Acute treatment of ATII and FGF23 did not have any effect on Ca^{2+} transient of 1Hz and 5Hz stimulated ARVMs

Treatment of ARVMs with ATII or FGF23 did not induce cellular hypertrophy with respect to hypertrophic marker gene expression and cell size. We further tried to elucidate whether these hypertrophic triggers have an early effect on Ca^{2+} homeostasis of ARVMs. Ca^{2+} imaging protocol was followed as shown schematically in Figure 5.4.

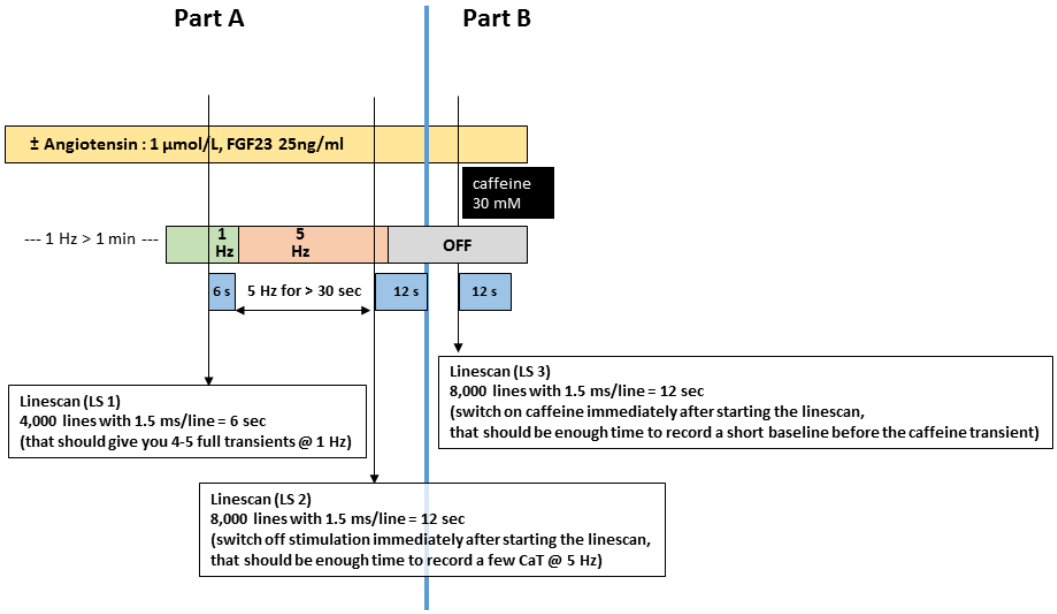

Figure 5.4 Ca^{2+} imaging protocol for studying effect of ATII (1uM) and FGF23 (25ng/ml) on CaT of ARVMs paced at 1z and 5 Hz.

In CMs an increase in stimulation frequency can cause increases in diastolic and systolic [Ca^{2+}]. Since there is distinctly slower kinetics of nucleoplasmic CaTs as compared to cytoplasmic CaTs, an increase in stimulation frequency affected [Ca^{2+}]nuclear and [Ca^{2+}]cytoplasmic differentially, in particular, the diastolic [Ca^{2+}].

Thus, an increase in stimulation frequency may be sufficient for the differential regulation of diastolic[Ca^{2+}] in the nucleus vs. cytoplasm(Ljubojević *et al.* 2014). We included 5Hz along with 1Hz stimulation frequency to study the effect of triggers on CaT in cytosolic and nuclear compartment. The original recording of a typical CaT is illustrated in Figure 5.5.

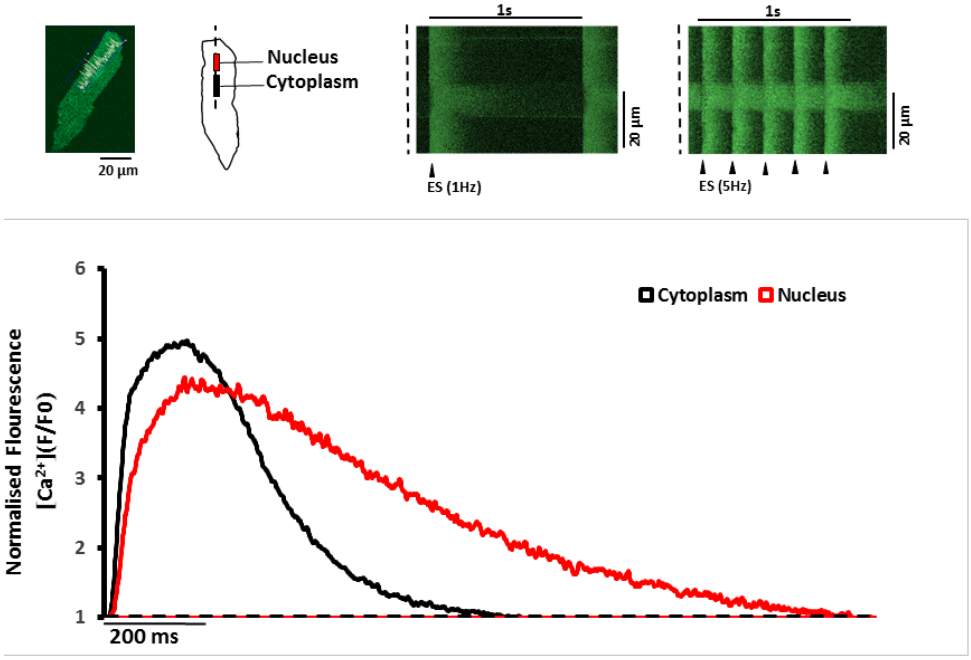

Figure 5.5 Electrical Stimulation (ES) protocol (above) and representative CaT (below) of ARVMs paced at 1Hz with black trace constituting cytoplasmic CaT and red trace indicating nuclear CaT.

As expected, an increase in diastolic calcium F0 was observed in all the treatment groups on 5Hz stimulation as compared to 1Hz. In addition, there was enhanced the increase in the nucleus as compared to the cytoplasm in all the groups.

Moreover, both ATII (trend), as well as FGF23, significantly increased F0 in the cytoplasm as well as a nucleus at 1Hz and more heightened at 5Hz (Figure 5.6A, B).

We normalized nuclear F0 to corresponding cytoplasm value (F0 Nuc/Cyt) in order to detect any nucleus-specific changes. However, no alterations of F0 Nuc/Cyt was observed in all the groups at a stimulation frequency of 1Hz and 5Hz (Figure 5.6C, D).

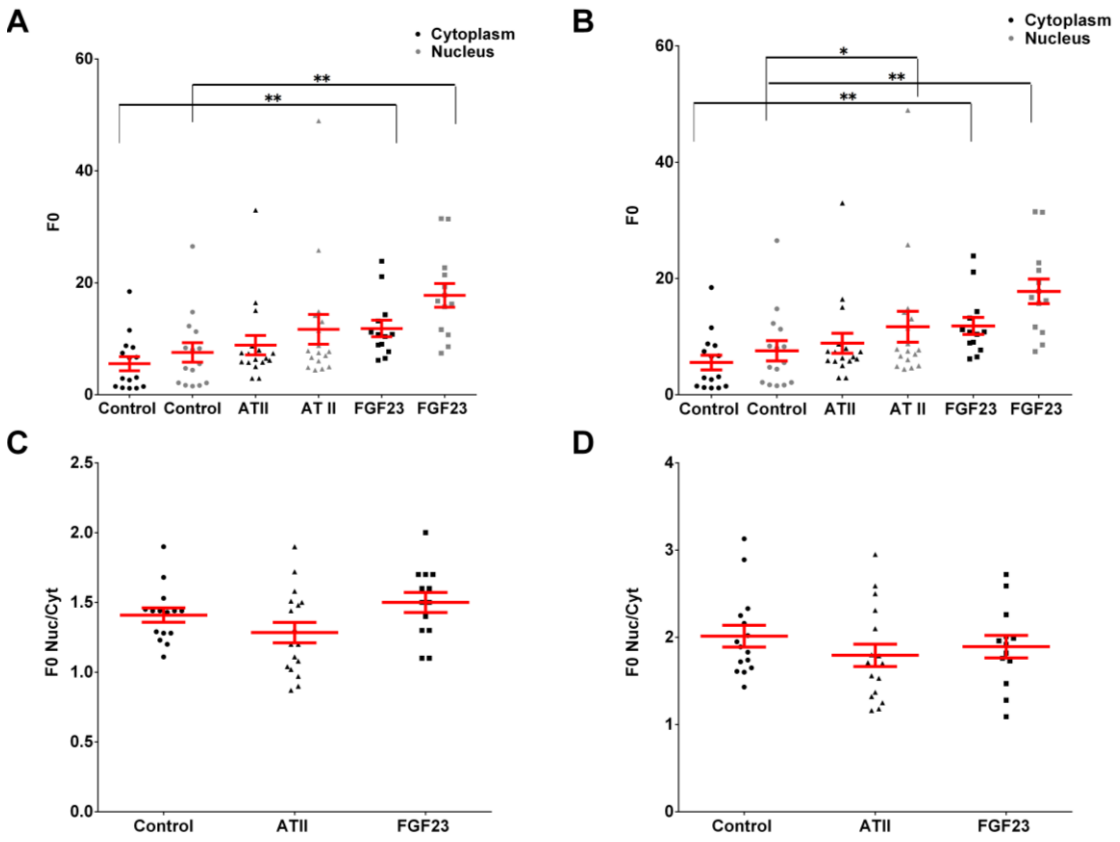

Figure 5.6 Effect of acute treatment of ATII (1µM) and FGF23 (25ng/ml) on F0 of CaT of ARVMs paced at 1Hz and 5 Hz.

A F0 of CaT in ARVMs paced at 1Hz after ATII (triangle) and FGF23 (square) treatment vs. control NRVMs (circle) for 15-90mins in the cytoplasm (black) and in the nucleus (grey). **B** F0 of CaT in ARVMs paced at 1Hz after ATII (triangle) and FGF23 (square) treatment vs. control NRVMs (circle) for 15-90mins in the cytoplasm (black) and in the nucleus (grey). **C** Effect of ATII and FGF23 on F0 in nucleus normalized to corresponding cytoplasmic F0 (F0 Nuc/Cyt) in ARVMs paced at 1Hz **D** and 5Hz (each symbol represents 1 cell; mean±SEM; n>15 cells for each group and region; N=3 isolations of NRVMs; *P<0.05, **P<0.01, compared with corresponding vehicle-treated control; Kruskal-Wallis followed by Dunn's test).

Here single-wavelength indicators were used to measure relative changes in Ca^{2+} concentration between different treatments. A simple approach to correct for uneven

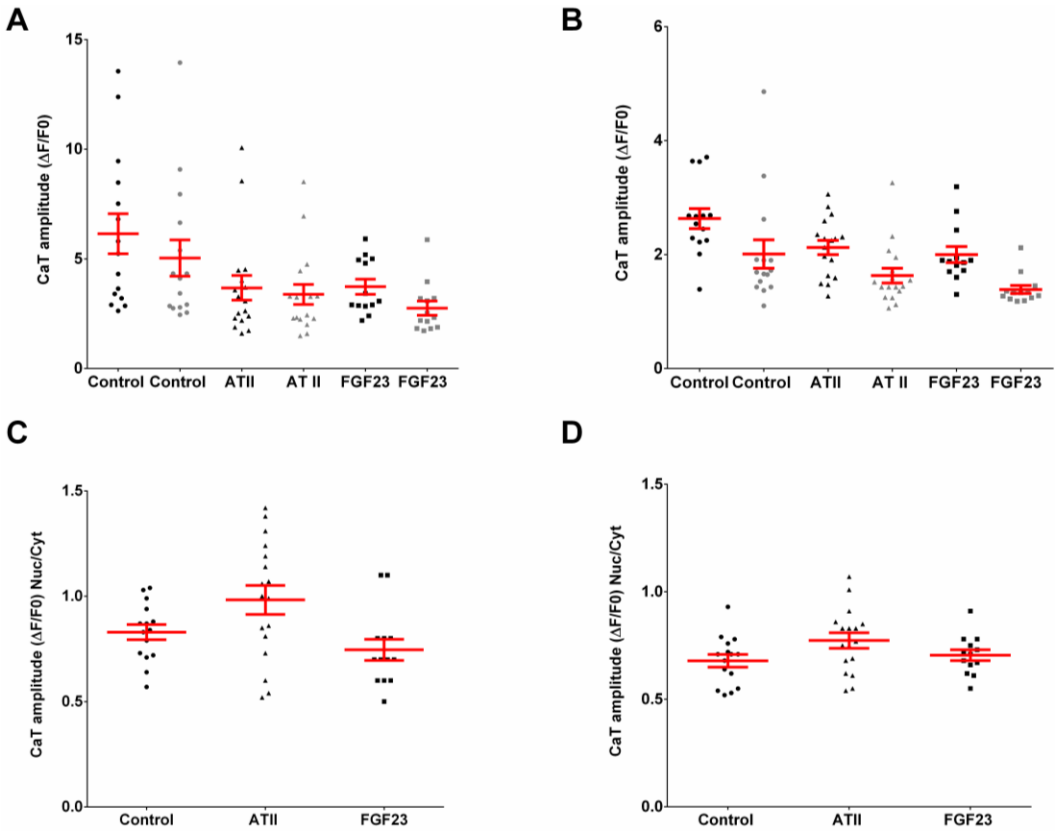

Figure 5.7 Effect of acute treatment of ATII (1µM) and FGF23 (25ng/ml) on ΔF/F0 of CaT of ARVMs paced at 1Hz and 5 Hz.

A ΔF/F0 of CaT in ARVMs paced at 1Hz B and at 5Hz after ATII (triangle) and FGF23 (square) treatment vs. control NRVMs (circle) for 15-90mins in the cytoplasm (black) and in the nucleus (grey). **C** Effect of ATII and FGF23 on ΔF/F0 in nucleus normalized to corresponding cytoplasmic ΔF/F0 (ΔF/F0 Nuc/Cyt) in ARVMs paced at 1Hz **D** and 5Hz (each symbol represents 1 cell; mean±SEM; n>15 cells for each group and region; N=3 isolations of NRVMs; *P<0.05, **P<0.01, compared with corresponding vehicle-treated control; Kruskal-Wallis followed by Dunn's test).

indicator loading is to express the fluorescence signal relative to the lowest fluorescence signal before Ca release (F0) (Kockskämper *et al.* 2008a). This CaT peak amplitude is denoted as ΔF/F0 (change in fluorescence).

In adult cardiomyocytes, there was no significant difference between the treatment and control groups with respect to CaT amplitude in both cytoplasm and nucleus at 1Hz (Figure 5.7A) and 5Hz (Figure 5.7B). The ratio of CaT peak amplitude

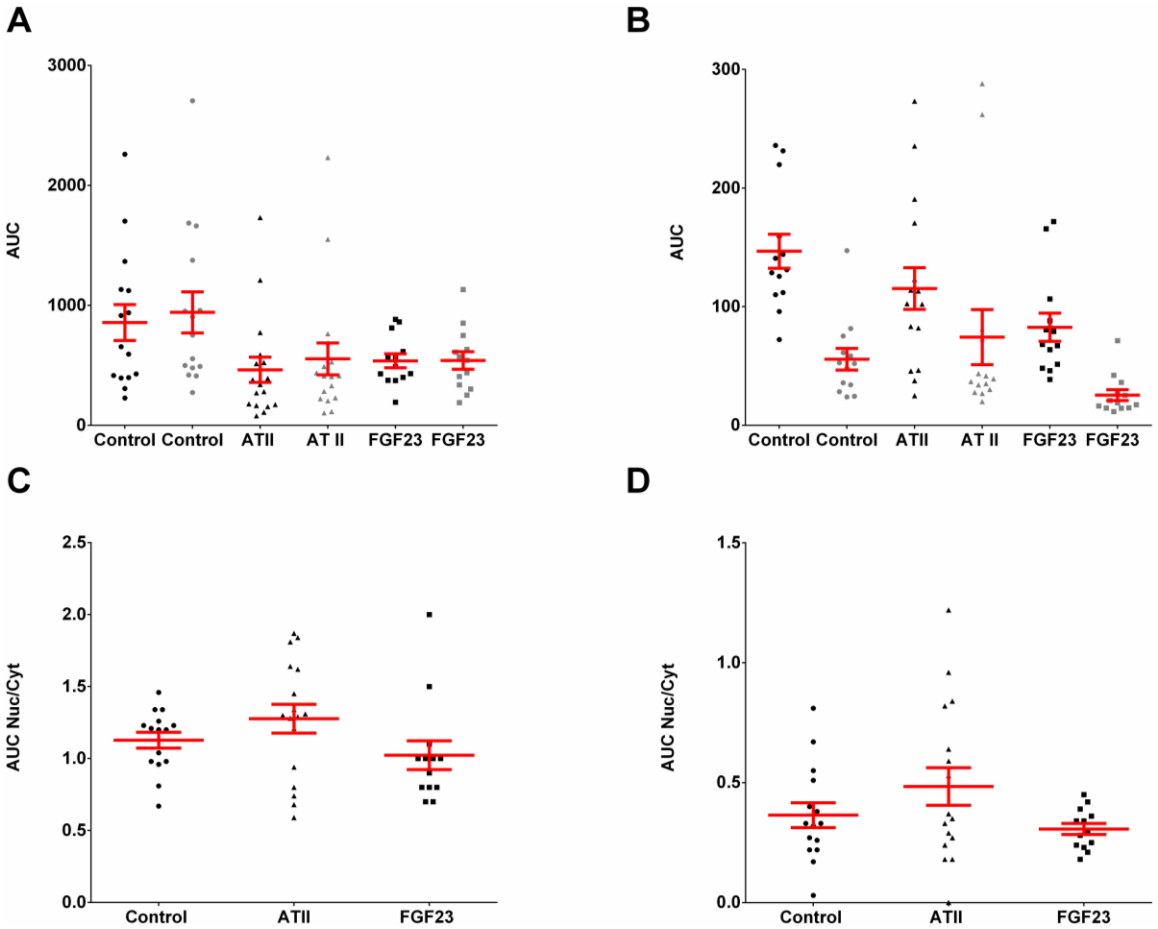

Figure 5.8 Effect of acute treatment of ATII (1μM) and FGF23 (25ng/ml) on AUC of CaT of ARVMs paced at 1Hz and 5 Hz.

A AUC of CaT in ARVMs paced at 1Hz after ATII (triangle) and FGF23 (square) treatment vs. control NRVMs (circle) for 15-90mins in the cytoplasm (black) and in the nucleus (grey). **B** AUC of CaT in ARVMs paced at 1Hz after ATII (triangle) and FGF23 (square) treatment vs. control NRVMs (circle) for 15-90mins in the cytoplasm (black) and in the nucleus (grey). **C** Effect of ATII and FGF23 on AUC in nucleus normalized to corresponding cytoplasmic AUC (AUC Nuc/Cyt) in ARVMs paced at 1Hz **B** and 5Hz (each symbol represents 1 cell; mean±SEM; n>15 cells for each group and region; N=3 isolations of NRVMs; *P<0.05, **P<0.01, compared with corresponding vehicle-treated control; Kruskal-Wallis followed by Dunn's test).

also did not show any nuclear specific changes at 1Hz (Figure 5.7C) and 5Hz (Figure 5.7D).

The AUC of the CaT is a function of the total intracellular Ca^{2+} exposure during one Ca^{2+} cycle and depends not only on the CaT amplitude but also on the Ca^{2+} release and decay kinetics. The AUC remained unchanged for both the treatment in both cytoplasm and nucleus at both the frequencies in ARVMs (Figure 5.8).

In conclusion, both ATII and FGF23 did not have any significant effect on a Ca^{2+} transient in ARVMs. This result is in line with the lack of downstream hypertrophic response of ARVMs to the chronic treatment of ATII.

5.1.4. Study of FGF23/FGFR expression in Nephrectomy rat model

In parallel with ARVM experiments, we studied FGF23 in a CKD rat model. CKD was induced in rats by 5/6 nephrectomy as mentioned in methods. Along CKD, 5/6 nephrectomy (NXT) is also a good model of HFpEF with early induction of cellular hypertrophy at the early time point of 8 weeks post-operation(Primessnig *et al.* 2016). In addition, NXT rats have increase FGF23 serum levels after induction as compared to sham-operated (SOP) rats(Di Marco *et al.* 2014).

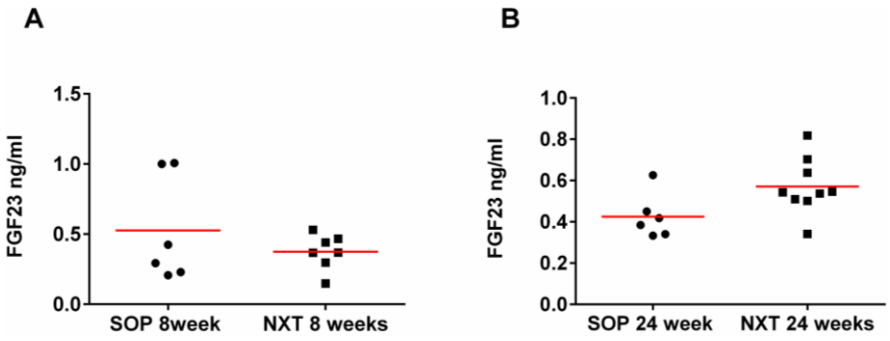

Figure 5.9 FGF23 serum concentration in Nephrectomy rats (NXT) at 8 and 24 weeks timepoint post-operation vs Sham operated rats (SOP)

A FGF23 serum lev els in ng/ml in NXT and SOP rats at 8 weeks (left) and **B** 24 weeks (right) time point post-operation. (red line denotes mean; N≥6 rats per group, quantified by EMD Millipore ELISA).

We measured the FGF23 serum levels in NXT vs SOP rats at 8 weeks and 24 weeks. However, there was no significant difference in the FGF23 levels between both the groups at these time-points (Figure 5.9A, B).

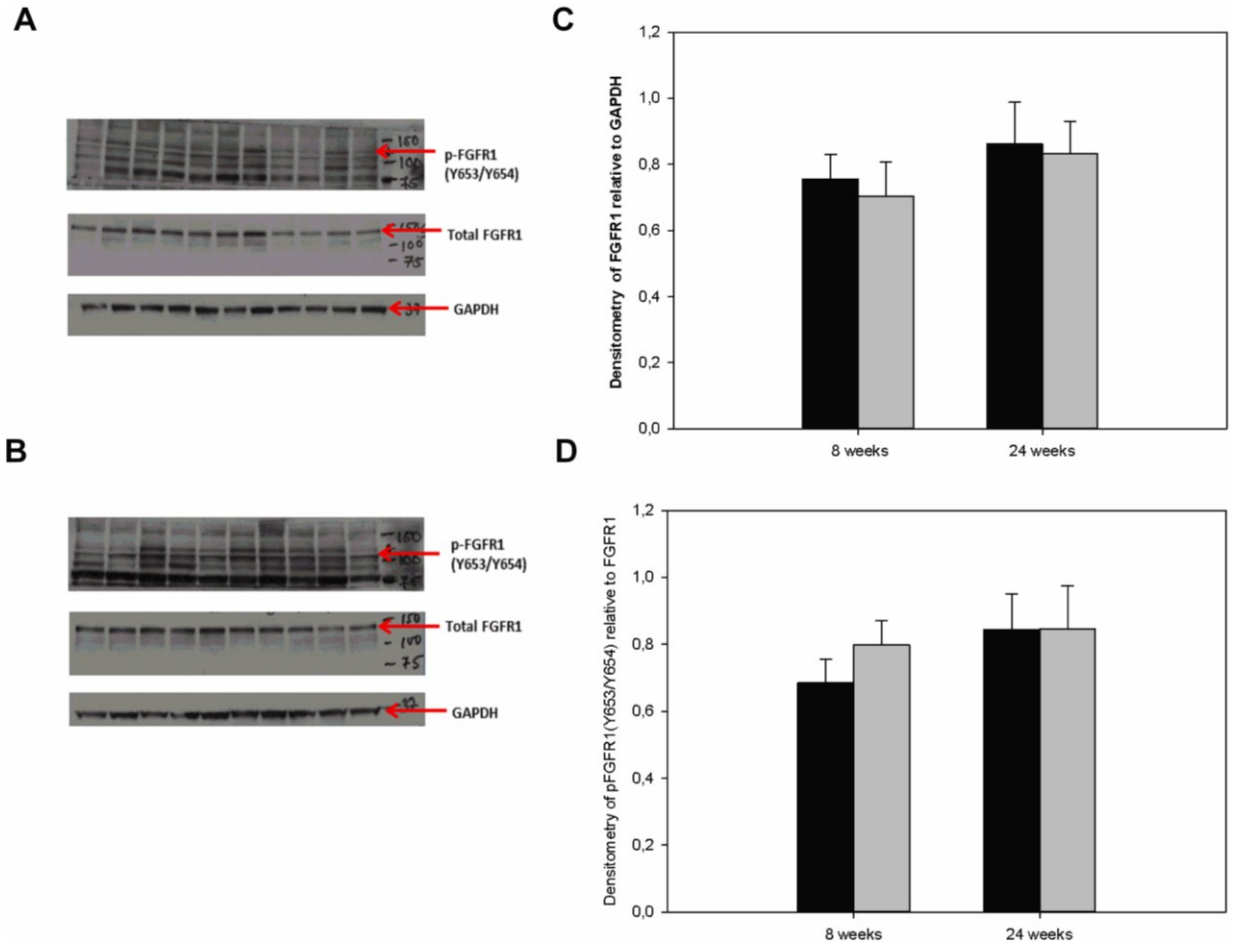

Figure 5.10 Level of FGFR1 expression and phosphorylation in LV samples of Nephrectomy rats (NXT) at 8 and 24 weeks timepoint post-operation vs Sham operated rats (SOP)

A Immunoblot of FGFR1 (130kDa) and pFGFR1 at at site (Tyr653/Tyr654) present in LV samples of NXT rats vs SOP (mixed) at 8 and **B** 24 week's time point post-operation. GAPDH is used as a loading control **C** Bar graphs derived from the immunoblot (left) in NXT (grey) vs. SOP (black) at 8 and 24 week's time point depicting the FGFR1 levels normalized to GAPDH **D** Phosphorylation levels of FGFR1 at site (Tyr653/Tyr654) normalized to FGFR1 (N≥6 rats per group).

We further studied the expression of the FGF23 specific receptor (FGFR1) and its phosphorylation levels at the site (Tyr653/Tyr654) involved in PLC-γ activation, which is involved in the further hypertrophic signaling(Grabner *et al.* 2015). There was no change in the expression of FGFR1 expression in LV myocardium both the groups at 8 and 24 weeks after nephrectomy (Figure 5.10C). While a trend ($p<0.2$) of increase in phosphorylation at the site (Tyr653/Tyr654) was observed at 8-week samples (Figure 5.10D).

5.2. Hypertrophy induced in NRVMs by Angiotensin and FGF23

5.2.1. FGF23 and ATII induced an increase of cell size in NRVMs

Here, we compared the response of isolated neonatal rat ventricular cardiomyocytes (NRVMs) to 48 hours of treatment with FGF23 or ATII at concentrations that induced hypertrophy in previous studies (Fig. 6). We immunostained the cells with sarcomeric protein desmin to differentiate CMs from fibroblast (). A significant increase in cell surface area in response to ATII (46.8±2.6%; $P<0.01$) and FGF23 (37.4±2.5%; $P<0.01$) treatment respectively was observed as compared to control cells from 5 independent isolations with >1000 cells analyzed per conditions (Figure 5.11B, C, D).

5.2.2. Treatment of FGF23 and ATII triggered hypertrophic gene expression in NRVMs

Since the findings of 48h stimulus suggest induction of hypertrophic growth of NRVMs, we used RT-PCR analysis to compare the expression levels of pro-hypertrophic gene markers of pathological cardiac hypertrophy. To investigate upstream hypertrophic signaling pathways, we quantified the classical target genes for cardiac hypertrophy and fibrotic remodeling, ACTA-1, natriuretic peptides NPPA and NPPB and TGF-β, at an early time point following the hypertrophic triggers. We also measured the calcineurin reporter gene, RCAN-1, which is involved in Ca^{2+}-dependent cardiac hypertrophic signaling(Kreusser *et al.* 2014). To match acute experimental conditions, we chose an

early time point (1-3h) as well as 24h to investigate changes in mRNA expression of marker genes.

Cellular hypertrophy was reflected by augmented expression of the hypertrophic genes with ATII treatment of 1h. ATII significantly increased ACTA-1 (1.98 ± 0.12fold) and RCAN-1 (1.91±0.09fold) gene expression (Figure 5.12A, B).

Whereas acute treatment of FGF23 induced a significant increase in expression of (Figure 5.12A, C) ACTA-1 (5.2±1.99fold; $p \leq 0.05$) while the trend of increase in RCAN-1 (2.42±0.62 fold; $p=0.07$) at the 6h time point. Thus similar to ATII, cellular hypertrophy was reflected by increased expression of hypertrophic genes induced by FGF23 (Figure 5.12A).

Furthermore, we also analyzed gene expression levels of natriuretic peptides ANP and BNP along with ACTA1, RCAN1, and TGF-β at 5-time points from 1-24h with FGF23, ATII, and phenylephrine (PE) treatment. FGF23, ATII, and PE-induced upregulation of gene expression with respect to selected marker genes, albeit at different time points (Figure 5.12A). These results suggest, like ATII, FGF23 might activate similar transcription factors to upregulate similar hypertrophic gene programs.

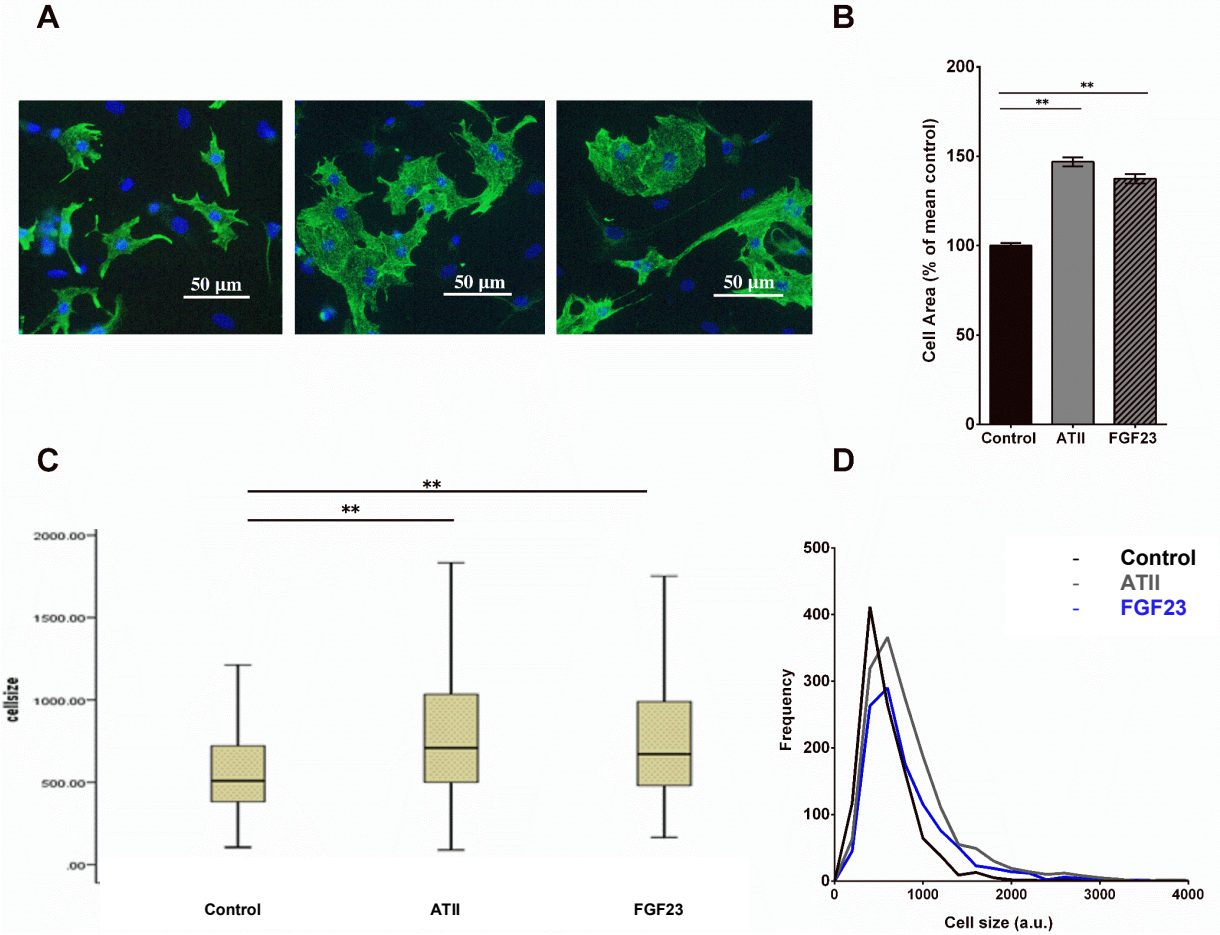

Figure 5.11 Effect of treatment of ATII (1µM) and FGF23 (25ng/ml) on NRVMs cell size recorded at 48h time point

A Representative images of isolated NRVMs after 48h treatment ATII and FGF23, as revealed by immuno-cytochemical analysis using antibodies to cardiomyocyte-specific Desmin (green) and DAPI (blue) used to identify nuclei (scale bar: 50µm). **B** The bar graph shows relative percentage change which was analyzed compared with that of vehicle-treated control cells (black) for 48 hours of treatment of NRVMs with ATII (grey) and FGF23 (pattern) (mean±SEM; n=5 independent isolations; n>1000 cells per group; **P<0.01, compared with control cells; Kruskal-Wallis followed by Dunn's test).**C** Box and whisker plot of cell size (a.u.); the black line across each box represents the median and box limits indicate 25th and 75th percentile **D** The frequency map of cell size (a.u) of NRVMs in all treatment groups.

The figure is adapted from "Mhatre, K.N., Wakula, P., Klein, O., Bisping, E., Völkl, J., Pieske, B., and Heinzel, F.R., 2018. Crosstalk between FGF23- and angiotensin II-mediated Ca2+ signaling in pathological cardiac hypertrophy. *Cellular and Molecular Life Sciences*, (0123456789). Copyright 2018 by Springer Nature. Reprinted with permission.

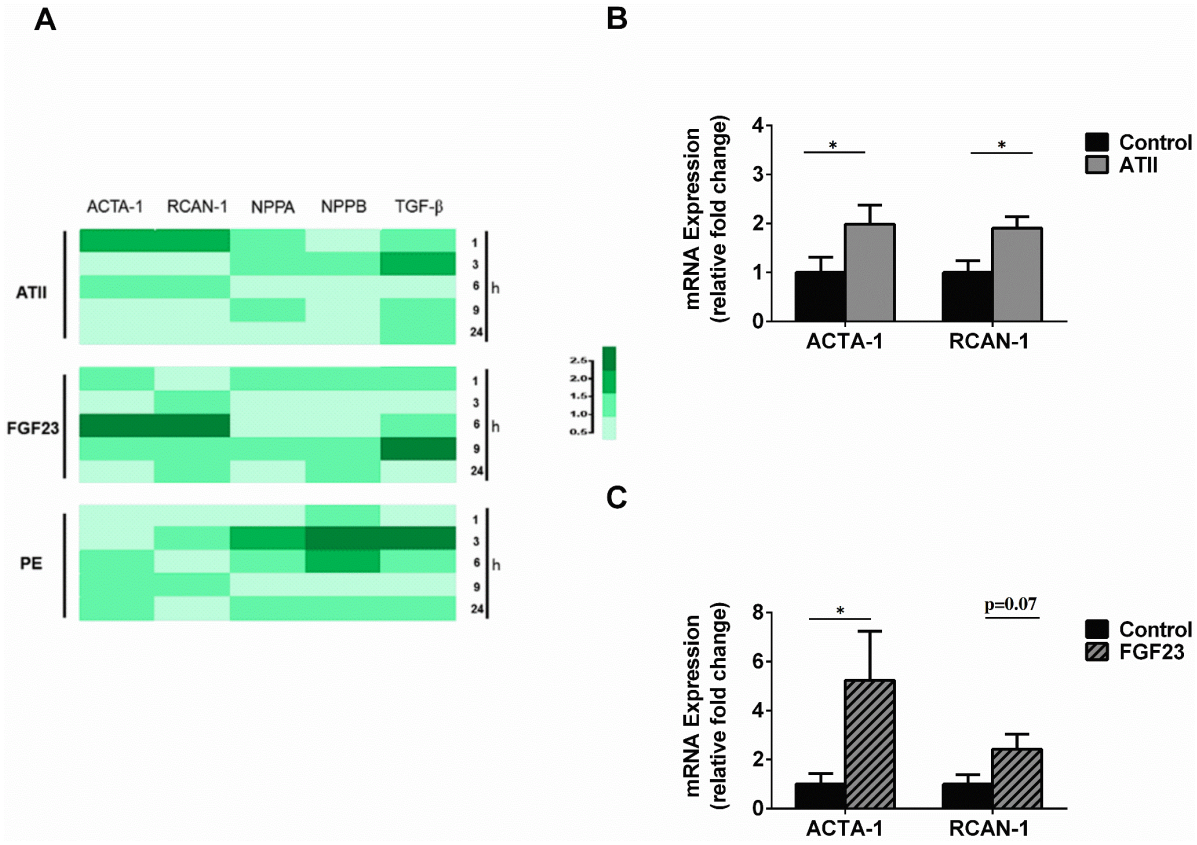

Figure 5.12 Effect of treatment of ATII (1μM) and FGF23 (25ng/ml) on hypertrophic gene expression in NRVMs at different time points

A The heat map exhibits the fold change in gene expression of genes ACTA-1, RCAN-1, NPPA, NPPB, TGF-β at timepoints 1h, 3h, 6h, 9h, 24h in ATII and FGF23-treated NRVMs as compared to corresponding vehicle-treated controls. **B** Compared to control cells (black), expression of genes ACTA-1 and RCAN-1 at 1h of ATII treatment (grey). **C** Compared to control cells (black), expression of genes ACTA-1 and RCAN-1 at 6h of FGF23 treatment (pattern) (mean±SEM; N=5 independent isolations quantified by RT-PCR normalized to GAPDH gene expression; *P<0.05, compared with corresponding control; unpaired t-test or Mann-Whitney U test).

The figure is adapted from “Mhatre, K.N., Wakula, P., Klein, O., Bisping, E., Völkl, J., Pieske, B., and Heinzel, F.R., 2018. Crosstalk between FGF23- and angiotensin II-mediated Ca2+ signaling in pathological cardiac hypertrophy. *Cellular and Molecular Life Sciences*, (0123456789). Copyright 2018 by Springer Nature. Reprinted with permission.

5.2.3. Activation of the hypertrophic CAMKII-HDAC4 pathway in NRVM by FGF23 stimulation

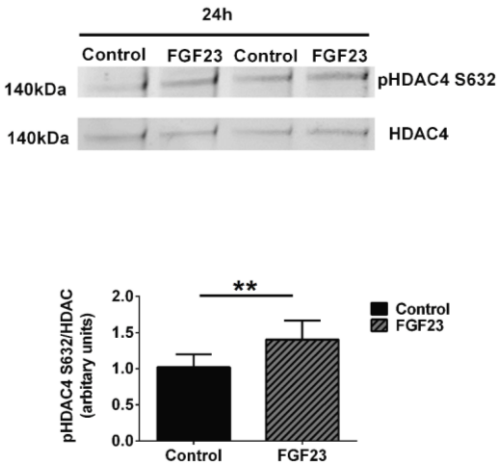

Figure 5.13 Effect of FGF23 treatment on HDAC4 phosphorylation at Serine 632 site in NRVMs

The immunoblot (above) of HDAC4 (140kDa) and corresponding pHDAC S632 in cell lysate samples form vehicle treated control and FGF23 treated group. The bar graph (below) depict degree of phosphorylation of HDAC4 at Serine 632 site normalized to HDAC-4 protein expression in both the treatment groups. The bar graph is from N=6 independent isolations (mean±SEM; **P<0.01, compared with control cells; paired t-test).

The figure is adapted from "Mhatre, K.N., Wakula, P., Klein, O., Bisping, E., Völkl, J., Pieske, B., and Heinzel, F.R., 2018. Crosstalk between FGF23- and angiotensin II-mediated Ca2+ signaling in pathological cardiac hypertrophy. *Cellular and Molecular Life Sciences*, (0123456789). Copyright 2018 by Springer Nature. Reprinted with permission.

Hence, next, we investigated the phosphorylation state at site Serine 632(S632) of HDAC4, which is known to be activated by ATII. In CMs, upon stimulation by a hypertrophic trigger like ATII, nuclear Ca^{2+}-CaMKII has been shown to tightly regulate epigenetic processes controlled by class II histone deacetylases (e.g. HDAC4) leading to transcriptional activation of gene programs that drive pathological remodeling.

Using immunoblotting, we observed significant increase by 1.4±0.1 fold in S632 phosphorylation of HDAC4 in FGF23 treated cells for 24h as compared to that of vehicle-treated control cells from 6 independent NRVM isolations (Figure 5.13).

5.2.4. FGF23 and ATII induces Ca^{2+} Transient changes in the cytoplasm as well as the nucleus

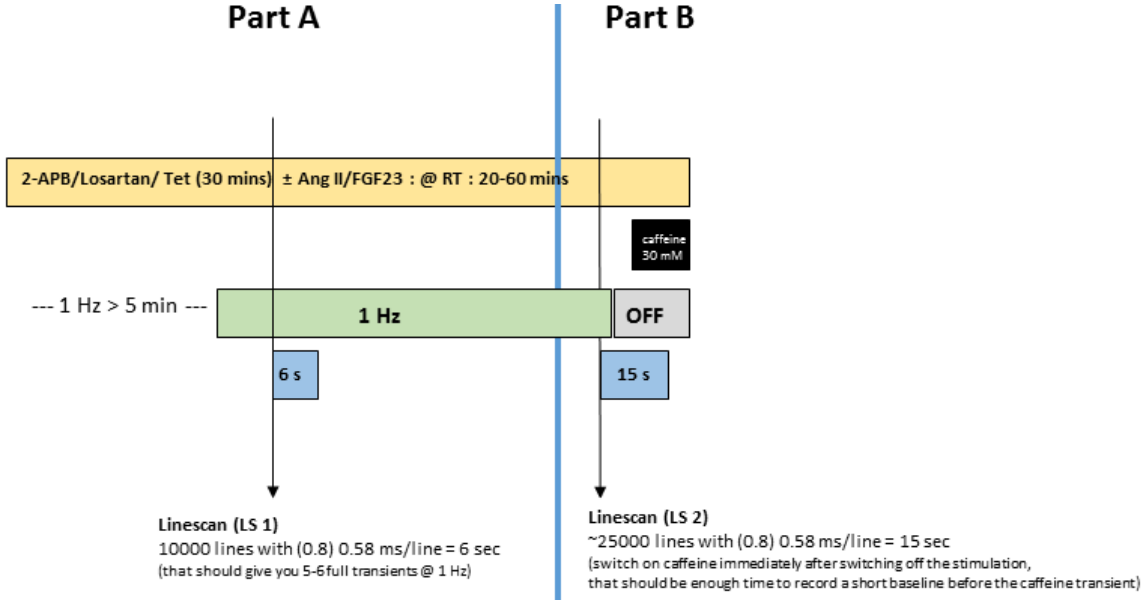

Figure 5.14 Ca^{2+} imaging protocol for studying effect of ATII (1uM) and FGF23 (25ng/ml) on CaT of NRVMs paced at 1Hz.

We investigated Ca^{2+} signals in the cytoplasm and nucleus of NRVMs electrically stimulated at 1Hz using protocol described in Figure 5.14. Following acute treatment for the duration of 15 to 90min, the cytosolic CaT amplitude tended to increase by 1.7±0.3 fold with ATII (P=0.05) and increased by 2.0±0.6 fold with FGF23 (P<0.01) (Figure 5.15A), whereas there was an augmentation of the nuclear CaT amplitudes by both the treatments though less pronounced (Figure 5.15B).

A substantial increase in AUC was elicited by ATII and FGF23 in both cytosol and nucleus (Figure 5.15C, D). Cytoplasmic CaT AUC increased by 2.4±0.4 fold (P<0.01) with ATII and by 2.9±0.3 fold (P<0.01) with FGF23 treatment respectively. Nuclear CaT AUC increased by 3.8±0.5 fold (P<0.01) with ATII and by 4.3±0.5 fold (P<0.01) with FGF23 treatment (Figure 5.15D).

Thus, both the hormones enhanced cytoplasmic as well as nuclear Ca^{2+} exposure, as was reflected best by the CaT AUC.

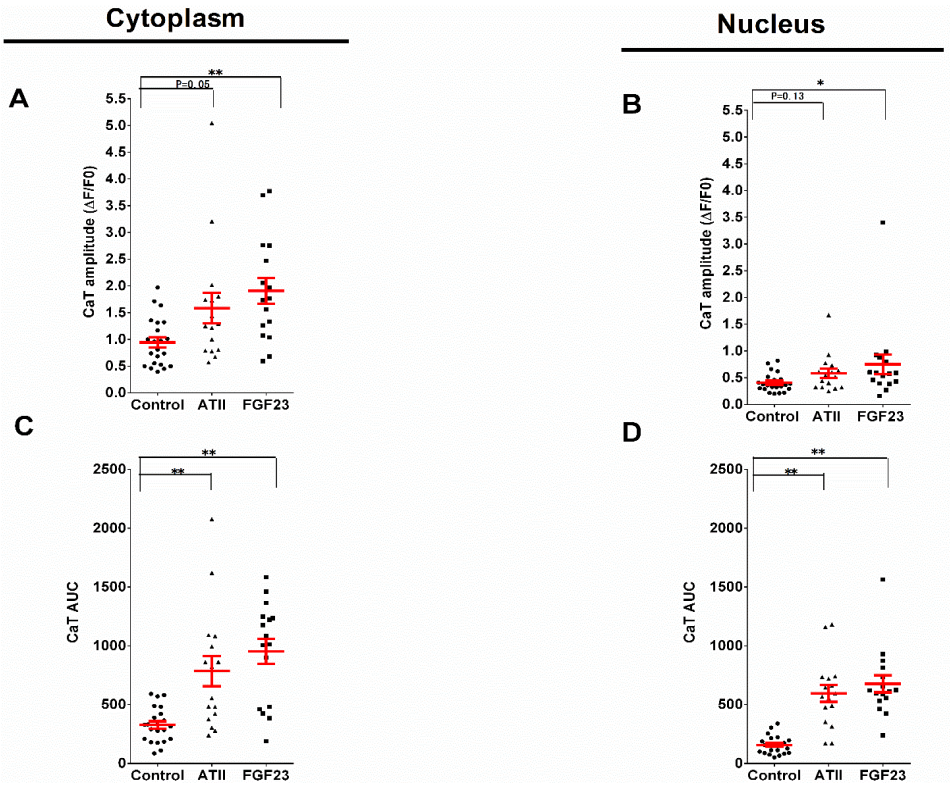

Figure 5.15 Effect of acute treatment of ATII (1µM) and FGF23 (25ng/ml) on CaT of NRVMs.

A Ca^{2+} transient peak amplitude after ATII (triangle) and FGF23 (square) treatment vs. vehicle-treated control NRVMs (circle) for 15-90mins in the cytoplasm (left) and in the **B** nucleus (right). **C** Ca^{2+} transient AUC in cytoplasm (left) and in **D** nucleus (right) after both the treatments vs. control NRVMs (circle) (each symbol represents 1 cell; mean±SEM; n>15 cells for each group and region; N=3 isolations of NRVMs; *P<0.05, **P<0.01, compared with corresponding vehicle-treated control; Kruskal-Wallis followed by Dunn's test).

The figure is adapted from "Mhatre, K.N., Wakula, P., Klein, O., Bisping, E., Völkl, J., Pieske, B., and Heinzel, F.R., 2018. Crosstalk between FGF23- and angiotensin II-mediated Ca2+ signaling in pathological cardiac hypertrophy. *Cellular and Molecular Life Sciences*, (0123456789). Copyright 2018 by Springer Nature. Reprinted with permission.

5.2.5. FGF23 induced increase in nuclear Ca^{2+} sparks in NRVMs

In addition, we also tested spontaneous spark activity in both the compartment for all the treatment groups. Significantly, more cells in FGF23 and ATII treatment groups exhibited

nuclear sparks as compared to control cells (Figure 5.16A, B). Ca^{2+} spark frequency was significantly increased in the nucleus of FGF23 treated cells vs. that of control cells but not in the cytoplasm (Figure 5.16C).

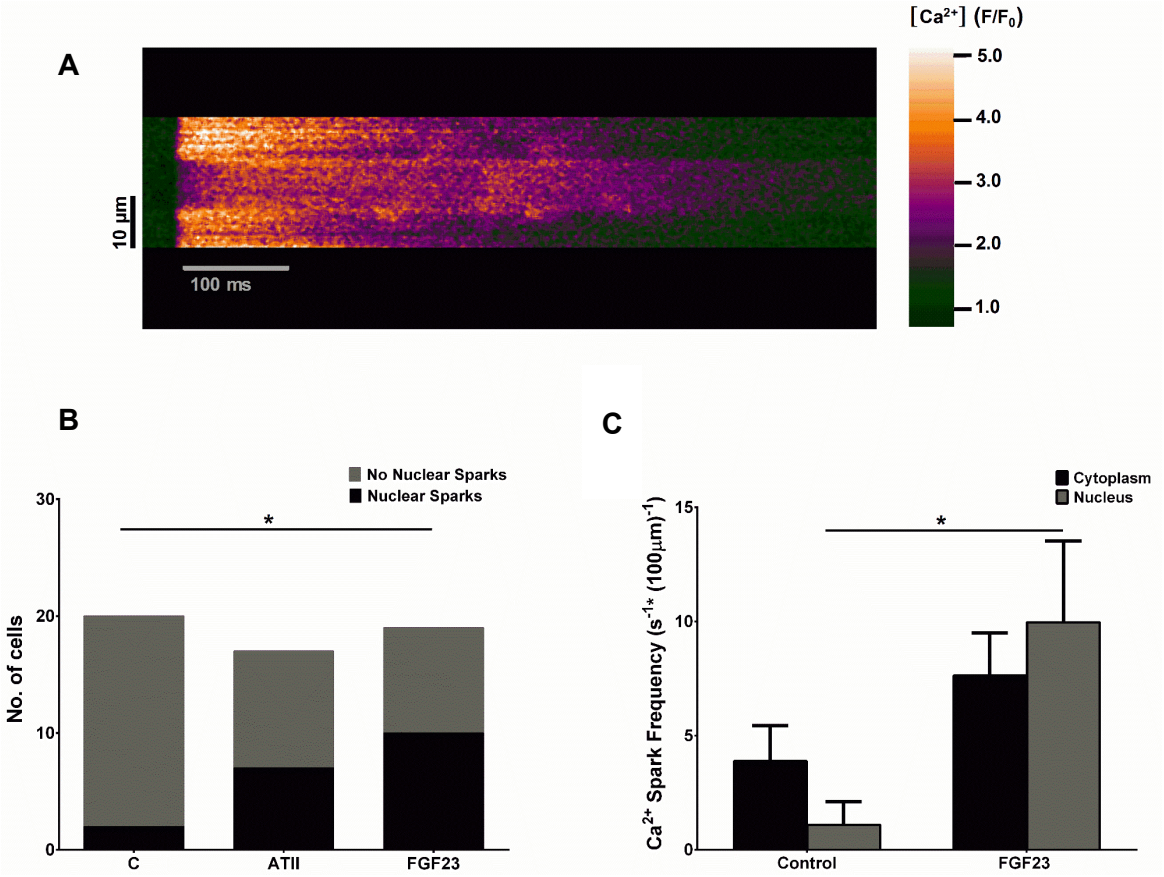

Figure 5.16 FGF23-evoked spontaneous Ca^{2+} sparks in the nucleus

A A typical example of original recordings of electrically stimulated Ca^{2+} transients and visible nuclear sparks in cell treated with FGF23. **B** Bar graph representation of the correlation between occurrence of nuclear Ca^{2+} sparks and treatments (Chi Square test; p=0.0145). **C** Quantification of Ca^{2+} spark frequency (n/100µm/sec) in vehicle-treated control cells and FGF23 treated cells in cytoplasm (black) and nucleus (grey). All the cells with or without sparks where included for this analysis (n>15 cells for each group and region; N=3 isolations of NRVMs; *P<0.05, compared with Two-way ANOVA followed by Tukey's test).

The figure is reproduced from "Mhatre, K.N., Wakula, P., Klein, O., Bisping, E., Völkl, J., Pieske, B., and Heinzel, F.R., 2018. Crosstalk between FGF23- and angiotensin II-mediated Ca2+ signaling in pathological cardiac hypertrophy. *Cellular and Molecular Life Sciences*, (0123456789). Copyright 2018 by Springer Nature. Reprinted with permission.

Thus, these results suggest an increase in specifically nuclear Ca^{2+} release events with ATII or FGF23 treatment of NRVMs.

5.2.6. FGF23-induced nuclear Ca^{2+} sparks have no detectable effects on the kinetics of nuclear CaT.

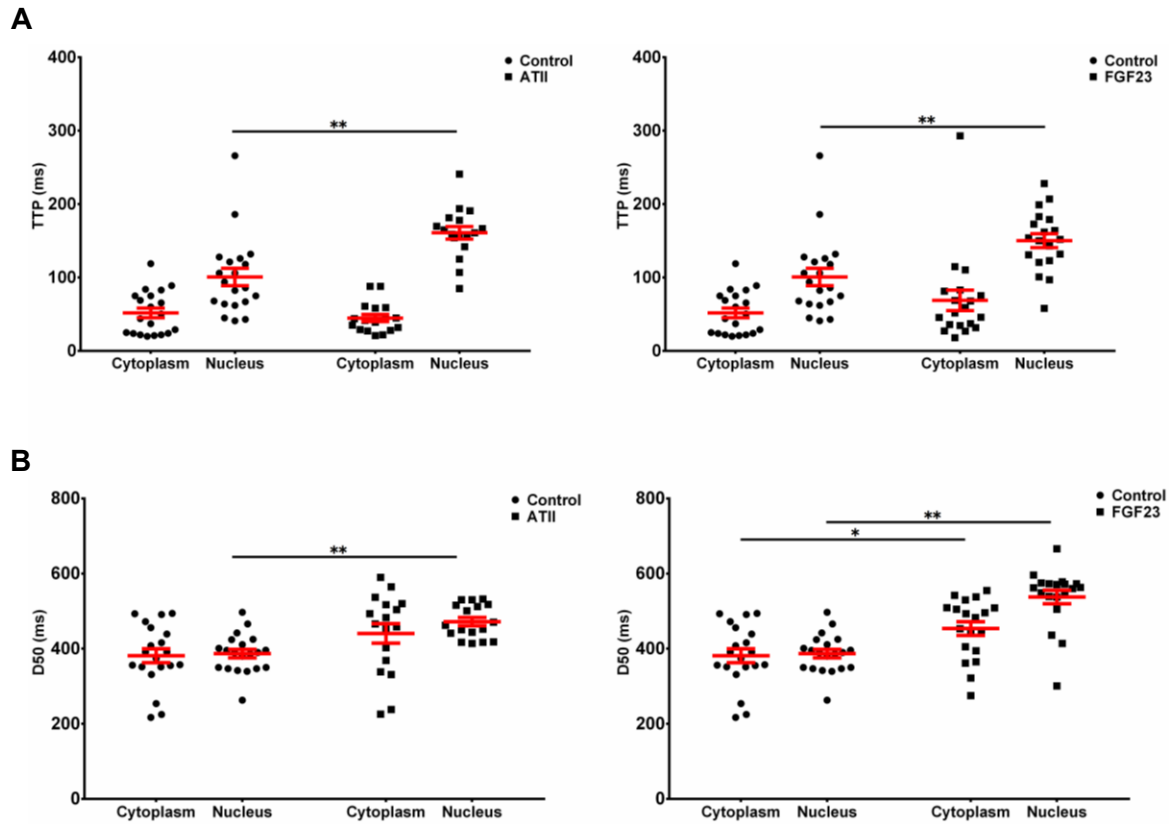

Figure 5.17 Effect of FGF23 and ATII on CaT kinetic parameters in NRVMs

A Time to peak (TTP) in ms of Ca^{2+} transient after ATII (square) (left) and FGF23 (square) (right) treatment for 15-90mins in cytoplasm and in the nucleus. **B** Time from peak [Ca^{2+}] to 50% decline (DT50) in ms of Ca^{2+} transient in both the compartments after both the treatments (each symbol represents 1 cell; mean±SEM; n>15 cells for each group and region; N=3 isolations of NRVMs; *P<0.05, **P<0.01, compared with Two-way ANOVA followed by Tukey's test).

Next, we wanted to check if the increased number of nuclear sparks influence overall nuclear Ca^{2+} transient and kinetics in FGF23-treated NRVMs. Time to peak (TTP) was used to quantify kinetics of Ca^{2+} release. We compared TTP of CaT in cytoplasm and nucleus in ATII or FGF23 treated vs. vehicle-treated controls cells. TTP was different between compartments and significantly prolonged with both the treatments (Figure 5.17A). However, the treatment effect does not significantly depend on the compartment, so the FGF23-induced increased nuclear sparks had no detectable effect on nuclear CaT TTP. In addition, the half decay time of CaT (D50) was obtained as a parameter of Ca^{2+} removal. A significant difference with FGF23 vs. control treatment was observed but that was again independent of the compartment (Figure 5.17B).

Thus, FGF23-induced change on the kinetics of CaT in NRVMs was not specifically for nuclear compartment.

5.3. ATII and FGF23 induced nuclear Ca^{2+} transient changes via IP3-IP3R in NRVMs.

It is known that Ca^{2+} signals generated via mechanisms distinct from excitation-contraction coupling control hypertrophic gene transcription. The stimulation of IP3-induced nuclear Ca^{2+} release (IICR) downstream of plasma membrane receptors (i.e. Angiotensin type 1 receptor) acts as a regulator of hypertrophic gene transcription (Higazi *et al.* 2009, Plačkić *et al.* 2016). Membrane-permeant 2-APB (5-10μM) and Xestospongin. C. (10μM), inositol trisphosphate receptor (IP3R) blockers, were used to further investigate the role of IP3 in this augmented nuclear Ca^{2+} release (Figure 5.15) due to ATII or FGF23 treatment.

5.3.1. 2-APB impedes FGF23-evoked active Ca^{2+} release in the nucleus

2-APB pretreatment did not have any effect on CaT peak amplitudes of both the treatments in the cytoplasm and nucleus (Figure 5.18A, B). However, it does impede ATII as well as FGF23 induced increase in nuclear CaT AUC. Although no effect of 2-APB was observed on cytoplasmic CaT AUC changes triggered by ATII and FGF23

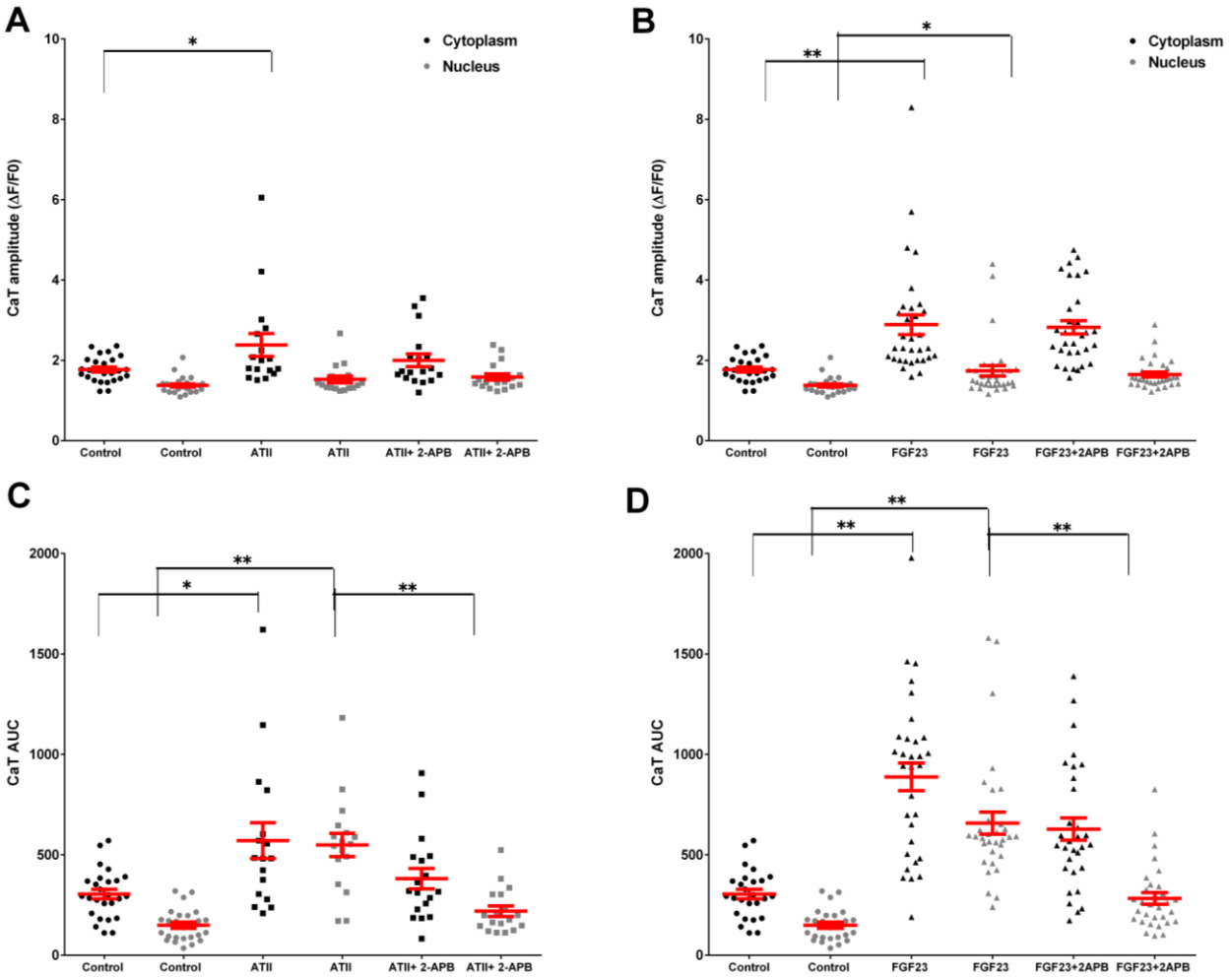

Figure 5.18 Effect of 2-APB on FGF23 and ATII-evoked CaT changes in NRVMs.

A Effect of 2-APB on Ca^{2+} transient amplitude in cytoplasm and nucleus in NRVMs treated with ATII (square) and **B** FGF23 (triangle) **C** Effect of 2-APB on Ca^{2+} transient AUC in cytoplasm and nucleus in NRVMs treated with ATII (square) and **D** FGF23 (triangle) (each symbol represents 1 cell; mean±SEM; n>15 cells for each group and region; N=3 isolations of NRVMs; *P<0.05, **P<0.01, compared with corresponding compartment of vehicle-treated control; Kruskal-Wallis followed by Dunn's test).

The figure is adapted from "Mhatre, K.N., Wakula, P., Klein, O., Bisping, E., Völkl, J., Pieske, B., and Heinzel, F.R., 2018. Crosstalk between FGF23- and angiotensin II-mediated Ca2+ signaling in pathological cardiac hypertrophy. *Cellular and Molecular Life Sciences*, (0123456789). Copyright 2018 by Springer Nature. Reprinted with permission.

(Figure 5.18C, D). Typical recordings of 1Hz stimulated Ca^{2+} transients in NRVMs treated with FGF23 and pretreated with 2-APB for 30mins before FGF23 stimulation show a visible decrease by 2-APB in FGF23 induced increase of nuclear Ca^{2+} release (Figure 5.19).

The nuclear Ca^{2+} transient (CaT) in ventricular CMs is constituted of two components, passive cytoplasmic Ca^{2+} diffusion through nuclear pore complexes and active IP3-mediated nuclear Ca^{2+}release(Ljubojević *et al.* 2011). In order to detect a selective effect of stimuli on active nuclear Ca^{2+} release independent of cytoplasmic Ca^{2+} diffusion, as specified before we normalized the nuclear CaT parameters to corresponding

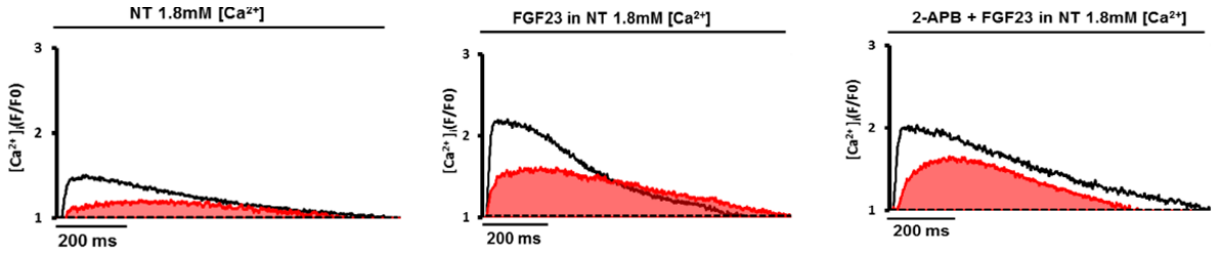

Figure 5.19 Examples of CaT exhibiting effect of 2-APB on FGF23-evoked active nuclear Ca2+ release in NRVMs

Typical examples of original recordings of electrically stimulated Ca2+ transients in the vehicle-treated control cell (above), cell treated with FGF23 (middle) and the cell pretreated with 2-APB for 30mins before FGF23 stimulation (below). The area covered in under the nuclear CaT (red) is considered as nuclear CaT AUC.

The figure is adapted from "Mhatre, K.N., Wakula, P., Klein, O., Bisping, E., Völkl, J., Pieske, B., and Heinzel, F.R., 2018. Crosstalk between FGF23- and angiotensin II-mediated Ca2+ signaling in pathological cardiac hypertrophy. *Cellular and Molecular Life Sciences*, (0123456789). Copyright 2018 by Springer Nature. Reprinted with permission.

cytoplasmic CaT (Plačkić *et al.* 2016). The ratio of nuclear to cytosolic CaT amplitudes was unchanged with both the treatments (Figure 5.20B). However, the ratio of nuclear CaT AUC to cytosolic CaT AUC revealed an increase in local nuclear Ca^{2+} release for both FGF23 and ATII (Figure 5.20A).

2-APB reduced the augmented Ca^{2+} release into the nucleus induced by FGF23. These results suggest that similar to ATII (Figure 5.20A), FGF23-triggered enhancement of nuclear Ca^{2+} signaling irrespective of cytosolic Ca^{2+} changes were mediated by IP3-dependent Ca^{2+} release. Thus, FGF23 induced hypertrophic Ca^{2+} signaling in CMs might be IP3-dependent as observed for ATII.

5.3.2. Xestospongin.C. (Xest.C.) also hinders FGF23-evoked active Ca^{2+} release in the nucleus

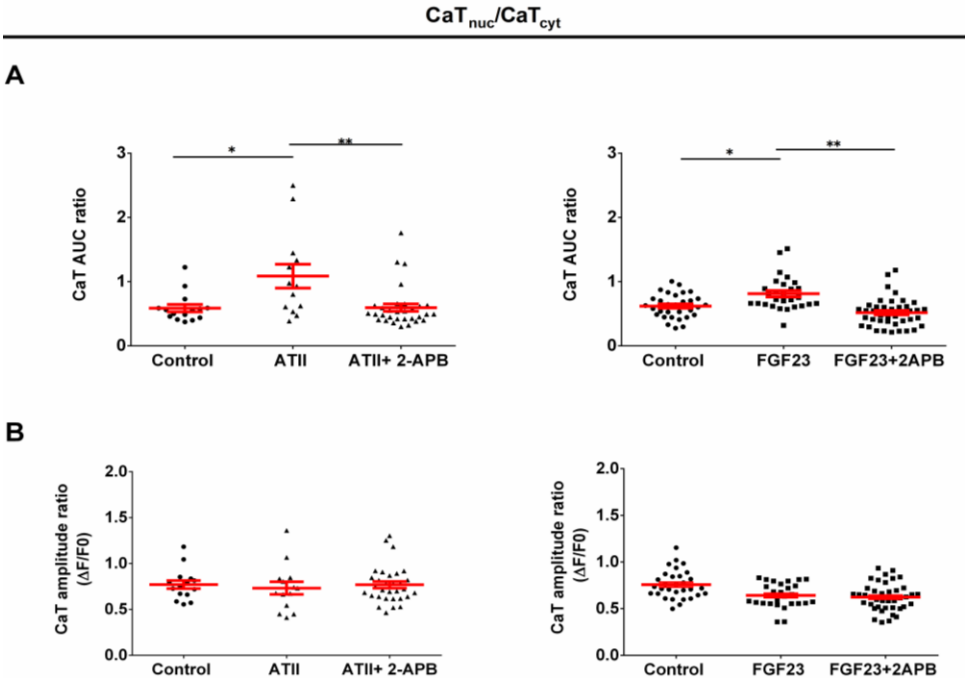

Figure 5.20 Effect of 2-APB on FGF23 and ATII-evoked nuclear Ca^{2+} release normalized to cytoplasmic CaT.

A Effect of 2-APB on Ca^{2+} transient AUC and **B** on Ca^{2+} transient amplitude in nucleus normalized to that of corresponding cytoplasmic Ca^{2+} transient (ratio) in NRVMs treated with ATII (triangle) and FGF23 (square) (each symbol represents 1 cell; mean±SEM; n>10 cells for each group and region; N=4 isolations of NRVMs; *P<0.05, **P<0.01, compared with corresponding compartment of vehicle-treated control; Kruskal-Wallis followed by Dunn's test).

The figure is adapted from "Mhatre, K.N., Wakula, P., Klein, O., Bisping, E., Völkl, J., Pieske, B., and Heinzel, F.R., 2018. Crosstalk between FGF23- and angiotensin II-mediated Ca2+ signaling in pathological cardiac hypertrophy. *Cellular and Molecular Life Sciences*, (0123456789). Copyright 2018 by Springer Nature. Reprinted with permission.

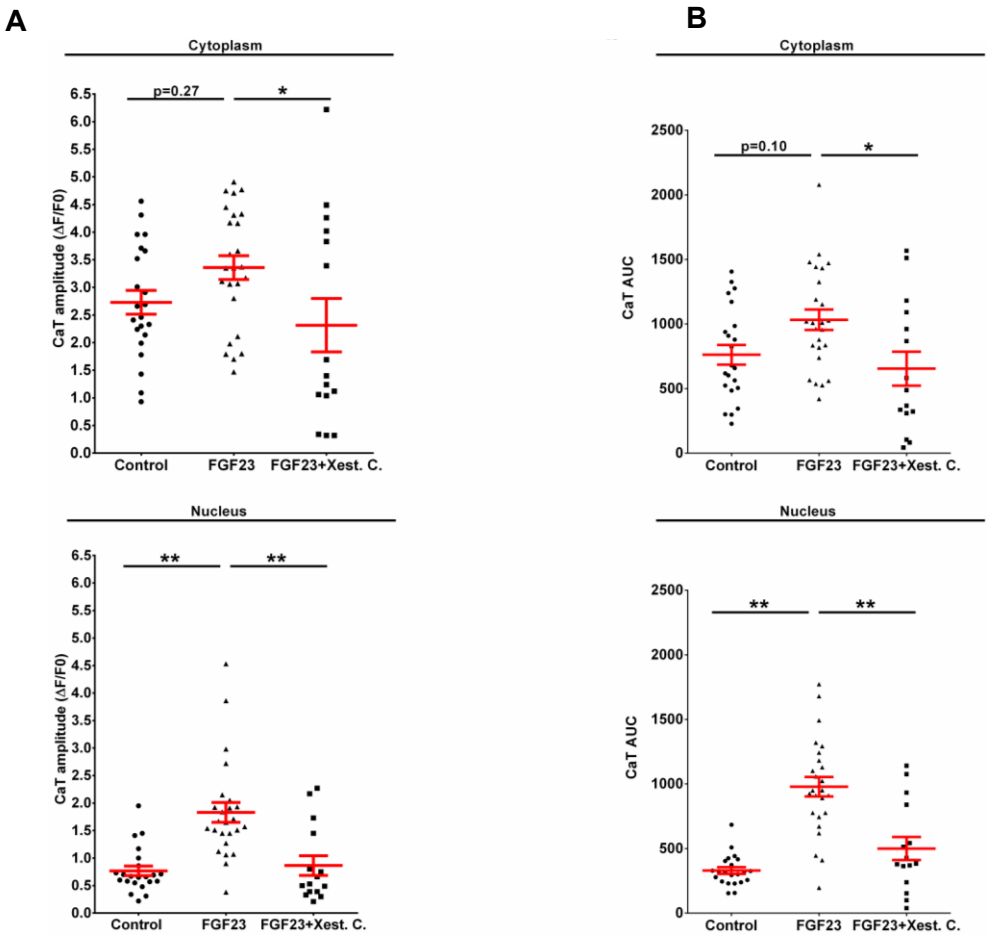

Figure 5.21 Effect of Xestospongin C (10 µM) on FGF23-evoked changes in Ca^{2+} transient

A Ca^{2+} transient peak amplitude in the vehicle-treated control cell (circle), cell treated with FGF23 (triangle) and the cell pretreated with Xestopsongin C (10 µM) for 30mins before FGF23 stimulation (square) in the cytoplasm (above) and in the nucleus (below). **B** Ca^{2+} transient AUC in the vehicle-treated control cell (circle), cell treated with FGF23 (triangle) and the cell pretreated with Xest. C. (10 µM) for 30mins before FGF23 stimulation (square) in the cytoplasm (above) and in the nucleus (below) (each symbol represents 1 cell; mean±SEM; n≥15 cells for each group and region; N=3 isolations of NRVMs; *P<0.05, **P<0.01; Kruskal-Wallis followed by Dunn's test). The figure is reproduced from Mhatre *et al.* 2018 with permission of Springer international publishing.

The figure is adapted from "Mhatre, K.N., Wakula, P., Klein, O., Bisping, E., Völkl, J., Pieske, B., and Heinzel, F.R., 2018. Crosstalk between FGF23- and angiotensin II-mediated Ca2+ signaling in pathological cardiac hypertrophy. *Cellular and Molecular Life Sciences*, (0123456789). Copyright 2018 by Springer Nature. Reprinted with permission.

Pretreatment of Xest.C. (10 μM) for 30mins before FGF23 stimulation offsets both, FGF23- induced increase in cytoplasmic as well as a nuclear Ca^{2+} release with respect to CaT amplitude and CaT AUC (Figure 5.21). Thus, both the compounds, 2-ABP and Xest. C. yielded similar results. Overall, these results suggest that irrespective of cytosolic Ca^{2+} changes, FGF23-triggered enhancement of nuclear Ca^{2+} signaling is mediated by IICR.

5.4. ATII-AT1R plays a role in FGF23-induced maladaptive Ca^{2+} signaling

As illustrated above, FGF23 had similar effects as ATII on NRVMs with respect to cellular hypertrophy and Ca^{2+} homeostasis changes. This implies the possibility of involvement of ATII signaling in FGF23-induced hypertrophy. To investigate whether there is an overlap between FGF23 and ATII/AT1R signaling, we used losartan, an AT1R antagonist.

5.4.1. Losartan blocks FGF23-induced CaT changes

NRVMs were pretreated with losartan for 30mins and then exposed to FGF23. Losartan (1μM) pretreatment effect was studied on the CaT changes induced by FGF23. Surprisingly, Losartan attenuated the FGF23-mediated increase in CaT amplitude as well as in total Ca^{2+} (CaT AUC) released into the cytosol and nucleus (Figure 5.22). Whereas, losartan alone did not have a significant effect on CaT amplitude in NRVMs vs. vehicle-treated control cells in the cytoplasm (0.73±0.13 and 0.76±0.07 in losartan-treated and control n≥8cells) and nucleus (0.38±0.07 and 0.30±0.03 in losartan-treated and control). CaT AUC in NRVMs was also not affected by losartan in the cytoplasm (253.4±45.6 and 252±17.3 in losartan-treated and control; n≥8cells) and nucleus (153.2±24.9 and 118.3±11.5 in losartan-treated and control).

5.4.2. Losartan inhibits FGF23-induced cellular hypertrophy

We went ahead and checked if losartan has an effect on FGF23 triggered cellular hypertrophy. Likewise, pretreatment with losartan significantly attenuated the FGF23-induced increase in CM size (Figure 5.23).

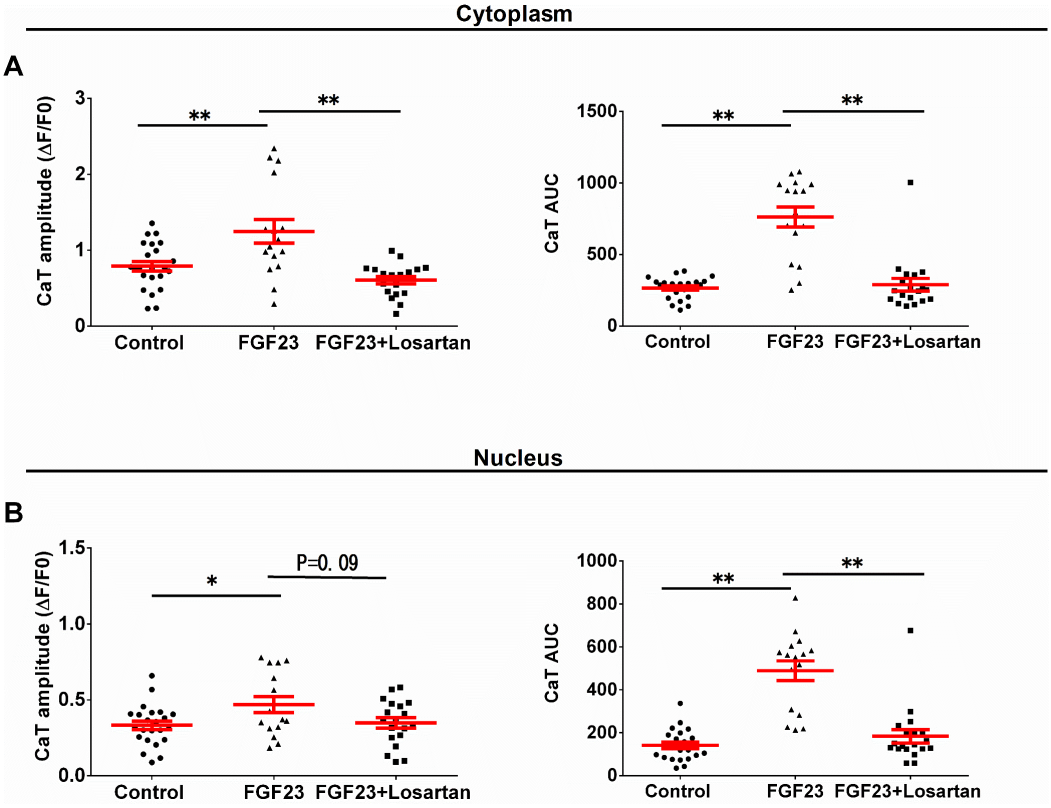

Figure 5.22 Effect of Losartan (1µM) on FGF23-evoked changes in Ca^{2+} transient

A Effect of 30 mins pre-treatment of losartan (square) on Ca^{2+} transient peak amplitude (left) and AUC (right) in cytoplasm **B** in nucleus of FGF23 (triangle) treated NRVMs (mean±SEM; n>15 cells for each group and region; N=3 isolations of NRVMs; *P<0.05, **P<0.01, compared with corresponding vehicle-treated control).

The figure is adapted from "Mhatre, K.N., Wakula, P., Klein, O., Bisping, E., Völkl, J., Pieske, B., and Heinzel, F.R., 2018. Crosstalk between FGF23- and angiotensin II-mediated Ca2+ signaling in pathological cardiac hypertrophy. *Cellular and Molecular Life Sciences*, (0123456789). Copyright 2018 by Springer Nature. Reprinted with permission.

Thus, inhibition of ATII/AT1R signaling leads to blocking of FGF23-induced Ca^{2+} changes in ventricular CMs. Consequently, our cell size data shows the possible involvement of ATII-AT1R activation in FGF23-induced maladaptive signaling in CMs.

Furthermore, pretreatment with losartan significantly attenuated the FGF23-induced upregulation of hypertrophy gene, ACTA-1 (Figure 5.24).

Thus, inhibition of ATII/AT1R signaling leads to blocking of FGF23-induced cellular hypertrophy in ventricular CMs.

5.4.3. Losartan does not have any inhibitory effect on FGF23 specific receptor FGFR4

There was a possibility that Losartan inhibitory effect on FGF23-triggered hypertrophy was due to interference with FGF23 specific receptor FGFR4. FGFR4, FGFR isoform, is a receptor tyrosine kinase. Following the FGF23-induced auto-phosphorylation of FGFR, PLCγ can be recruited to bind directly to one specific phosphorylated tyrosine residue (Tyr783) in the FGFR cytoplasmic tail (Grabner *et al.* 2015). Subsequent phosphorylation of PLCγ induces the generation of diacylglycerol and IP3, which further activates Ca^{2+} mediated hypertrophy signaling.

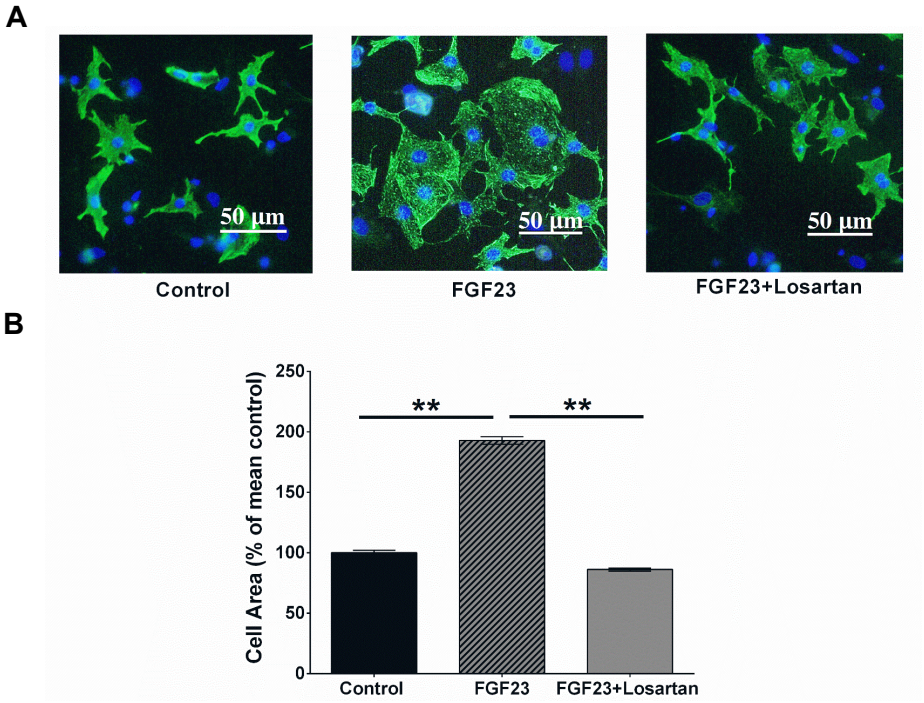

Figure 5.23 Effect of Losartan (1µM) on FGF23-evoked changes NRVM cell size.

A Representative images of isolated NRVMs for each condition after immunocytochemical analysis using antibodies to cardiomyocyte-specific Desmin (green), DAPI (blue) was used to identify nuclei (scale bar: 50µm). **B** The bar graph represents relative percentage change compared to vehicle-treated control cells (black) in NRVMs treated with FGF23 (pattern) for 48 hours or after 30 min pre-treatment of losartan (grey) (mean±SEM; n>1000 cells per group; N=3 isolations of NRVMs; *P<0.05, **P<0.01; one-way ANOVA with Bonferroni post-test or Kruskal–Wallis followed by Dunn's test).

The figure is adapted from "Mhatre, K.N., Wakula, P., Klein, O., Bisping, E., Völkl, J., Pieske, B., and Heinzel, F.R., 2018. Crosstalk between FGF23- and angiotensin II-mediated Ca2+ signaling in pathological cardiac hypertrophy. *Cellular and Molecular Life Sciences*, (0123456789). Copyright 2018 by Springer Nature. Reprinted with permission.

.

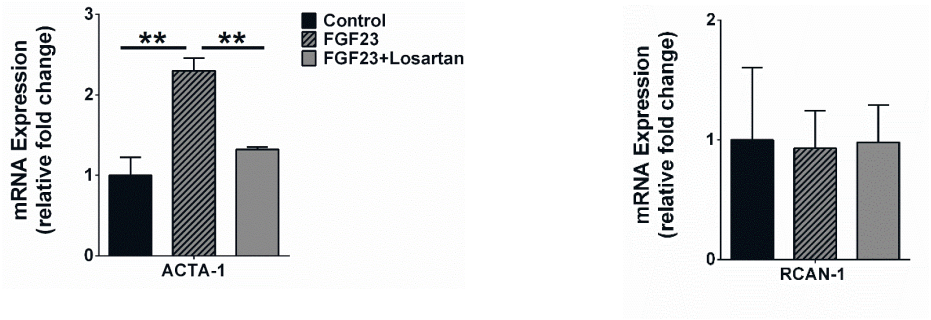

Figure 5.24 Effect of Losartan (1μM) on FGF23-triggered upregulation in hypertrophic gene expression.

Compared to control cells (black), expression of genes ACTA-1 (right) and RCAN-1 (left) at 6h of FGF23 treatment (pattern) or after 30 min pre-treatment of losartan (grey) (mean±SEM; N=4 independent isolations quantified by RT-PCR normalized to GAPDH gene expression; **P<0.01; unpaired t-test or Mann-Whitney U test).

The figure is adapted from "Mhatre, K.N., Wakula, P., Klein, O., Bisping, E., Völkl, J., Pieske, B., and Heinzel, F.R., 2018. Crosstalk between FGF23- and angiotensin II-mediated Ca2+ signaling in pathological cardiac hypertrophy. *Cellular and Molecular Life Sciences*, (0123456789). Copyright 2018 by Springer Nature. Reprinted with permission.

In order, to check the effect of pretreatment of losartan on FGFR4 in NRVMs, we checked the phosphorylation status at Tyr783 of FGFR4 by western blot technique.

Epidermal growth factor (EGF) is known to act via PLCγ phosphorylation of its receptor EGFR to induce downstream signaling. We used EGF as our positive control. The PLCγ phosphorylation quantified was normalized to that of vehicle-treated control NRVMs. EGF induced an almost 2-fold increase in PLCγ phosphorylation levels at 10min stimulation time point while FGF-23 and losartan pretreated FGF23 stimulated NRVMs did not show much difference with control cells (Figure 5.25). Thus, Losartan is not likely to interfere with the FGFR4 activity.

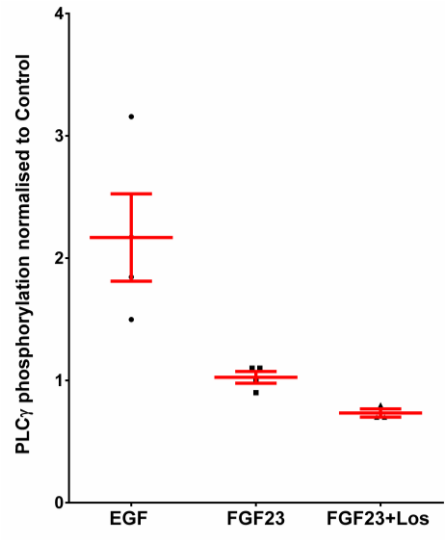

Figure 5.25 Effect of Losartan (1μM) on PLCγ phosphorylation levels related to FGF23-specific receptor FGFR4

The degree of phosphorylation of PLCγ at Tyr783 site was examined by immunoblot in NRVMs treated with EGF, FGF23 and FGF23 pre-treated with Losartan normalized to vehicle-treated control at 10mins timepoint. The bar graph (below) is from N≥3 independent isolations (mean±SEM).

5.5. FGF23 stimulates formation of intracellular ATII in NRVMs

Earlier studies have shown that ATII can be produced intracellularly in CMs in response to different stimuli (Singh *et al.* 2007). Based on our Losartan study, we hypothesized ATII might be an upstream activator of FGF23-hypertrophic signaling in CMs. Hence, we examined whether FGF23 induces a rise in formation of ATII and its precursors in CMs. Intracellular ATII formation-dependent immunofluorescence was quantified in NRVMs treated with FGF23 for 90min and 24h by thresholding method (Figure 4.1, Material and methods 4.5.2).

High extracellular glucose has also been shown to trigger ATII production (Singh *et al.* 2007) and served as a positive control. The glucose content in NRVM culture medium is 10mM (DMEM-F12 and M199 GlutaMAX Supplement, Thermo Scientific, Rockford, IL, USA), for our experiments, we used 25mM as our high glucose concentration. We choose 24h time point as well as 90min in order to incorporate the early changes observed in Ca^{2+} homeostasis triggered by FGF23 (Figure 5.22).

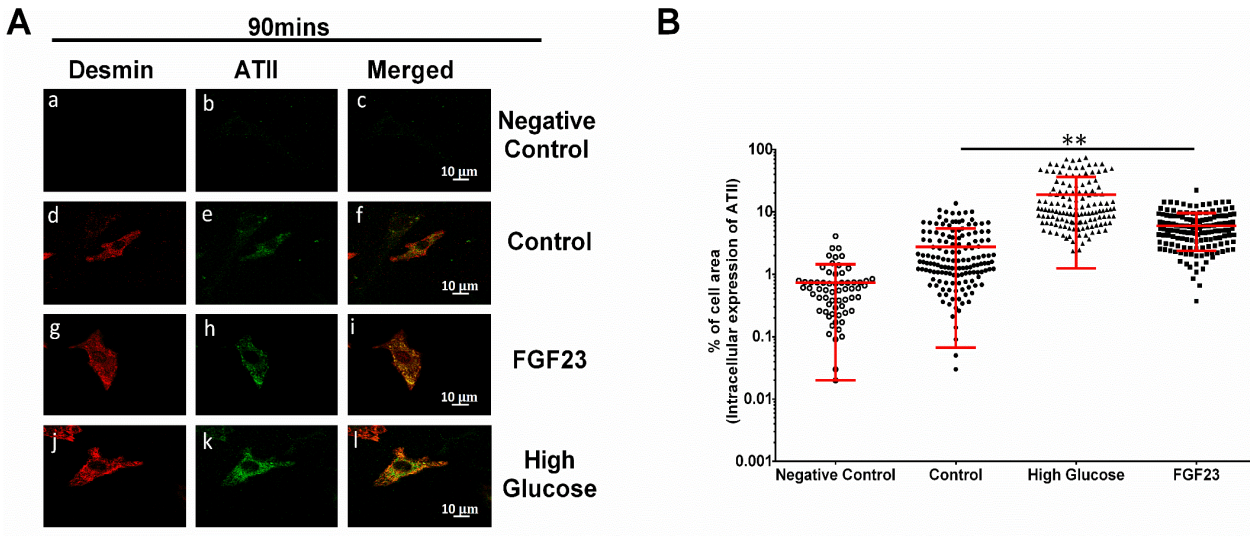

Figure 5.26 Formation of intra-cardiac ATII induced by FGF23 treatment for 90mins

A Representative confocal images of NRVM immunofluorescence in negative control (a,b,c) , vehicle-treated control (d,e,f) , FGF23 (g,h,i) and high glucose (25mM) (j,k,l) conditions after 90mins of treatment (scale bar: 10µm). **B** Quantitative analysis by thresholding (see 4.5.2.) of ATII-specific cellular immunofluorescence for all the treatments at 90mins (each symbol represents 1 cell; mean±SD; n_{cells}≥40 for each group; N≥3 isolations of NRVMs; **P<0.01, compared with corresponding vehicle-treated control cells; Kruskal-Wallis followed by Dunn's test).

The figure is adapted from "Mhatre, K.N., Wakula, P., Klein, O., Bisping, E., Völkl, J., Pieske, B., and Heinzel, F.R., 2018. Crosstalk between FGF23- and angiotensin II-mediated Ca2+ signaling in pathological cardiac hypertrophy. *Cellular and Molecular Life Sciences*, (0123456789). Copyright 2018 by Springer Nature. Reprinted with permission.

Remarkably, FGF23 significantly increased the fraction of cell area expressing ATII in NRVMs already early at the time point of Ca^{2+} changes (5.9±0.3% of cell area vs. 2.7±0.2% in control at 90min, Figure 5.26). A time-dependent increase was observed in FGF23-treated CMs with ATII formation (13.6±1.6%) compared with untreated control cells (3.24±0.5%) at 24h (Figure 5.27). As expected, high glucose had a significant effect on intracellular ATII levels at 90min and 24h (18.8±1.5 and 8.3±1.3% cell area, respectively) as compared to untreated control cells.

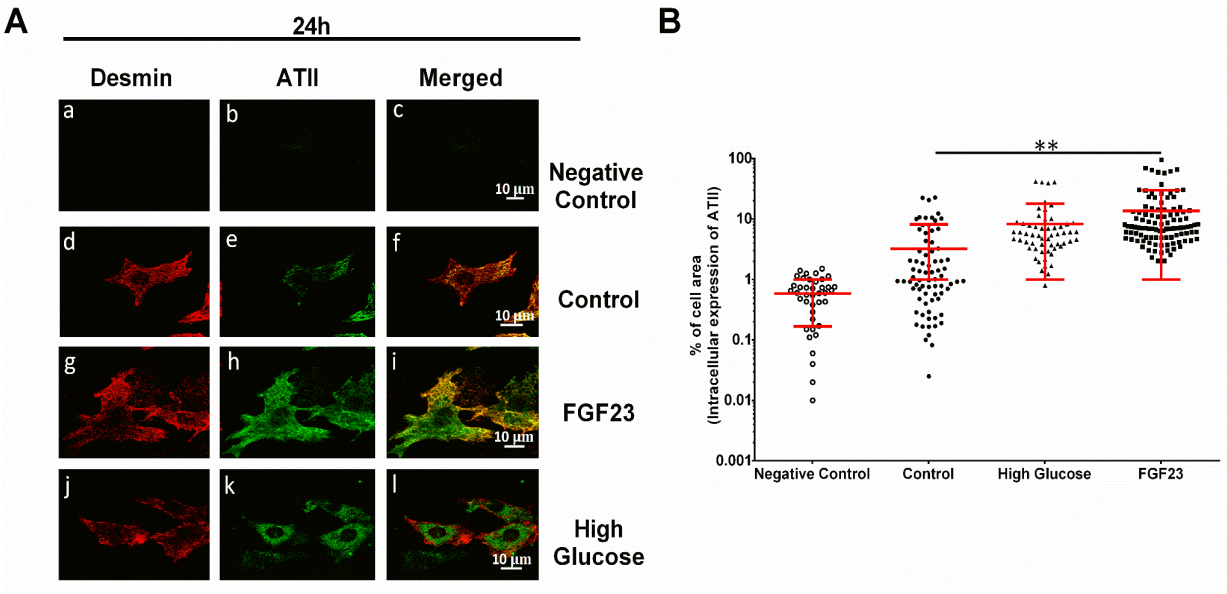

Figure 5.27 Formation of intra-cardiac ATII induced by FGF23 treatment for 24h

A Representative confocal images of NRVM immunofluorescence in negative control (a,b,c) , vehicle-treated control (d,e,f) , FGF23 (g,h,i) and high glucose (25mM) (j,k,l) conditions after 24h of treatment (scale bar: 10µm). **B** Quantitative analysis by thresholding (see 4.5.2.) of ATII-specific cellular immunofluorescence for all the treatments at 24h (each symbol represents 1 cell; mean±SD; n_{cells}≥40 for each group; N≥3 isolations of NRVMs; **P<0.01, compared with corresponding vehicle-treated control cells; Kruskal-Wallis followed by Dunn's test).

The figure is adapted from "Mhatre, K.N., Wakula, P., Klein, O., Bisping, E., Völkl, J., Pieske, B., and Heinzel, F.R., 2018. Crosstalk between FGF23- and angiotensin II-mediated Ca2+ signaling in pathological cardiac hypertrophy. *Cellular and Molecular Life Sciences*, (0123456789). Copyright 2018 by Springer Nature. Reprinted with permission.

Overall, in presence of FGF23, there was a persistent increase in ATII synthesis in CMs already at 90min. In our case, FGF23 might be increasing the ATII formation and secretion, which might be involved in FGF23-mediated hypertrophy. This explains the effect of Angiotensin II type 1 receptor (AT1R) antagonist effect on hypertrophy induced by FGF23.

5.6. FGF23 stimulates secretion of ATII in NRVMs

In order to detect the secretion of FGF23-mediated ATII, we performed mass spectrometry analysis of the conditioned medium from the 24h FGF23-treated NRVMs and vehicle-treated control NRVMs. The conditioned medium samples collected were processed to be ready for mass spectrometry analysis (Figure 4.2).

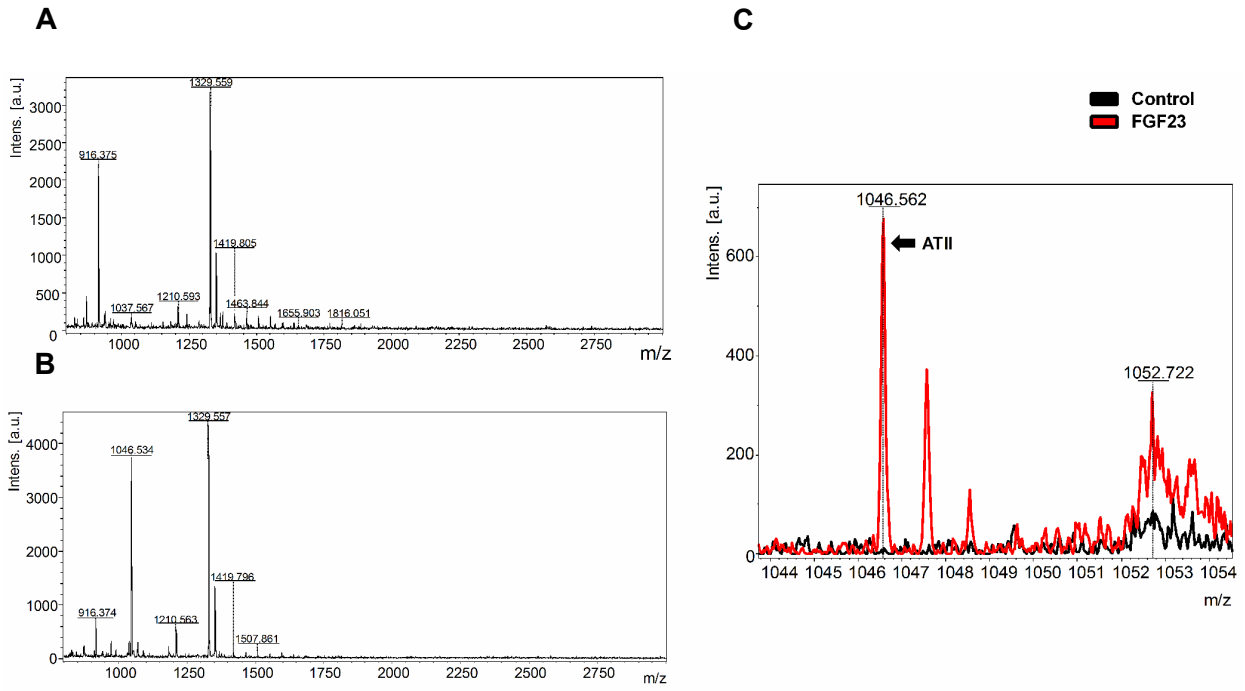

Figure 5.28 Detection of secreted ANG II from NRVM exposed to FGF23 by mass spectrometry

A Representative mass spectra (m/z 800–3000) of conditioned media samples from vehicle-treated control NRVMs (above) and **B** FGF23 treated NRVMs (below) for 24h. **C** Superimposed representative mass spectra (m/z 1044–1054) were extracted and amplified from full mass chromatogram of 24h FGF23 treated-conditioned medium (red) and conditioned medium from control cells (black). ATII (m/z 1046.562) peak is highlighted by red arrow.

The figure is adapted from “Mhatre, K.N., Wakula, P., Klein, O., Bisping, E., Völkl, J., Pieske, B., and Heinzel, F.R., 2018. Crosstalk between FGF23- and angiotensin II-mediated Ca2+ signaling in pathological cardiac hypertrophy. *Cellular and Molecular Life Sciences*, (0123456789). Copyright 2018 by Springer Nature. Reprinted with permission.

Qualitative results were gathered from MALDI-IMS as represented in the mass spectra (Figure 5.28A, B). The initial inspection of the mass spectra revealed a number of prominent peaks found between m/z 800–3000 with the intensity and profile clearly altered between the two groups. In Figure 5.28C, superimposed representative mass spectra (m/z range: 1044–1054) evidently showed the presence of a peak of ATII peptide (m/z 1046.562) in the supernatant collected from FGF23 treated NRVMs. Whereas, the ATII peak was absent in the supernatant collected from untreated NRVMs.

These results suggest that in FGF23 treated NRVMs; ATII peptide was synthesized in the secretory pathway. Overall, our results indicate an activation of production, secretion, and signaling of ATII in FGF23-mediated hypertrophy in ventricular CMs(Mhatre *et al.* 2018).

6. Discussion

In this study, we were the first to explore the effects of FGF23 on intracellular Ca^{2+} homeostasis related to cellular hypertrophy. We provide primary evidence suggesting that, in CMs, FGF23 and ATII share a common Ca^{2+}-mediated signaling pathway. Similar to ATII-dependent signaling, we show that hypertrophy induced by FGF23 was associated with the IP3-dependent nuclear Ca^{2+} release. We also demonstrated that the ATII/AT1R-antagonist 'losartan' attenuated FGF23-induced effects on CM hypertrophy and Ca^{2+} signaling. Lastly, we demonstrated that FGF23 enhances ATII formation and secretion in CMs. Based on these results; we suggest a cross-talk between FGF23- and ATII-mediated signaling in CMs(Mhatre *et al.* 2018).

Prospective studies have shown that increased FGF23 concentrations are associated with increased risk of cardiovascular disease events independently of established risk factors and co-morbidities like CKD (Kestenbaum *et al.* 2014). Moreover, this association has been strongly observed for heart failure, which is one of the most common presentations of heart disease in individuals with CKD(Di Giuseppe *et al.* 2014). The reason why elevated FGF23 appears to demonstrate this strong association between heart failure-related CVD phenotypes was still unclear. In this project, we try to find the answer to this question in our *in vitro* cellular model of hypertrophy.

We instigated this study in adult rat ventricular cardiomyocytes (ARVMs). An established hypertrophic trigger like ATII did not have a significant effect on cell size or hypertrophic marker gene expression as compared to the vehicle-treated control cells (Figure 5.1, Figure 5.2, Figure 5.3). The possible reason might be a constant reduction in the viability of ARVMs in culture conditions as seen in (Figure 5.1). The dead cells might be masking the possible hypertrophic effect of ATII in the case of cell size and gene expression. In addition, there is the possibility of excretion from the dead, apoptotic cells that interfere with the physiology of healthy living cells. In addition, no or minimal effect of ATII

stimulation was observed on Ca^{2+} homeostasis of ARVMs (Figure 5.5, Figure 5.7, and Figure 5.8), which was in line with the lack of hypertrophic effects.

There is strong evidence that ATII infusion induces hypertrophy in the heart *in vivo*(McCarthy *et al.* 2017). However, very few papers document the effect of ATII on ARVMs in long-term culture conditions. Serum from different sources was added in the culture medium to keep the ARVMs stable for long-term culture(Pellieux *et al.* 2009). However, serum itself can induce a hypertrophic response in ARVMs irrespective of ATII stimulus(Dambrot *et al.* 2014). Thus, additional triggers may be necessary to facilitate hypertrophy in these fully differentiated adult CMs. Nonetheless, these triggers themselves can act as hypertrophic, which might overshadow the effects of the stimulus in question (ATII). Therefore, we repeated this study in Neonatal rat ventricular cardiomyocytes (NRVMs).

NRVMs are commonly used model systems for cardiac hypertrophy and can be maintained in a stable state in cell culture as compared to adult CMs(Luo *et al.* 2008; Arantes *et al*. 2012). We chose this model of healthy CMs because our aim was to study early adaptation to hypertrophic triggers. NRVM are less differentiated but fully functional, contracting CMs. NRVM are much more susceptible to hypertrophic triggers and growth than adult terminally differentiated CMs *in vitro*. We chose NRVM as a model to allow quantitative recordings of subcellular Ca^{2+} transients in controlled extracellular conditions. While this approach ignores additional mechanical, neurohumoral and paracrine triggers, it allows us to dissect single receptor-mediated signaling pathways. However, our *in vitro* observations should be extrapolated cautiously to the *in vivo* setting where CMs are coupled with other cardiac cell types. While NRVMs are in a premature state with respect to Ca^{2+}-handling, this bears resemblance to long-term cultured as well as diseased adult CMs where there is a loss of t-tubule organization and web like the arrangement of contractile proteins (Louch *et al*. 2015). Nonetheless, functional signaling pathways for ATII and FGF23 have been demonstrated previously in NRVM (Faul *et al.* 2011).

One possibility of FGF23 association with HF may be that FGF23 either directly or indirectly promotes adverse left ventricular remodeling. In previous studies with NXT rats and further with CKD patients, elevated serum FGF23 concentrations were independently associated with LVH (Leifheit-Nestler *et al.* 2016). However, we did not observe the elevation of FGF23 serum levels in NXT vs SOP rats at 8 weeks and 24 weeks timepoint (Figure 5.9A, B). The increase serum levels of FGF23 observed by other groups in the CKD animal models was measured at the early timepoint of 2 weeks unlike our samples and might be the reason of lack of difference(Di Marco *et al.* 2014; Silswal *et al.* 2014). Regarding the absence of an increase in activation of FGFR1 in LV of NXT rats (Figure 5.10), there might be different FGFR type involved in FGF23-mediated maladaptive hypertrophic signaling. Animal studies have shown that FGF23 trigger FGF receptor 4 (FGFR4)-dependent but Klotho-independent signaling leading to pathological LVH (Grabner et al. 2015). Further, by blocking FGF23 binding to FGFR4 in CKD rat model, the development of LVH was halted despite the development of severe hypertension (Di Marco *et al.* 2014). In other studies, FGF23 have shown to altering Ca^{2+}- homeostasis in CMs, resulting in increased contractility, arrhythmogenesis etc.(Touchberry *et al.* 2013; Kao *et al.* 2014). Taken together, these data support that excess of serum FGF23 as a causal mechanism for pathological cardiac remodeling and heart failure. Even though FGF23 is known to induce hypertrophy, mechanistic details of this signaling pathway involved are not well understood**.** In the present study, we confirmed the direct hypertrophic effects of FGF23 in CMs and found them comparable to ATII.

ATII, an important mediator of the RAAS cascade, is a major trigger of cardiac hypertrophy. In CMs, ATII acts via the angiotensin II receptor type 1 (AT1R), a classical G-protein-coupled receptor (GPCR). Downstream of GPCR, IICR plays a pivotal role in regulating cardiac hypertrophy(Nakayama *et al.* 2010). IP3-mediated enhanced intracellular nuclear Ca^{2+} and activation of Ca^{2+}-sensors such as Ca^{2+} /calmodulin-dependent protein kinase II (CaMKII) triggers the development of ATII-induced cardiac hypertrophy(Zhang *et al.* 2010). CaMKII specifically regulates the phosphorylation (Ser-632) of anti-hypertrophic transcription repressor histone deacetylase 4 (HDAC4) (Kee *et*

al. 2006; Backs *et al.* 2009). As a result, HDAC4 is exported from the nucleus to cytoplasm, where it no longer serve anti-hypertrophic functions against transcription factors MEF2 and SRF resulting in activation of hypertrophic gene programs that are controlled by these transcription factors (Backs *et al.* 2006; Kreusser *et al.* 2014).

Angiotensin receptor blockers (ARBs) are drugs which selectively block AT1R by directly preventing the binding of ATII and hence impedes downstream maladaptive signaling(Tamura *et al.* 2000). Numerous clinical trials with ARBs have suggested that this class of drugs are most effective in LVH regression(Cuspidi *et al.* 2008; Heinzel *et al.* 2015).

Based on this rationale, we used ATII as a reference Ca^{2+}-regulated hypertrophy trigger for comparison with FGF23(Mhatre *et al.* 2018).

It is shown that FGF23 exclusively activates FGFR4 on CMs to stimulate PLCγ/calcineurin/NFAT cell signaling(Grabner *et al.* 2015). FGFR4 is a receptor tyrosine kinase (RTK), phosphorylates PLCγ and leads to the generation of IP3. Production of IP3 stimulates Ca^{2+} from intracellular stores, especially nucleus. Furthermore, activation of FGFR4 is required for the FGF23-induced hypertrophy as FGFR4-specific blocking antibody prevents FGF23-induced cellular hypertrophy in NRVMs. These results are consistent with the *in vivo* studies demonstrating an absence of hypertrophy induced by FGF23 in FGFR4-/- mice(Grabner *et al.* 2015).

FGF23 acts on intracellular Ca^{2+} handling in a similar manner as ATII in CMs(Touchberry *et al.* 2013). Our results indicate the positive effect of FGF23 on both cytoplasmic as well as nuclear calcium cycling (Figure 5.15). Both ATII and FGF23 induced cell hypertrophy with respect to cell size along with similarities in Ca^{2+} changes (Figure 5.11). Interestingly, FGF23 triggered hypertrophic gene response along with an elevation in Ca^{2+} signal similar to ATII (Figure 5.12B, C). Additionally, FGF23 treatment showed a trend towards an increase in TGF-β gene expression in NRVMs, which is an important mediator of the fibrotic and hypertrophic response of the heart to ATII (Figure 5.12A). As stated earlier,

ATII activates CAMKII-HDAC-4 hypertrophic signaling via IICR mediated nuclear Ca^{2+} elevation. With immunoblotting experiments, we found that FGF23 too increased CAMKII-mediated HDAC-4 phosphorylation (Figure 5.13), suggesting nuclear Ca^{2+} involvement in FGF23-induced cellular hypertrophy. Thus, we observed similar effects of FGF23 on NRVMs compared to ATII, even though these two stimuli act via a different type of receptor(Mhatre *et al.* 2018).

We and others have previously shown that the nucleus surrounded by the nuclear envelope (NE) forms a compartment with differentially regulated Ca^{2+} signaling(Ljubojević *et al.* 2014). While the nucleus participates in global cytosolic Ca^{2+} changes during excitation-contraction coupling (ECC), amplitude and kinetics of nuclear Ca^{2+} transients may differ from the cytosols. This in part can be explained by the additional release of Ca^{2+} into the nucleus from the NE via IP3-receptors (IICR)(Wu *et al.* 2006; Ljubojević and Bers 2015). This excess nuclear Ca^{2+} has been shown to be important for hypertrophic signaling (Ljubojević *et al.* 2014; Hohendanner *et al.* 2015). While our results indicate an increase in nuclear [Ca^{2+}] and activation of Ca^{2+}-dependent nuclear signaling (HDAC4), where nuclear [Ca^{2+}] is sensitive to both the IP3 blockers (see below), the Ca^{2+}-dependent fluorescence signal is also influenced by the dye properties in the respective compartments(Ljubojević *et al.* 2011). Furthermore, to quantify the accurate difference between the groups and subcellular compartments, it would have been beneficial to do calibration and quantification using ratiometric Ca^{2+} dyes in order to negate the effects of the different subcellular environments on the characteristics of the Ca^{2+} dye and its loading(Ljubojević *et al.* 2011). However, our aim of this project was to compare the relation between cytosolic and nuclear Ca^{2+} signaling in response to different triggers in the same cells. The ratio of Ca^{2+} concentrations in the nucleus and cytosol in the present study is, therefore, a surrogate marker for differential changes in these compartments but not necessarily a ratio in absolute terms.

ATII modulates intracellular [Ca^{2+}] and influences CMs both *in vivo* and *in vitro*. Acute treatment with ATII on not only increases the three parameters in cytosol resting

intracellular Ca^{2+}, Ca^{2+} sparks, and wave frequency but also has a specific effect on nuclear Ca^{2+} in CMs(Wang *et al.* 2014). ATII increases nuclear systolic and diastolic Ca^{2+} vs. vehicle-treated CMs and this effect is aggravated in a LVH mice model(Ljubojević *et al.* 2014). As stated earlier, IP3 is known to regulate nuclear CaTs by localized Ca^{2+} release via IP3R located on the inner membrane of the nuclear envelope(Bootman *et al.* 2009; Ljubojević *et al.* 2014). Stimulation of AT1R, via classical cytosolic Gq signaling, involves the activation of phospholipase C-β (PLC-β) that leads to release of IP3 in the cytosol. The IP3-mediated perinuclear Ca^{2+} increase is involved in the expression of hypertrophic marker genes via translocation of histone deacetylases and activation of Ca^{2+}-regulated transcription factors leading to hypertrophy of the heart(Plačkić *et al.* 2016; Guatimosim *et al.* 2008; Ljubojević *et al*. 2014; Backs *et al.* 2006; Anderson *et al.* 2011). Essentially, ATII stimulation generates an increase in IP3 concentration which excites local nuclear Ca^{2+} release to induce LVH(Bootman *et al.* 2009; Arantes *et al.* 2012; Sedej *et al.* 2014)

The role of IICR in FGF23-mediated hypertrophy has not been tested so far. We planned to test this hypothesis in 1Hz paced NRVMs. Even though IP3 signaling may have a more prominent role in neonatal vs. (healthy) adult rat CMs (Louch *et al.* 2015), IP3-dependent signaling is similarly relevant for cardiac hypertrophy in adult CMs (Wu *et al.* 2006). We chose to study paced CMs, as the duality of large amounts of Ca^{2+} -induced Ca^{2+}release (CICR) during ECC and local Ca^{2+} signaling (IICR) for Ca^{2+}-dependent hypertrophic remodeling, is an important feature of differentiated beating CMs. In the present study, we show that similar to ATII, excess nuclear [Ca^{2+}] via IICR is involved in FGF23-induced hypertrophy (Figure 5.18, Figure 5.19).

2-APB is widely used IP3R blocker and majorly used to study IP3-mediated Ca^{2+}release in CMs(Kockskämper *et al.* 2008a; Luo *et al.* 2008; Hohendanner *et al.* 2015). Like many pharmacological IP3R inhibitors, 2-APB suffer from variable degrees of specificity and unwanted side effects(Kockskämper *et al.* 2008a). In addition to its effects on IP3-induced Ca^{2+} release, it has been shown to have nonspecific effects on Ca^{2+} signaling

mechanisms such as store-operated channels (SOC) (Bootman *et al.* 2002). However, these side effects have been observed on a higher concentration of 2-APB (Bootman *et al.* 2002). In all our experiments, we have used 2-APB in the range of 5-10μM concentration. Furthermore, 2-APB had a specific effect on CaT AUC ratio than on CaT amplitude ratio (Figure 5.20), thus discrediting its side effect on SOCE (Bilmen *et al.* 2002; Hohendanner *et al.* 2014). Though limited specificity of all current IP3R blockers warrants caution in the interpretation of pharmacological IP3R inhibition, to address this concern, we confirmed the experiments using another IP3R blocker, Xestospongin C. (Xest.C., 10μM). Xestospongins are the commonly used membrane-permeant IP3R antagonists (Gafni *et al.* 1997). Pre-treatment with Xest. C. attenuated both FGF23-induced nuclear as well as cytoplasmic changes with respect to CaT peak amplitude and CaT AUC (Figure 5.21). Thus, both InsP3R blockers corroborate the observation of FGF23-induced IP3-IP3R specific nuclear Ca^{2+} release.

The distinct features of nuclear IP3-IP3R signaling include prolonged and sustained nuclear CaT response along with greater basal spark rate and higher sparks due to IP3 on GPCR stimulation changing the nuclear Ca^{2+} dynamics(Hohendanner *et al.* 2014). Our Ca^{2+} imaging experiments demonstrated a similar increase in nuclear along with cytoplasmic CaT AUC in ATII-treated CMs (Figure 5.15). However, we found significantly more cells with nuclear sparks in the ATII treatment group vs. the vehicle-treated control group (Figure 5.16B). In parallel experiments, FGF23-induced comparable augmentation in nuclear CaT (Figure 5.19, Figure 5.20) along with a similar increase in cells with nuclear sparks in the FGF23 treatment group (Figure 5.16A, B). Furthermore, spark frequency within the nucleus; was significantly increased in FGF23-treated cells vs. control cells (Figure 5.16C). Thus, like ATII, the rise in nuclear local Ca^{2+} release and CaT may be involved in instigating FGF23-induced hypertrophy in NRVMs(Mhatre *et al.* 2018).

Based on the similarity between cellular effects of FGF23 and ATII, we hypothesized that there must be an overlap between the FGF23 and ATII mediated Ca^{2+}-hypertrophy signaling.

To investigate this hypothesis, we used Losartan, which is an AT1R antagonist and a competitive inhibitor of ATII signaling. It inhibits the rapid internalization of AT1R upon agonist stimulation with ATII, thus inhibiting further downstream pathological signaling. *In vivo*, it inhibits hypertrophy induced by ATII in CMs from spontaneously hypertensive rat models as well as in individual CMs under stress conditions like a mechanical stretch(Sadoshima *et al.* 1993; Cerbai *et al.* 2000).

In addition to its canonical effect, strikingly, losartan seemed to protect the CMs from the hypertrophic effect of FGF23. We discovered that losartan inhibited changes in cytoplasmic Ca^{2+} homeostasis induced by FGF23 and had a similar inhibitory effect on nuclear CaT with respect to FGF23 treatment (Figure 5.22). Furthermore, losartan not only interfered with the FGF23 induced nuclear Ca^{2+} changes but also inhibits successive cell hypertrophy with respect to cell size (Figure 5.23) and hypertrophic gene upregulation (Figure 5.24). Overall, these results indicate the possible involvement of ATII-AT1R signaling in FGF23 activity(Mhatre *et al.* 2018).

Additionally, other groups and our experiments have revealed that FGFR4 has weak kinase activity that results in less pronounced auto-phosphorylation and weaker phosphorylation of PLCγ on the binding of FGF23(Grabner *et al.* 2015) (Figure 5.25). We also showed that losartan did not have an effect on FGF23-FGFR4 activity by studying its effect on PLCγ phosphorylation (Figure 5.25). This suggests that the IP3 involved in FGF23 induced hypertrophy (Figure 5.19) may be due to the coupling of other isoforms of PLC with PLCγ activation or simultaneous activation of other signaling pathway having overlapping secondary messengers. Thus, in FGF23 hypertrophic signaling, ATII might be acting upstream to activate PLCβ-IP3 activation further leading to Ca^{2+}-mediated hypertrophy(Mhatre *et al.* 2018).

RAAS is activated in various pathological conditions, such as hypertension, diabetes, obesity, and other cardiovascular conditions. It plays a significant role in the etiology and morbidity associated with these diseases(Paul *et al.* 2006). ATII is classically synthesized in the circulation by the sequential cleavage steps of kidney-derived renin and

endothelium-anchored angiotensin-converting enzyme (ACE) on liver-generated angiotensinogen (AGT) (Figure 2.9). However, several components of the RAAS are found in different tissues. This has led to a concept of a tissue or local RAAS, whose regulation is independent of the systemic RAAS(Dostal and Baker 1999). Most cell types have ATII type 1 (AT1) receptors on their plasma membranes, via which locally synthesized ATII may act in an autocrine/ paracrine manner.

Although, the site of ATII synthesis, whether it is intracellular and/or extracellular is debatable (Dostal and Baker 1999). We and other groups have shown that ATII can be produced intracellularly and possibly secreted by cultured NRVMs as the effect of the different stimulus. CMs do express angiotensinogen, Angiotensin-converting enzyme (ACE) and renin (chymase)(Malhotra *et al.* 1999). ATII has been shown to act from an intracellular location as an intracrine peptide in neonatal and adult CMs and fibroblasts, inducing CM growth and hypertrophy(Baker *et al.* 2004; Baker and Kumar 2006). Furthermore, the levels of intracellular ATII in CMs is altered during cardiomyopathies and the increased levels of intracellular ATII have shown to play a role in the induction of hypertrophy in CMs(Baker *et al.* 2004).

Based on this background, we wanted to investigate the underlying molecular mechanism for the potential activation of the ATII-AT1R pathway by FGF23. We investigated this possibility by studying the formation of intracellular ATII in FGF23 treated NRVM. We provide proof by immunostaining experiments that FGF23 treated CMs had increased intracellular formation of ATII in a time-dependent fashion. We observed FGF23-induced sustained increase of ATII levels in CMs after, as early as, 90 min (Figure 5.26) and at 24h (Figure 5.27) as compared to vehicle-treated control cells. However, a systematic study is warranted of the ATII synthesis pathway in CM treated with FGF23. Angiotensinogen (ATG) gene-specific transcription factor, ATG gene expression, ATII synthesis specific enzyme expression and activity should be studied with respect to FGF23 stimulus. Nonetheless, it still needs to be tested with good control where we still observe FGF23-induced hypertrophic effect if we eliminate FGF23 ability to activate

intracellular ATII by gene deletion. Largely, our results indicate that FGF23-induced activation of ATII synthesis in ventricular CMs(Mhatre *et al.* 2018).

There are number of hypothesis about how the ATII can act as an intracrine peptide in CMs to induce hypertrophy. One of them is the via cognate AT1Rs present on nuclear membrane accompanying corresponding AT1Rs located on the plasma membrane in CMs. The preferential nuclear signaling observed in ATII treatment might be due to the presence of AT1R on the inner nuclear membrane (Tadevosyan *et al.* 2010). There is a possibility that nuclear AT1R might couple with IP3R to induce nuclear signaling pathways and regulate transcription involved in hypertrophy. In addition, the nuclear AT1R expression levels have shown to increase along with intracellular ATII in cardiac fibroblast in the heart failure animal model, but it is still to be explored in CMs(Tadevosyan *et al.* 2017). The mechanism of access and binding of the mature ATII peptide to the ligand-binding site of their cognate receptor located within the perinuclear space is not clear. Possibilities include intracellular biosynthesis and maturation of ATII in cytoplasm followed by active or passive transport across the nuclear membrane in CMs. Hence, there is the possibility of FGF23 stimulation increasing intracellular ATII, which may act as an intracrine ligand able to trigger an IP3 mediated release of Ca^{2+} from perinuclear stores and regulating hypertrophic transcription.

One more mechanism to explain the FGF23-ATII interaction is activation of FGFR4, via AT1R. This phenomenon is called transactivation where GPCR on stimulation with its ligand can activate neighboring RTKs. It is quite common in different cell type for activation of GPCRs to stimulate growth factor RTKs in the absence of added growth factor and is an important pathway that contributes to the growth-promoting activity of many GPCR ligands(Wisler *et al.* 2015). Reciprocally, an increasing body of evidence has revealed that RTKs utilize GPCR signaling molecules to transduce signals and that RTK ligands themselves can transactivate GPCRs. This process which places GPCR signaling downstream of RTKs requires the production of a GPCR ligand of the transactivated GPCR Activation of GPCR by activated RTK by synthesis and secretion of

the ligand (Mira *et al.* 2001). A likely strategy to check this in case of FGF23-ATII signaling would be to compare the FGF23 effect on CMs from wild-type with transgenic animals that lack cardiac AT1R or by silencing AT1R. However, it stands to be tested if FGF23 leads to secretion of this surplus ATII and this ATII acts in an autocrine manner to induce FGF23 -mediated hypertrophic effects.

There are few studies that have demonstrated that ATII is not only synthesized intracellularly by CMs but also secreted (Sadoshima *et al.* 1993). However, the ATII secretion mechanism and its regulation in CMs are still unknown. CMs have shown to secrete different signaling molecules via exosomes under different stressor like stretch, hypoxia(Pironti *et al.* 2015). These signaling molecules may include angiogenic, pro-survival factors, miRNAs etc. This activity is essential for communication between different cell types in heart and induces repair and healing of the infarcted myocardium. IP3Rs are prominently expressed in classical secretory cells including exocrine cells of the pancreas, salivary glands etc.(Futatsugi *et al.* 2005). IP3 stimulation during hypertrophy is proposed to be involved in secretion from CMs too. Secretory granules act as an IP3-sensitive intracellular Ca^{2+} store. IP3-mediated Ca^{2+} release from secretory granules in CMs contributes to secretion of chromogranins and natriuretic peptides, aggravating pathological hypertrophy(Heidrich *et al.* 2008). Thus, there is a possibility of FGF23-induced IP3 to play a role in the secretion of ATII by CMs. In this case, ATII could act in an autocrine manner inducing a downstream cascade of FGF23 triggered hypertrophic signaling. However, it is not yet clear whether this action of ATII is due to the secretory or non-secretory pathway in the case of FGF23 stimulation.

Therefore, to answer this question, we tried to detect secreted ATII in the conditioned medium from CMs treated with FGF23. ATII is a small octapeptide, so it is difficult to detect the peptide using standard methods like Western blot. Further, commercial available ATII ELISA is low on specificity where it can detect other peptides (Ang1-7, Ang III, and Ang IV) formed on further digestion of ATII. In this study, *MALDI TOF*/*TOF* tandem mass spectrometry method was used. This approach has the advantage of being highly

specific and robust due to the assignment of the target compound by mass, thereby eliminating cross-reactivity as a source of error (Cui *et al.* 2007). Thus, this approach was used to specifically detect the presence of angiotensin (ATII) depending on its molecular weight as oppose to Ang1-7, AngIII, and AngIV in our samples.

Remarkably, we could detect secreted ATII in processed conditioned medium from NRVMs incubated with FGF23 using *MALDI TOF*/*TOF* tandem mass spectrometry technique (Figure 5.28B). An ATII peptide-specific peak in mass spectra at m/z 1046.562 was observed (Figure 5.28C). In contrast, no ATII peptide was detected in the processed supernatant from untreated NRVMs (Figure 5.28A, C). Thus, indeed FGF23 induces ATII secretion in CMs. These results also suggest that in FGF23 treated NRVMs, ATII peptide was synthesized in the secretory pathway possibly involving ACE (Singh *et al.* 2007). Overall, our results indicate an activation of production, secretion, and signaling of ATII in FGF23-mediated hypertrophy in ventricular CMs(Mhatre *et al.* 2018).

These studies confirm an unexpected involvement of ATII secretion in the FGF23-dependent induction of hypertrophy in NVRMs. Our results suggest that the local cardiac renin-angiotensin system is activated in CMs on the FGF23 action. It seems like FGF23 acts as a bystander while stimulated ATII, in an autocrine manner triggers an IP3 mediated release of Ca^{2+} from perinuclear stores and regulate hypertrophic transcription. However, the secretory pathway of intracellular ATII and its regulation in FGF23/FGFR4-induced Ca^{2+} mediated hypertrophy remains to be elucidated in detail(Mhatre *et al.* 2018).

Based on the evidence collected in this study, we propose that, at least in the cultured neonatal cardiac myocytes, ATII is the initial mediator of the FGF23 triggered response and activates the subsequent autocrine/paracrine production of other factors, which may act in concert to produce hypertrophic responses. As summarized in Figure 6.1, FGF23 activates ATII signaling pathway by an increase of ATII formation and its secretion in cardiomyocytes.

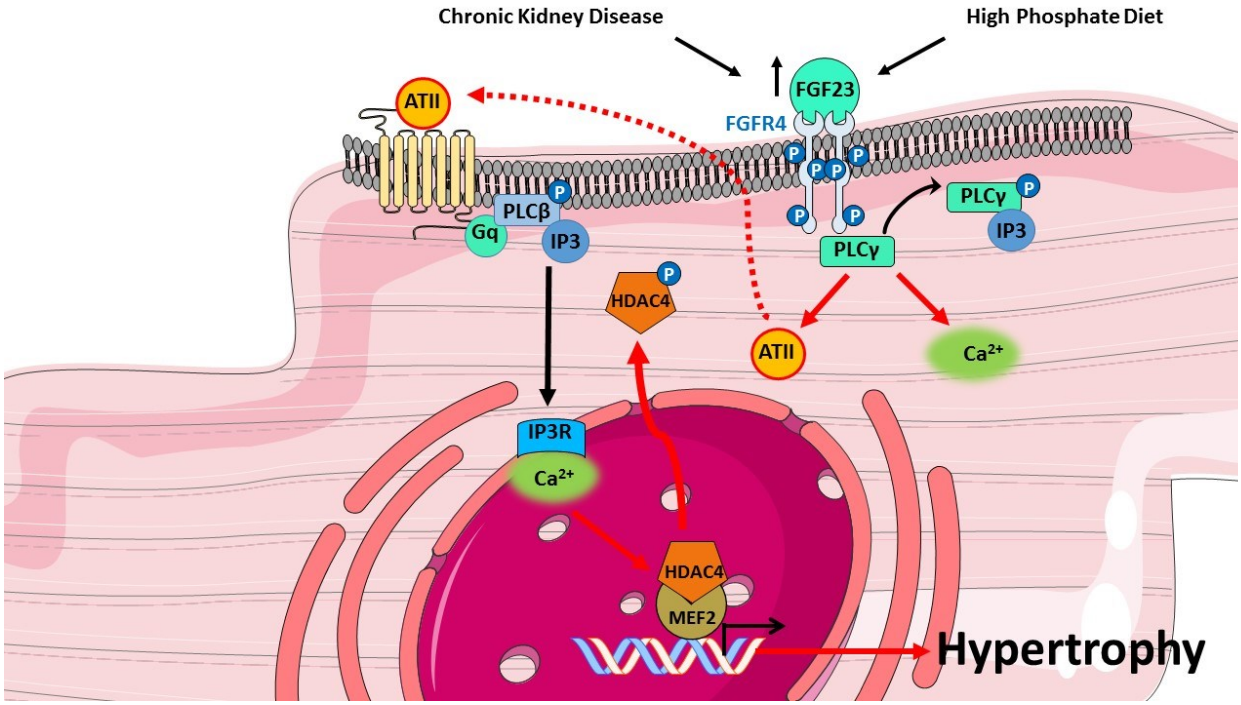

Figure 6.1 Crosstalk between Ca^{2+}-mediated hypertrophic signaling by ATII and FGF23 in cardiomyocytes

Schematic diagram depicting the proposed activation of ATII signaling pathway by which FGF23/FGFR4 stimulates cardiac hypertrophy. Current studies support a model whereby FGF23 activates formation and secretion of ATII from cardiomyocytes, which in an autocrine manner lead to the subsequent stimulation of IP3-nuclear Ca^{2+}-CAMKII-HDAC4 mediated pathways resulting in cellular hypertrophy. ATII indicates Angiotensin II; ATIIR, Angiotensin type1 receptor; PLC-β/γ, Phospholipase C- β/γ; IP3, inositol 1, 4, 5-triphosphate; CAMKII, Ca2+/calmodulin-dependent protein kinase II; HDAC-4, Histone deacetylase-4; MEF-2, Myocyte enhancer factor-2. The novel findings are highlighted with red arrows.

Simultaneously, there is an IP3-mediated Ca^{2+} release from nucleoplasm on FGF23 stimulation, which mediates Ca^{2+}-dependent hypertrophic signaling in cardiomyocytes. Cooperatively, both events might play an important role in cellular hypertrophy triggered by FGF23. Thus, our results provide direct proof that the local renin-angiotensin system plays a pathophysiological role in FGF23 effect on cardiomyocytes. It opens up a different

aspect of the FGF23-FGFR4 pathway in eliciting cardiac hypertrophy, which can be further investigated *in vivo* and in patients.

6.1. Limitations and future directions:

We used NRVMs as the established model to study cellular hypertrophy and Ca^{2+} signaling as ARVMs in culture were much less responsive to our hypertrophic stimuli. Our result provide the basis for future studies to investigate the role of ATII blockers in FGF-mediated hypertrophy but need to be validated *in vivo*. However, we chose the cell model for proof-of-concept because mechanistic interpretation of such *in vivo* experiments is complicated by the systemic effects of FGF23 on RAAS signaling(Kovesdy and Quarles 2016).

However, further studies are required in vivo, validating correlation of levels of circulating FGF23 and myocardial ATII levels. The process of ATII formation and secretion induced by FGF23 should be elucidated in details. The expression and regulation of angiotensinogen, renin and chymase should be screened in cardiomyocytes following FGF23 stimulation. The crosstalk or transactivation possibilities between FGF23 and ATII receptor should be further investigated. If ATII is essential for FGF23-induced hypertrophy should be tested in appropriate model. The CAMKII-HDAC4 pathway and gene program activation by FGF23 should be further explored.

6.2. Clinical relevance:

Cardiac hypertrophy is an adaptive response of the heart most commonly to hypertension. It is an independent risk factor for heart failure. The study of underlying cellular mechanisms is crucial for developing new treatment strategies and improving the prognosis of multi-morbidity disease like heart failure.

There is a prognostic role of FGF23 in individuals with heart failure. Studies have shown that circulating FGF23 concentrations are elevated in heart failure patients, correlate with heart failure severity and poor outcomes, even among individuals with preserved kidney

function. FGF23 has been found to be expressed in heart tissue. FGF23 expression and secretion in myocardial tissue markedly increased after induction of experimental myocardial infarction in rats(Wohlfahrt *et al.* 2015). The expression levels of FGFR4, calcineurin, and NFAT are elevated in myocardial tissue of patients with CKD and positively correlates with the presence of LVH, suggesting that this FGF23 driven pro-hypertrophic pathway also exists in humans(Leifheit-Nestler *et al.* 2016). Faul and group have indicated possible treatment for FGF23-induced hypertrophy(Faul *et al.* 2011; Grabner *et al.* 2015) LVH induced by FGF23 is found to be reversible, on the removal of the trigger. Anti-FGFR4 treatment of NXT rat completely prevented progression of LVH, but no difference in cardiac collagen deposition and cardiac function(Grabner *et al.* 2017).

Unfortunately, current therapeutic approaches in CKD and end-stage renal diseases inadequately control pathological cardiac remodeling and heart failure. Current manuscript and our earlier work support the observation that altered state of nucleoplasmic [Ca^{2+}] is an early event during hypertrophy acting via CaMKII-HDAC4 transcription pathway and may contribute to the development and progression of heart failure. Hence, correction of impaired nucleoplasmic [Ca^{2+}] regulation mediated transcription pathway in the case of patients with high FGF23 levels may be a possible therapeutic approach (Ljubojević *et al.* 2014).

Here we found an additional factor, ATII to be involved in development and progression of LVH in CKD and suggest a novel pathway, which can be targeted to reduce the burden of cardiovascular diseases in this high-risk population. In the heart, blood pressure-independent cardioprotective effects of angiotensin receptor blockers (ARBs) and angiotensin-converting enzyme (ACEi) inhibitors therapy have demonstrated the significance of the cardiac RAS (Dostal and Baker 1999). Based on our data and other studies, increased FGF23 may identify a subset of HF patients benefiting from ARB therapy(Wohlfahrt *et al.* 2015). Thus, reemphasizing the prognostic value of FGF23 in the treatment of HF.

The question of intracellular ATII synthesis is important not only to elucidate the intracrine system but, also, from the perspective of therapeutic inhibition of the local RAS by commonly used ACE inhibitors and the potential use of renin and chymase inhibitors. The involvement of renin and ACE in intracellular synthesis of ATII would require further study in view of the secretory and membranous nature of these enzymes.

There is substantial evidence that there are internal pools of GPCRs like AT1R on nucleolemma and they are involved in maladaptive signaling(Tadevosyan *et al.* 2010). Pharmaceutical ligands selectively targeted to nuclear GPCRs would open up a novel range of drugs. Delivery of such precision drugs to the right address will insulate the signal within the cell, which could greatly increase the efficacy and reduce the side effects.

7. Conclusion

Exciting recent research related to FGF23 has elevated it into one of the most intensively studied proteins, implicated in the link between cardiovascular disease and chronic kidney disease. However, this is the first study (to our knowledge) to show a mechanistic link between FGF23 and local RAAS in cardiomyocytes with respect to cardiac hypertrophy. It is well established that FGF23/FGFR4 pathway causes left ventricular hypertrophy. The expression levels of FGF23 in serum and specific receptor FGFR4 in myocardial tissue are elevated in HF patients and positively correlates with the presence of LVH, suggesting FGF23 driven pro-hypertrophic pathway in HF(Leifheit-Nestler *et al.* 2016). The evidence collected in this study does imply that convergence of FGF23 and ATII signaling is essential for FGF23-induced cardiomyocyte hypertrophy. In fact, we could not only demonstrate that FGF23 induces similar effects like ATII on ventricular cardiomyocytes for e.g. cellular hypertrophy, fetal gene response, changes in nuclear Ca^{2+} handling but FGF23 can also induce ATII synthesis and secretion. Our findings thus led to the conclusion that, ATII plays an essential role in the development and progression of FGF23-induced cellular hypertrophy. Not only that local RAAS in context with FGF23 needs further experimental attention, but also targeting local RAAS may provide powerful means to prevent maladaptive cardiac remodeling and its progression to heart failure in CKD patients. To this end, the key findings of this thesis provide new incentives to further elucidate the full spectrum of ways that excess FGF23 impacts cardiac function and how this may ultimately contribute to the pathophysiology of heart failure in CKD.

8. References

Ai, X., Curran, J.W., Shannon, T.R., Bers, D.M., and Pogwizd, S.M., 2005. Ca2+/calmodulin-dependent protein kinase modulates cardiac ryanodine receptor phosphorylation and sarcoplasmic reticulum Ca2+ leak in heart failure. *Circulation Research*, 97 (12), 1314–1322.

Anderson, M.E., Brown, J.H., and Bers, D.M., 2011. CaMKII in myocardial hypertrophy and heart failure. *Journal of Molecular and Cellular Cardiology*, 51 (4), 468–473.

Angelin, B., Larsson, T.E., and Rudling, M., 2012. Circulating fibroblast growth factors as metabolic regulators--a critical appraisal. *Cell metabolism*, 16 (6), 693–705.

Anger, M., Lompre, A., Vallot, O., Marotte, F., Rappaport, L., and Samuel, J., 1998. Cellular Distribution of Ca2+ Pumps and Ca2+ Release Channels in Rat Cardiac Hypertrophy Induced by Aortic Stenosis.*Circulation,* 98 (22), 2477-2486.

Antoons, G., Willems, R., and Sipido, K.R., 2012. Alternative strategies in arrhythmia therapy: Evaluation of Na/Ca exchange as an anti-arrhythmic target. *Pharmacology and Therapeutics*, 134 (1), 26–42.

Arantes, L. A., Aguiar, C.J., Amaya, M.J., Figueiró, N.C.G., Andrade, L.M., Rocha-Resende, C., Resende, R.R., Franchini, K.G., Guatimosim, S., and Leite, M.F., 2012. Nuclear inositol 1,4,5-trisphosphate is a necessary and conserved signal for the induction of both pathological and physiological cardiomyocyte hypertrophy. *Journal of Molecular and Cellular Cardiology*, 53 (4), 475–486.

Archer, C.R., Robinson, E.L., Drawnel, F.M., and Roderick, H.L., 2017. Endothelin-1 promotes hypertrophic remodelling of cardiac myocytes by activating sustained signalling and transcription downstream of endothelin type A receptors. *Cellular Signalling*, 36, 240–254.

Backs, J. and Olson, E.N., 2006. Control of cardiac growth by histone acetylation/deacetylation. *Circulation Research*, 98 (1), 15–24.

Backs, J., Backs, T., Neef, S., Kreusser, M.M., Lehmann, L.H., Patrick, D.M., Grueter, C.E., Qi, X., Richardson, J.A., Hill, J.A., Katus, H.A., Bassel-Duby, R., Maier, L.S., and Olson, E.N., 2009. The delta isoform of CaM kinase II is required for pathological cardiac hypertrophy and remodeling after pressure overload. *Proceedings of the National Academy of Sciences*, 106 (7), 2342–2347.

Backs, J., Song, K., Bezprozvannaya, S., Chang, S., and Olson, E.N., 2006. CaM kinase II selectively signals to histone deacetylase 4 during cardiomyocyte hypertrophy. *Journal of Clinical Investigation*, 116 (7), 1853–1864.

Baker, K.M., and Kumar, R., 2006. Intracellular angiotensin II induces cell proliferation independent of AT 1 receptor. *American Journal of Physiology-Cell Physiology* , 291, C995–C100.

Baker, K.M., Chernin, M.I., Schreiber, T., Sanghi, S., Haiderzaidi, S., Booz, G.W., Dostal, D.E., and Kumar, R., 2004. Evidence of a novel intracrine mechanism in angiotensin II-induced cardiac hypertrophy. *Regulatory Peptides*, 120 (1–3), 5–13.

Balijepalli, R.C., Foell, J.D., Hall, D.D., Hell, J.W., and Kamp, T.J., 2006. Localization of cardiac L-type Ca2+ channels to a caveolar macromolecular signaling complex is required for {beta}2-adrenergic regulation. *Proceedings of the National Academy of Sciences*, 103 (19), 7500-7505.

Bare, D.J., Kettlun, C.S., Liang, M., Bers, D.M., and Mignery, G.A., 2005. Cardiac type 2 inositol 1,4,5-trisphosphate receptor: interaction and modulation by calcium/calmodulin-dependent protein kinase II. *Journal of Biological Chemistry*, 280 (16), 15912–15920.

Barry, S.P., Davidson, S.M., and Townsend, P.A., 2008. Molecular regulation of

cardiac hypertrophy. *International Journal of Biochemistry and Cell Biology*, 40 (10), 2023–2039.

Berridge, M.J., Bootman, M.D., and Roderick, H.L., 2003. Calcium Signalling: dynamics, homeostasis and remodelling. *Nature Reviews Molecular Cell Biology*, 4(7), 517-29.

Bers, D.M., 2000. Calcium fluxes involved in control of cardiac myocyte contraction. *Circulation Research*, 87 (4), 275–281.

Bers, D.M., 2001. Excitation-contraction coupling and cardiac contractile force. *Kluwer Academic Publisher*, 161–162.

Bers, D.M., 2002. Cardiac excitation-contraction coupling. *Nature,* 415(6868), 198-205.

Bers, D.M., 2006. Altered Cardiac Myocyte Ca Regulation In Heart Failure. *Physiology*, 21 (6), 380–387.

Bers, D.M., 2008. Calcium Cycling and Signaling in Cardiac Myocytes. *Annual Review of Physiology*, 70 (1), 23–49.

Bers, D.M., 2014. Cardiac Sarcoplasmic Reticulum Calcium Leak: Basis and Roles in Cardiac Dysfunction. *Annual Review of Physiology*, 76 (1), 107–127.

Bilmen, J.G., Wootton, L.L., Godfrey, R.E., Smart, O.S., and Michelangeli, F., 2002. Inhibition of SERCA Ca2+ pumps by 2-aminoethoxydiphenyl borate (2-APB): 2-APB reduces both Ca2+ binding and phosphoryl transfer from ATP, by interfering with the pathway leading to the Ca2+-binding sites. *European Journal of Biochemistry*, 269 (15), 3678–3687.

Bisping, E., Ikeda, S., Kong, S.W., Tarnavski, O., Bodyak, N., McMullen, J.R., Rajagopal, S., Son, J.K., Ma, Q., Springer, Z., Kang, P.M., Izumo, S., and Pu, W.T.,

2006. Gata4 is required for maintenance of postnatal cardiac function and protection from pressure overload-induced heart failure. *Proceedings of the National Academy of Sciences of the United States of America*, 103 (39), 14471–14476.

Bisping, E., Wakula, P., Poteser, M., and Heinzel, F.R., 2014. Targeting Cardiac Hypertrophy : Toward a Causal Heart Failure Therapy. *Journal of Cardiovascular Pharmacology* , 64 (4), 293–305.

Blaustein, M.P. and Lederer, W.J., 1999. Sodium calcium exchange: Its physiological implications. *Physiological Reviews*, 79 (3), 763–854.

Bobenko, A., Bartels, I., Münch, M., Trippel, T., Lindhorst, R., Nolte, K., Herrmann-Lingen, C., Halle, M., Duvinage, A., Düngen, H. D., Gelbrich, G., Tschöpe, C., Hasenfuss, G., Wachter, R., Pieske, B., and Edelmann, F., 2018. Amount or intensity? Potential targets of exercise interventions in patients with heart failure with preserved ejection fraction. *ESC Heart Failure*, 5(1), 53-62.

Bodi, I., Mikala, G., Koch, S.E., Akhter, S. A., and Schwartz, A., 2005. The L-type calcium channel in the heart : the beat goes on. *Journal of Clinical Investigation*, 115(12), 3306-3317.

Bootman, M.D., Collins, T.J., Mackenzie, L., Roderick, H.L., Berridge, M.J., and Peppiatt, C.M., 2002. 2-aminoethoxydiphenyl borate (2-APB) is a reliable blocker of store-operated Ca2+ entry but an inconsistent inhibitor of InsP3-induced Ca2+ release. *The FASEB journal : official publication of the Federation of American Societies for Experimental Biology*, 16 (10), 1145–1150.

Bootman, M.D., Fearnley, C., Smyrnias, I., MacDonald, F., and Roderick, H.L., 2009. An update on nuclear calcium signalling. *Journal of Cell Science*, 122 (14), 2337–2350.

Cerbai, E., Crucitti, A., Sartiani, L., De Paoli, P., Pino, R., Rodriguez, M.L., Gensini,

G., and Mugelli, A., 2000. Long-term treatment of spontaneously hypertensive rats with losartan and electrophysiological remodeling of cardiac myocytes. *Cardiovascular Research*, 45 (2), 388–396.

Chow, B.S.M. and Allen, T.J., 2016. Angiotensin II type 2 receptor (AT2R) in renal and cardiovascular disease. *Clinical Science*, 130 (15), 1307–1326.

Correll, R.N., Makarewich, C.A., Zhang, H., Zhang, C., Sargent, M.A., York, A.J., Berretta, R.M., Chen, X., Houser, S.R., and Molkentin, J.D., 2017. Caveolae-localized L-type Ca2+ channels do not contribute to function or hypertrophic signalling in the mouse heart. *Cardiovascular Research*, 113 (7), 749–759.

Cui, L., Nithipatikom, K., and Campbell, W.B., 2007. Simultaneous Analysis of Angiotensin Peptides by LC-MS and LC- MS/MS: Metabolism by Bovine Adrenal Endothelial Cells. *Analytical Biochemistry*, 369 (1), 27–33.

Cuspidi, C., Negri, F., and Zanchetti, A., 2008. Angiotensin II receptor blockers and cardiovascular protection: Focus on left ventricular hypertrophy regression and atrial fibrillation prevention. *Vascular Health and Risk Management*, 4 (1), 67–73.

Dambrot, C., Braam, S.R., Tertoolen, L.G.J., Birket, M., Atsma, D.E., and Mummery, C.L., 2014. Serum supplemented culture medium masks hypertrophic phenotypes in human pluripotent stem cell derived cardiomyocytes. *Journal of Cellular and Molecular Medicine*, 18 (8), 1509–1518.

Dewenter, M., Von Der Lieth, A., Katus, H.A., and Backs, J., 2017. Calcium signaling and transcriptional regulation in cardiomyocytes. *Circulation Research*, 121 (8), 1000–1020.

Di Giuseppe, R., Buijsse, B., Hirche, F., Wirth, J., Arregui, M., Westphal, S., Isermann, B., Hense, H.W., Dierkes, J., Boeing, H., Stangl, G.I., and Weikert, C., 2014. Plasma fibroblast growth factor 23, parathyroid hormone, 25-hydroxyvitamin D3, and risk of

heart failure: A prospective, case-cohort study. *Journal of Clinical Endocrinology and Metabolism*, 99 (3), 947–955.

Di Marco, G.S., Reuter, S., Kentrup, D., Grabner, A., Amaral, A.P., Fobker, M., Stypmann, J., Pavenstädt, H., Wolf, M., Faul, C., and Brand, M., 2014. Treatment of established left ventricular hypertrophy with fibroblast growth factor receptor blockade in an animal model of CKD. *Nephrology Dialysis Transplantation*, 29 (11), 2028–2035.

Dickstein, K., Cohen-Solal, A., Filippatos, G., McMurray, J.J.V., Ponikowski, P., Poole-Wilson, P.A., Strömberg, A., van Veldhuisen, D.J., Atar, D., Hoes, A.W., Keren, A., Mebazaa, A., Nieminen, M., Priori, S.G., Swedberg, K., Vahanian, A., Camm, J., De Caterina, R., Dean, V., Dickstein, K., Filippatos, G., Funck-Brentano, C., Hellemans, I., Kristensen, S.D., McGregor, K., Sechtem, U., Silber, S., Tendera, M., Widimsky, P., Zamorano, J.L., Tendera, M., Auricchio, A., Bax, J., Böhm, M., Corrà, U., della Bella, P., Elliott, P.M., Follath, F., Gheorghiade, M., Hasin, Y., Hernborg, A., Jaarsma, T., Komajda, M., Kornowski, R., Piepoli, M., Prendergast, B., Tavazzi, L., Vachiery, J.L., Verheugt, F.W.A., and Zannad, F., 2008. ESC Guidelines for the diagnosis and treatment of acute and chronic heart failure 2008. The Task Force for the Diagnosis and Treatment of Acute and Chronic Heart Failure 2008 of the European Society of Cardiology. Developed in collaboration with the Heart. *European Journal of Heart Failure*, 10 (10), 933–989.

Dolmetsch, R.E., Lewis, R.S., Goodnow, C.C., and Healy, J.I., 1997. Differential activation of transcription factors induced by Ca2+ response amplitude and duration. *Nature*, 386(6627), 855-858.

Dolmetsch, R.E., Xu, K., and Lewis, R., 1998. Calcium oscillations increase the efficiency and specificity of gene expression. *Nature*, 392(6679), 933-936.

Dorn II, G.W., Force, T., and Ii, G.W.D., 2005. Protein kinase cascades in the regulation of cardiac hypertrophy. *Journal of Clinical Investigation*, 115 (3), 527–537.

Dostal, D. and Baker, K., 1999. The cardiac rennin-angiotensin system conceptual, or a regulator of cardiac function? *Circulation Research*, 97, 1037–1041.

Dunlay, S.M., Pereira, N.L., and Kushwaha, S.S., 2014. Contemporary Strategies in the Diagnosis and Management of Heart Failure. *Mayo Clinic Proceedings*, 89(5), 662-676.

Eckardt, K.U., Coresh, J., Devuyst, O., Johnson, R.J., Köttgen, A., Levey, A.S., and Levin, A., 2013. Evolving importance of kidney disease: From subspecialty to global health burden. *The Lancet*, 382 (9887), 158–169.

Edelmann, F., 2015. Facts and numbers on epidemiology and pharmacological treatment of heart failure with preserved ejection fraction. *ESC Heart Failure*, 2 (2), 41–45.

Engelhardt, S., Hein, L., Wiesmann, F., and Lohse, M.J., 1999. Progressive hypertrophy and heart failure in beta1-adrenergic receptor transgenic mice. *Proceedings of the National Academy of Sciences of the United States of America*, 96 (12), 7059–7064.

Escobar, M., Cardenas, C., Colavita, K., Petrenko, N.B., and Franzini-Armstrong, C., 2011. Structural evidence for perinuclear calcium microdomains in cardiac myocytes. *Journal of Molecular and Cellular Cardiology*, 50 (3), 451–459.

Eswarakumar, V.P., Lax, I., and Schlessinger, J., 2005. Cellular signaling by fibroblast growth factor receptors. *Cytokine and Growth Factor Reviews*, 16 (2), 139–149.

Faul, C., 2012. Fibroblast growth factor 23 and the heart. *Current Opinion in Nephrology and Hypertension*, 21 (4), 369–375.

Faul, C., Amaral, A.P., Oskouei, B., Hu, M., Sloan, A., Isakova, T., Gutiérrez, O.M., Aguillon-prada, R., Lincoln, J., Hare, J.M., Mundel, P., Morales, A., Scialla, J., Fischer, M., Soliman, E.Z., Feldman, H.I., St, M., Sutton, J., Ojo, A., Gadegbeku, C., Seno, G.,

Marco, D., Reuter, S., Kentrup, D., Tiemann, K., Brand, M., Hill, J. A., Moe, O.W., Kuro-o, M., Kusek, J.W., Keane, M.G., and Wolf, M., 2011. FGF23 induces left ventricular hypertrophy. *Journal of Clinical Investigation*, 121 (11), 4393–4408.

Ferrario, C.M., Trask, A.J., and Jessup, J.A., 2005. Advances in biochemical and functional roles of angiotensin-converting enzyme 2 and angiotensin-(1–7) in regulation of cardiovascular function. *American Journal of Physiology-Heart and Circulatory Physiology*, 289 (6), 2281–2290.

Frey, N., McKinsey, T.A., and Olson, E.N., 2000. Decoding calcium signals involved in cardiac growth and function. *Nature Medicine*, 6 (11), 1221–1227.

Fricker, M., Hollinshead, M., White, N., and Vaux, D., 1997. Interphase nuclei of many mammalian cell types contain deep, dynamic, tubular membrane-bound invaginations of the nuclear envelope. *Journal of Cell Biology*, 136 (3), 531–544.

Futatsugi, A., Nakamura, T., Yamada, M.K., Ebisui, E., Nakamura, K., Uchida, K., Kitaguchi, T., Takahashi-Iwanaga, H., Noda, T., Aruga, J., and Mikoshiba, K., 2005. IP3 receptor types 2 and 3 mediate exocrine secretion underlying energy metabolism. *Science*, 309 (5744), 2232–4.

Gaasch, W.H. and Little, W.C., 2007. Assessment of Left Ventricular Diastolic Function and Recognition of Diastolic Heart Failure. *Circulation*, 116 (6), 591–593.

Gafni, J., Munsch, J.A., Lam, T.H., Catlin, M.C., Costa, L.G., Molinski, T.F., and Pessah, I.N., 1997. Xestospongins: Potent membrane permeable blockers of the inositol 1,4,5- trisphosphate receptor. *Neuron*, 19 (3), 723–733.

Galbiati, F., Engelman, J.A., Volonte, D., Zhang, X.L., Minetti, C., Li, M., Hou, H., Kneitz, B., Edelmann, W., and Lisanti, M.P., 2001. Caveolin-3 Null Mice Show a Loss of Caveolae, Changes in the Microdomain Distribution of the Dystrophin-Glycoprotein Complex, and T-tubule Abnormalities. *Journal of Biological Chemistry*, 276 (24),

21425–21433.

Garcia, M.I., Karlstaedt, A., Amione-Guerra, J., Youker, K.A., Taegtmeyer, H., and Boehning, D., 2016. Functionally redundant control of cardiac hypertrophic signaling by inositol 1,4,5-trisphosphate receptors. *Journal of Molecular and Cellular Cardiology*, 112, 95–103.

Gattineni, J., Alphonse, P., Zhang, Q., Mathews, N., Bates, C.M., and Baum, M., 2014. Regulation of renal phosphate transport by FGF23 is mediated by FGFR1 and FGFR4. *American Journal of Physiology-Renal Physiology*, 306 (3), F351–F358.

Genka, C., Ishida, H., Ichimori, K., Hirota, Y., Tanaami, T., and Nakazawa, H., 1999. Visualization of biphasic Ca2+ diffusion from cytosol to nucleus in contracting adult rat cardiac myocytes with an ultra-fast confocal imaging system. *Cell Calcium*, 25 (3), 199–208.

Gerasimenko, O. and Gerasimenko, J., 2004. New aspects of nuclear calcium signalling. *Journal of Cell Science*, 117 (15), 3087–3094.

Gorski, P.A., Ceholski, D.K., and Hajjar, R.J., 2015. Altered myocardial calcium cycling and energetics in heart failure - A rational approach for disease treatment. *Cell Metabolism*, 21 (2), 183–194.

Grabner, A., Amaral, A.P., Schramm, K., Singh, S., Sloan, A., Yanucil, C., Li, J., Shehadeh, L. a., Hare, J.M., David, V., Martin, A., Fornoni, A., Di Marco, G.S., Kentrup, D., Reuter, S., Mayer, A.B., Pavenstadt, H., Stypmann, J., Kuhn, C., Hille, S., Frey, N., Leifheit-Nestler, M., Richter, B., Haffner, D., Abraham, R., Bange, J., Sperl, B., Ullrich, A., Brand, M., Wolf, M., and Faul, C., 2015. Activation of Cardiac Fibroblast Growth Factor Receptor 4 Causes Left Ventricular Hypertrophy. *Cell Metabolism*, 22, 1020–1032.

Grabner, A., Schramm, K., Silswal, N., Hendrix, M., Yanucil, C., Czaya, B., Singh, S.,

Wolf, M., Hermann, S., Stypmann, J., Di Marco, G.S., Brand, M., Wacker, M.J., and Faul, C., 2017. FGF23/FGFR4-mediated left ventricular hypertrophy is reversible. *Scientific Reports*, 7 (1), 1993.

Gruver, C.L., Demayo, F., Goldstein, M., and Means, A., 1993. Targeted Developmental Overexpression of Calmodulin Induces Proliferative and Hypertrophic Growth of Cardiomyocytes in Transgenic Mice. *Endocrinology*, 133 (1), 376–388.

Guatimosim, S., Amaya, M.J., Guerra, M.T., Aguiar, C.J., Goes, A.M., Gomez-Viquez, N.L., Rodrigues, M.A., Gomes, D.A., Martins-Cruz, J., Lederer, W.J., and Leite, M.F., 2008. Nuclear Ca2+ regulates cardiomyocyte function. *Cell Calcium*, 44 (2), 230–242.

Gutierrez, O., Isakova, T., Rhee, E., Shah, A., Holmes, J., Collerone, G., Juppner, H., and Wolf, M., 2005. Fibroblast Growth Factor-23 Mitigates Hyperphosphatemia but Accentuates Calcitriol Deficiency in Chronic Kidney Disease. *Journal of the American Society of Nephrology*, 16 (7), 2205–2215.

Gutiérrez, O.M., Januzzi, J.L., Isakova, T., Laliberte, K., Smith, K., Collerone, G., Sarwar, A., Hoffmann, U., Coglianese, E., Christenson, R., Wang, T.J., DeFilippi, C., and Wolf, M., 2009. Fibroblast growth factor 23 and left ventricular hypertrophy in chronic kidney disease. *Circulation*, 119 (19), 2545–2552.

Gwathmey, J.K., Copelas, L., Mackinnon, R., Schoen, F.J., Feldman, M.D., Grossman, W., and Morgan, J.P., 1987. Abnormal Intracellular Calcium Handling in Myocardium From Patients With End-Stage Heart Failure. *Circulation*, 61, 70–76.

Harrison, B.C., Kim, M., van Rooij, E., Craig, F., Papst, P.J., Vega, R.B., Mcanally, J.A., Richardson, J.A., Bassel-duby, R., Olson, E.N., Mckinsey, T.A., and Plato, C.F., 2006. Regulation of Cardiac Stress Signaling by Protein Kinase D1. *Molecular and Cellular Biology*, 26 (10), 3875–3888.

Harzheim, D., Movassagh, M., Foo, R.S., Ritter, O., Tashfeen, A., Conway, S.J.,

Bootman, M.D., and Roderick, H.L., 2009. Increased InsP3Rs in the junctional sarcoplasmic reticulum augment Ca2+ transients and arrhythmias associated with cardiac hypertrophy. *Proceedings of the National Academy of Sciences*, 106 (27), 1–6.

Hasenfuss, G. and Pieske, B., 2002. Calcium cycling in Congestive Heart Failure. *Journal of Molecular and Cellular Cardiology*, 34 (8), 951–969.

Hasenfuss, G., Reinecke, H., Studer, R., Meyer, M., Pieske, B., Holtz, J., Holubarsch, C., Posival, H., Just, H., and Drexler, H., 1994. Relation between myocardial function and expression of sarcoplasmic reticulum Ca(2+)-ATPase in failing and nonfailing human myocardium. *Circulation Research*, 75 (3), 434–442.

Hasenfuss, G., Schillinger, W., Lehnart, S.E., Preuss, M., Pieske, B., and Maier, L.S., 1999. Relationship Between Na2+-Ca2+-Exchanger Protein Levels and Diastolic Function of Failing Human Myocardium. *Circulation*, 99 (5), 641–648.

Heger, J., Peters, S.C., Piper, H.M., and Euler, G., 2009. SMAD-proteins as a molecular switch from hypertrophy to apoptosis induction in adult ventricular cardiomyocytes. *Journal of Cellular Physiology*, 220 (2), 515–523.

Heidrich, F.M., Zhang, K., Estrada, M., Huang, Y., Giordano, F.J., and Ehrlich, B.E., 2008. Chromogranin B regulates calcium signaling, nuclear factor κb activity, and brain natriuretic peptide production in cardiomyocytes. *Circulation Research*, 102 (10), 1230–1238.

Heinzel, F.R., Bito, V., Biesmans, L., Wu, M., Detre, E., Von Wegner, F., Claus, P., Dymarkowski, S., Maes, F., Bogaert, J., Rademakers, F., D'Hooge, J., and Sipido, K., 2008. Remodeling of T-tubules and reduced synchrony of Ca2+ release in myocytes from chronically ischemic myocardium. *Circulation Research*, 102 (3), 338–346.

Heinzel, F.R., Hohendanner, F., Jin, G., Sedej, S., and Edelmann, F., 2015.

Myocardial hypertrophy and its role in heart failure with preserved ejection fraction. *Journal of Applied Physiology*, 119 (10), 1233–1242.

Higazi, D.R., Fearnley, C.J., Drawnel, F.M., Talasila, A., Corps, E.M., Ritter, O., McDonald, F., Mikoshiba, K., Bootman, M.D., and Roderick, H.L., 2009. Endothelin-1-Stimulated InsP3-Induced Ca2+ Release Is a Nexus for Hypertrophic Signaling in Cardiac Myocytes. *Molecular Cell*, 33 (4), 472–482.

Hilgemann, D., Nicoll, D., and Philipson, K., 1991. Charge movement during Na+ translocation by native and cloned cardiac Na+/Ca2+ exchanger. *Nature*, 352 (6337), 715-718.

Hobai, I.A. and Rourke, B.O., 2000. Enhanced Ca2+-activated Na2+-Ca2+ exchange activity in Canine pacing-induced Heart Failure. *Circulation Research*, 87, 690-698.

Hoch, B., Meyer, R., Hetzer, R., Krause, E., and Karczewski, P., 1999. Identification and Expression of delta-Isoforms of the Multifunctional Calcium/Calmodulin-Dependent Protein Kinase in Failing and Nonfailing Human Myocardium. *Circulation Research*, 84, 713–721.

Hohendanner, F., Maxwell, J.T., and Blatter, L. A., 2015. Cytosolic and nuclear calcium signaling in atrial myocytes: IP3 -mediated calcium release and the role of mitochondria. *Channels (Austin)*, 9 (3), 129–138.

Hohendanner, F., McCulloch, A.D., Blatter, L. a., and Michailova, A.P., 2014. Calcium and IP3 dynamics in cardiac myocytes: Experimental and computational perspectives and approaches. *Frontiers in Pharmacology*, 5 (35), 1–10.

Houser, S.R. and Molkentin, J.D., 2008. Does Contractile Ca^{2+} Control Calcineurin-NFAT Signaling and Pathological Hypertrophy in Cardiac Myocytes? *Science Signaling,* 1 (25), 31.

Hu, M.C., Shiizaki, K., Kuro-o, M., and Moe, O.W., 2013. Fibroblast Growth Factor 23

and Klotho: Physiology and Pathophysiology of an Endocrine Network of Mineral Metabolism. *Annual Review of Physiology*, 75 (1), 503–533.

Humbert, J.P., Matte, N., Artault, J.C., Köppler, P., and Malviya, A.N., 1996. Inositol 1,4,5-trisphosphate receptor is located to the inner nuclear membrane vindicating regulation of nuclear calcium signaling by inositol 1,4,5-trisphosphate. Discrete distribution of inositol phosphate receptors to inner and outer nuclear membranes. *Journal of Biological Chemistry*, 271 (1), 478–485.

Isakova, T., Xie, H., Yang, W., Xie, D., Anderson, A.H., Scialla, J., Wahl, P., Gutierrez, O.M., Steigerwalt, S., He, J., Schwartz, S., Lo, J., Ojo, A., Sondheimer, J., Hsu, C.Y., Lash, J., Leonard, M., Kusek, J.W., Feldman, H.I., Wolf, M., and Chronic Renal Insufficiency Cohort (CRIC) Study Group, 2011. Fibroblast growth factor 23 and risks of mortality and end-stage renal disease in patients with chronic kidney disease. *JAMA*, 305 (23), 2432–2439.

Itoh, N. and Ohta, H., 2013. Pathophysiological roles of FGF signaling in the heart. *Frontiers in physiology*, 4, 247.

Jaconi, M., Bony, C., Richards, S.M., Terzic, A., Arnaudeau, S., Vassort, G., and Pucéat, M., 2000. Inositol 1,4,5-trisphosphate directs Ca(2+) flow between mitochondria and the Endoplasmic/Sarcoplasmic reticulum: a role in regulating cardiac autonomic Ca(2+) spiking. *Molecular Biology of the Cell*, 11 (5), 1845–1858.

Jha, V., Garcia-Garcia, G., Iseki, K., Li, Z., Naicker, S., Plattner, B., Saran, R., Wang, A.Y.M., and Yang, C.W., 2013. Chronic kidney disease: Global dimension and perspectives. *The Lancet*, 382 (9888), 260–272.

Kao, Y.H., Chen, Y.C., Lin, Y.K., Shiu, R.J., Chao, T.F., Chen, S.A., and Chen, Y.J., 2014. FGF-23 dysregulates calcium homeostasis and electrophysiological properties in HL-1 atrial cells. *European Journal of Clinical Investigation*, 44 (8), 795–801.

Kaye, D.M., Lefkovits, J., Jennings, G.L., Bergin, P., Broughton, A., and Esler, M.D., 1995. Adverse consequences of high sympathetic nervous activity in the failing human heart. *Journal of the American College of Cardiology*, 26 (5), 1257–1263.

Kee, H.J., Sohn, I.S., Nam, K.Il., Park, J.E., Qian, Y.R., Yin, Z., Ahn, Y., Jeong, M.H., Bang, Y.-J., Kim, N., Kim, J.-K., Kim, K.K., Epstein, J. A, and Kook, H., 2006. Inhibition of histone deacetylation blocks cardiac hypertrophy induced by angiotensin II infusion and aortic banding. *Circulation*, 113 (1), 51–59.

Kehat, I., Davis, J., Tiburcy, M., Accornero, F., Saba-El-Leil, M.K., Maillet, M., York, A.J., Lorenz, J.N., Zimmermann, W.H., Meloche, S., and Molkentin, J.D., 2011. Extracellular signal-regulated kinases 1 and 2 regulate the balance between eccentric and concentric cardiac growth. *Circulation Research*, 108 (2), 176–183.

Kehlenbach, R.H., Dickmanns, A., and Gerace, L., 1998. Nucleocytoplasmic shuttling factors including Ran and CRM1 mediate nuclear export of NFAT in vitro. *Journal of Cell Biology*, 141 (4), 863–874.

Keidar, S., Kaplan, M., and Gamliel-Lazarovich, A., 2007. ACE2 of the heart: from angiotensin I to angiotensin (1-7). *Cardiovascular Research*, 73 (3), 463–469.

Kestenbaum, B., Sachs, M.C., Hoofnagle, A.N., Siscovick, D.S., Ix, J.H., Robinson-Cohen, C., Lima, J.A.C., Polak, J.F., Blondon, M., Ruzinski, J., Rock, D., and De Boer, I.H., 2014. Fibroblast growth factor-23 and cardiovascular disease in the general population: the multi-ethnic study of atherosclerosis. *Circulation Heart Failure*, 7 (3), 409–417.

Kirchhof, P., Fabritz, L., Kilić, A., Begrow, F., Breithardt, G., and Kuhn, M., 2004. Ventricular arrhythmias, increased cardiac calmodulin kinase II expression, and altered repolarization kinetics in ANP receptor deficient mice. *Journal of Molecular and Cellular Cardiology*, 36 (5), 691–700.

Kockskämper, J., Seidlmayer, L., Walther, S., Hellenkamp, K., Maier, L.S., and Pieske, B., 2008a. Endothelin-1 enhances nuclear Ca2+ transients in atrial myocytes through Ins(1,4,5)P3-dependent Ca2+ release from perinuclear Ca2+ stores. *Journal of Cell Science*, 121 (Pt 2), 186–195.

Kockskämper, J., Zima, A. V., Roderick, H.L., Pieske, B., Blatter, L.A., and Bootman, M.D., 2008b. Emerging roles of Inositol 1,4,5-trisphosphate signaling in cardiac myocytes. *Journal of Molecular and Cellular Cardiology*, 45 (2), 128–147.

Kovesdy, C.P. and Quarles, L.D., 2016. FGF23 from bench to bedside. *American Journal of Physiology - Renal Physiology*, 310 (11), F1168–F1174.

Kreusser, M.M., Lehmann, L.H., Keranov, S., Hoting, M.O., Oehl, U., Kohlhaas, M., Reil, J.C., Neumann, K., Schneider, M.D., Hill, J.A., Dobrev, D., Maack, C., Maier, L.S., Gröne, H.J., Katus, H.A., Olson, E.N., and Backs, J., 2014. Cardiac CaM kinase II genes δ and γ contribute to adverse remodeling but redundantly inhibit calcineurin-induced myocardial hypertrophy. *Circulation*, 130 (15), 1262–1273.

Kuo, P.L., Lee, H., Bray, M.A., Geisse, N.A., Huang, Y.T., Adams, W.J., Sheehy, S.P., and Parker, K.K., 2012. Myocyte shape regulates lateral registry of sarcomeres and contractility. *American Journal of Pathology*, 181 (6), 2030–2037.

Leifheit-Nestler, M., große Siemer, R., Flasbart, K., Richter, B., Kirchhoff, F., Ziegler, W.H., Klintschar, M., Becker, J.U., Erbersdobler, A., Aufricht, C., Seeman, T., Fischer, D.C., Faul, C., and Haffner, D., 2016. Induction of cardiac FGF23/FGFR4 expression is associated with left ventricular hypertrophy in patients with chronic kidney disease. *Nephrology Dialysis Transplantation*, 31 (7), 1088–1099.

Levin, A. and Stevens, P.E., 2014. Summary of KDIGO 2012 CKD Guideline: Behind the scenes, need for guidance, and a framework for moving forward. *Kidney International*, 85 (1), 49–61.

Lim, H.W. and Molkentin, J.D., 1999. Calcineurin and human heart failure. *Nature Medicine*, 5, 246-247.

Lipp, P., Laine, M., Tovey, S.C., Burrell, K.M., Berridge, M.J., Li, W., and Bootman, M.D., 2000. Functional InsP3 receptors that may modulate excitation – contraction coupling in the heart. *Current Biology*, 10 (15), 939–942.

Lipp, P., Thomas, D., Berridge, M.J., and Bootman, M.D., 1997. Nuclear calcium signalling by individual cytoplasmic calcium puffs. *The EMBO journal*, 16 (23), 7166–7173.

Liu, S., Vierthaler, L., Tang, W., Zhou, J., and Quarles, L.D., 2008. FGFR3 and FGFR4 do not mediate renal effects of FGF23. *Journal of the American Society of Nephrology*, 19 (12), 2342–2350.

Ljubojević, S. and Bers, D.M., 2015. Nuclear Calcium in Cardiac Myocytes. *Journal of Cardiovascular Pharmacology*, 65 (3), 211–217.

Ljubojević, S., Radulovic, S., Leitinger, G., Sedej, S., Sacherer, M., Holzer, M., Winkler, C., Pritz, E., Mittler, T., Schmidt, A., Sereinigg, M., Wakula, P., Zissimopoulos, S., Bisping, E., Post, H., Marsche, G., Bossuyt, J., Bers, D.M., Kockskämper, J., and Pieske, B., 2014. Early remodeling of perinuclear Ca2+ stores and nucleoplasmic Ca2+ signaling during the development of hypertrophy and heart failure. *Circulation*, 130 (3), 244–255.

Ljubojević, S., Walther, S., Asgarzoei, M., Sedej, S., Pieske, B., and Kockskämper, J., 2011. In situ calibration of nucleoplasmic versus cytoplasmic Ca^{2}+ concentration in adult cardiomyocytes. *Biophysical journal*, 100 (10), 2356–66.

Löffler, B.M., Roux, S., Kalina, B., Clozel, M., and Clozel, J.P., 1993. Influence of congestive heart failure on endothelin levels and receptors in rabbits. *Journal of Molecular and Cellular Cardiology*, 25 (4), 407-416.

Lopaschuk, G.D., Collins-Nakai, R.L., and Itoi, T., 1992. Developmental changes in energy substrate use by the heart. *Cardiovascular Research*, 26 (12), 1172–1180.

Louch, W.E., Koivumäki, J.T., and Tavi, P., 2015. Calcium signalling in developing cardiomyocytes: implications for model systems and disease. *Journal of Physiology*, 593 (5), 1047–1063.

Lu, H.R., Vlaminckx, E., Van De Water, A., and Gallacher, D.J., 2006. Calmodulin antagonist W-7 prevents sparfloxacin-induced early afterdepolarizations (EADs) in isolated rabbit Purkinje fibers: Importance of beat-to-beat instability of the repolarization. *Journal of Cardiovascular Electrophysiology*, 17 (4), 415–422.

Lu, J., McKinsey, T.A., Nicol, R.L., and Olson, E.N., 2000. Signal-dependent activation of the MEF2 transcription factor by dissociation from histone deacetylases. *Proceedings of the National Academy of Sciences*, 97 (8), 4070–4075.

Lu, Y.M., Huang, J., Shioda, N., Fukunaga, K., Shirasaki, Y., Li, X., and Han, F., 2011. CaMKIIδb mediates aberrant NCX1 expression and the imbalance of NCX1/SERCA in Transverse Aortic Constriction-Induced Failing Heart. *PLoS ONE*, 6 (9), e24724.

Luo, D., Yang, D., Lan, X., Li, K., Li, X., Chen, J., Zhang, Y., Xiao, R.P., Han, Q., and Cheng, H., 2008. Nuclear Ca2+ sparks and waves mediated by inositol 1,4,5-trisphosphate receptors in neonatal rat cardiomyocytes. *Cell Calcium*, 43 (2), 165–174.

MacCarthy, P.A., Grocott-Mason, R., Prendergast, B.D., and Shah, A.M., 2000. Contrasting Inotropic Effects of Endogenous Endothelin in the Normal and Failing Human Heart: studies with an intracoronary ET(A) receptor antagonist. *Circulation,* 10 1 (2), 142-147

MacLennan, D.H. and Kranias, E.G., 2003. Phospholamban: A crucial regulator of cardiac contractility. *Nature Reviews Molecular Cell Biology*, 4 (7), 566–577.

Maier, L.S., 2005. CaMKIIdelta overexpression in hypertrophy and heart failure: Cellular consequences for excitation-contraction coupling. *Brazilian Journal of Medical and Biological Research*, 38 (9), 1293–1302.

Malhas, A., Goulbourne, C., and Vaux, D.J., 2011. The nucleoplasmic reticulum: Form and function. *Trends in Cell Biology*, 21 (6), 362–373.

Malhotra, R., Sadoshima, J., Brosius, F.C., and Izumo, S., 1999. Mechanical Stretch and Angiotensin II Differentially Upregulate the Renin-Angiotensin System in Cardiac Myocytes In Vitro. *Circulation Research*, 85 (2), 137–146.

McCarthy, J.C., Aronovitz, M., DuPont, J.J., Calamaras, T.D., Jaffe, I.Z., and Blanton, R.M., 2017. Short-Term Administration of Serelaxin Produces Predominantly Vascular Benefits in the Angiotensin II/L-NAME Chronic Heart Failure Model. *Journal of the American College of Cardiology*, 2 (3), 285–296.

McDonough, P.M. and Glembotski, C.C., 1992. Induction of atrial natriuretic factor and myosin light chain-2 gene expression in cultured ventricular myocytes by electrical stimulation of contraction. *Journal of Biological Chemistry*, 267 (17), 11665–11668.

Merlen, C., Farhat, N., Luo, X., Chatenet, D., Tadevosyan, A., Villeneuve, L.R., Gillis, M.A., Nattel, S., Thorin, E., Fournier, A., and Allen, B.G., 2013. Intracrine endothelin signaling evokes IP3-dependent increases in nucleoplasmic Ca2+ in adult cardiac myocytes. *Journal of Molecular and Cellular Cardiology*, 62, 189–202.

Mhatre, K.N., Wakula, P., Klein, O., Bisping, E., Völkl, J., Pieske, B., and Heinzel, F.R., 2018. Crosstalk between FGF23- and angiotensin II-mediated Ca2+ signaling in pathological cardiac hypertrophy. *Cellular and Molecular Life Sciences*, (0123456789).

Middlekauf, H.R. and Mark, A.L., 1998. The Treatment of Heart Failure: The Role of Neurohumoral Activation. *Internal Medicine*, 37 (2), 112–122.

Mira, E., Lacalle, R.A., González, M.A., Gómez-Moutón, C., Abad, J.L., Bernad, A., Martínez, C., and Santos, M., 2001. A role for chemokine receptor transactivation in growth factor signaling. *EMBO Reports*, 2 (2), 151–156.

Mishra, S., Gray, C.B.B., Miyamoto, S., Bers, D.M., and Brown, J.H., 2011. Location matters: Clarifying the concept of nuclear and cytosolic CaMKII subtypes. *Circulation Research*, 109 (12), 1354–1362.

Miyata, S. and Haneda, T., 1994. Hypertrophic growth of cultured neonatal rat heart cells mediated by type 1 angiotensin II receptor. *American Journal of Physiology*, 266 (6 Pt 2), H2443-H2451.

Molkentin, J.D., 2004. Calcineurin-NFAT signaling regulates the cardiac hypertrophic response in coordination with the MAPKs. *Cardiovascular Research*, 63 (3), 467–475.

Molkentin, J.D., Lu, J.R., Antos, C.L., Markham, B., Richardson, J., Robbins, J., Grant, S.R., and Olson, E.N., 1998. A calcineurin-dependent transcriptional pathway for cardiac hypertrophy. *Cell*, 93 (2), 215–228.

Mudd, J.O. and Kass, D. A., 2008. Tackling heart failure in the twenty-first century. *Nature*, 451 (7181), 919–928.

Nakayama, H., Bodi, I., Maillet, M., Desantiago, J., Domeier, T.L., Mikoshiba, K., Lorenz, J.N., Blatter, L.A., Bers, D.M., and Molkentin, J.D., 2010. The IP3 receptor regulates cardiac hypertrophy in response to select stimuli. *Circulation Research*, 107 (5), 659–666.

Paradis, P., Dali-Youcef, N., Paradis, F.W., Thibault, G., and Nemer, M., 2000. Overexpression of angiotensin II type I receptor in cardiomyocytes induces cardiac hypertrophy and remodeling. *Proceedings of the National Academy of Sciences of the United States of America*, 97 (2), 931–936.

Passier, R., Zeng, H., Frey, N., Naya, F.J., Nicol, R.L., McKinsey, T. A., Overbeek, P.,

Richardson, J. A., Grant, S.R., and Olson, E.N., 2000. CaM kinase signaling induces cardiac hypertrophy and activates the MEF2 transcription factor in vivo. *Journal of Clinical Investigation*, 105 (10), 1395–1406.

Pasumarthi, K.B., Jin, Y., Bock, M.E., Lytras, A., Kardami, E., and Cattini, P.A., 1995. Characterization of fibroblast growth factor receptor 1 RNA expression in the embryonic mouse heart. *Annals of the New York Academy of Sciences*, 752, 406–416.

Paul, M., Poyan Mehr, A., and Kreutz, R., 2006. Physiology of Local Renin-Angiotensin Systems. *Physiological Reviews*, 86 (3), 747–803.

Pavik, I., Jaeger, P., Ebner, L., Wagner, C.A., Petzold, K., Spichtig, D., Poster, D., Wüthrich, R.P., Russmann, S., and Serra, A.L., 2013. Secreted Klotho and FGF23 in chronic kidney disease stage 1 to 5: A sequence suggested from a cross-sectional study. *Nephrology Dialysis Transplantation*, 28 (2), 352–359.

Pellieux, C., Montessuit, C., Papageorgiou, I., and Lerch, R., 2009. Angiotensin II downregulates the fatty acid oxidation pathway in adult rat cardiomyocytes via release of tumour necrosis factor-α. *Cardiovascular Research*, 82 (2), 341–350.

Periasamy, M. and Kalyanasundaram, A., 2008. SERCA2a gene therapy for heart failure: Ready for primetime? *Molecular Therapy*, 16 (6), 1002–1004.

Peskoff, A. and Langer, G.A., 1998. Calcium concentration and movement in the ventricular cardiac cell during an excitation-contraction cycle. *Biophysical Journal*, 74 (1), 153–174.

Picht, E., Zima, A. V., Blatter, L. A., and Bers, D. M., 2008. SparkMaster: automated calcium spark analysis with ImageJ. *Methods in Cell Physiology*, 293 (3),1073-1081.

Pieske, B., Beyermann, B., Breu, V., Löffler, B.M., Schlotthauer, K., Maier, L.S., Schmidt-Schweda, S., Just, H., and Hasenfuss, G., 1999. Functional effects of

endothelin and regulation of endothelin receptors in isolated human nonfailing and failing myocardium. *Circulation*, 99 (14), 1802–1809.

Pinz, I., Zhu, M., Mende, U., and Ingwall, J., 2011. An Improved Isolation Procedure for Adult Mouse Cardiomyocytes. *Cell Biochemistry and Biophysics,* 61 (1), 93–101.

Pironti, G., Strachan, R.T., Abraham, D., Yu, S.M.W., Chen, M., Chen, W., Hanada, K., Mao, L., Watson, L.J., and Rockman, H.A., 2015. Circulating exosomes induced by cardiac pressure overload contain functional angiotensin II type 1 receptors. *Circulation*, 131 (24), 2120–2130.

Pitt, B., Poole-Wilson, P.A., Segal, R., Martinez, F.A., Dickstein, K., Camm, A.J., Konstam, M.A., Riegger, G., Klinger, G.H., Neaton, J., Sharma, D., and Thiyagarajan, B., 2000. Effect of losartan compared with captopril on mortality in patients with symptomatic heart failure: randomised trial—the Losartan Heart Failure Survival Study ELITE II. *The Lancet*, 355 (9215), 1582–1587.

Plačkić, J., Preissl, S., Nikonova, Y., Pluteanu, F., Hein, L., and Kockskämper, J., 2016. Enhanced nucleoplasmic Ca2+ signaling in ventricular myocytes from young hypertensive rats. *Journal of Molecular and Cellular Cardiology*, 101, 58–68.

Pogwizd, S.M., Schlotthauer, K., Li, L., Yuan, W., and Bers, D.M., 2001. Arrhythmogenesis and contractile dysfunction in heart failure: Roles of sodium-calcium exchange, inward rectifier potassium current, and residual beta-adrenergic responsiveness. *Circulation Research*, 88 (11), 1159–1167.

Ponikowski, P., Voors, A.A., Anker, S.D., Bueno, H., Cleland, J.G.F., Coats, A.J.S., Falk, V., González-Juanatey, J.R., Harjola, V.P., Jankowska, E.A., Jessup, M., Linde, C., Nihoyannopoulos, P., Parissis, J.T., Pieske, B., Riley, J.P., Rosano, G.M.C., Ruilope, L.M., Ruschitzka, F., Rutten, F.H., and Van Der Meer, P., 2016. 2016 ESC Guidelines for the diagnosis and treatment of acute and chronic heart failure. *European Heart Journal*, 37 (27), 2129–2200.

Primessnig, U., Schönleitner, P., Höll, A., Pfeiffer, S., Bracic, T., Rau, T., Kapl, M., Stojakovic, T., Glasnov, T., Leineweber, K., Wakula, P., Antoons, G., Pieske, B., and Heinzel, F.R., 2016. Novel pathomechanisms of cardiomyocyte dysfunction in a model of heart failure with preserved ejection fraction. *European Journal of Heart Failure*, 18 (8), 987–997.

Rajapurohitam, V., Javadov, S., Purdham, D.M., Kirshenbaum, L.A., and Karmazyn, M., 2006. An autocrine role for leptin in mediating the cardiomyocyte hypertrophic effects of angiotensin II and endothelin-1. *Journal of Molecular and Cellular Cardiology*, 41 (2), 265–274.

Remus, T.P., Zima, A. V., Bossuyt, J., Bare, D.J., Martin, J.L., Blatter, L.A., Bers, D.M., and Mignery, G.A., 2006. Biosensors to measure inositol 1,4,5-trisphosphate concentration in living cells with spatiotemporal resolution. *Journal of Biological Chemistry*, 281 (1), 608–616.

Rinne, A., Kapur, N., Molkentin, J.D., Pogwizd, S.M., Bers, D.M., Banach, K., and Blatter, L.A., 2010. Isoform- and tissue-specific regulation of the Ca2+-sensitive transcription factor NFAT in cardiac myocytes and heart failure. *American Journal of Physiology. Heart and Circulatory Physiology*, 298 (63), 2001–2009.

Rizzuto, R. and Pozzan, T., 2006. Microdomains of Intracellular Ca2+ : Molecular Determinants and Functional Consequences. *Physiological reviews*, 86 (1), 369–408.

Rossignol, P., Ménard, J., Fay, R., Gustafsson, F., Pitt, B., and Zannad, F., 2011. Eplerenone survival benefits in heart failure patients post-myocardial infarction are independent from its diuretic and potassium-sparing effects: Insights from an EPHESUS (Eplerenone Post-Acute Myocardial Infarction Heart Failure Efficacy and Survival Study) Substudy. *Journal of the American College of Cardiology*, 58 (19), 1958–1966.

Ruiz-Villalba, A., Mattiotti, A., Gunst, Q.D., Cano-Ballesteros, S., van den Hoff, M.J.B.,

and Ruijter, J.M., 2017. Reference genes for gene expression studies in the mouse heart. *Scientific Reports*, 7 (1), 24.

Sadoshima, J. and Izumo, S., 1993. Molecular characterization of angiotensin II--induced hypertrophy of cardiac myocytes and hyperplasia of cardiac fibroblasts. Critical role of the AT1 receptor subtype. *Circulation Research*, 73 (3), 413–423.

Sadoshima, J., Qiu, Z., Morgan, J.P., and Izumo, S., 1995. Angiotensin II and other hypertrophic stimuli mediated by G protein-coupled receptors activate tyrosine kinase, mitogen-activated protein kinase, and 90-kD S6 kinase in cardiac myocytes. *Circulation Research*, 76 (1), 1–15.

Sadoshima, J., Xu, Y., Slayter, H.S., and Izumo, S., 1993. Autocrine release of angiotensin II mediates stretch-induced hypertrophy of cardiac myocytes in vitro. *Cell*, 75 (5), 977–984.

Saito, T., Fukuzawa, J., Osaki, J., Sakuragi, H., Yao, N., Haneda, T., Fujino, T., Wakamiya, N., Kikuchi, K., and Hasebe, N., 2003. Roles of calcineurin and calcium/calmodulin-dependent protein kinase II in pressure overload-induced cardiac hypertrophy. *Journal of Molecular and Cellular Cardiology*, 35 (9), 1153–1160.

Salazar, N.C., Chen, J., and Rockman, H.A., 2007. Cardiac GPCRs: GPCR signaling in healthy and failing hearts. *Biochimica et Biophysica Acta - Biomembranes*, 1768 (4), 1006–1018.

Schmitt, J.P., Kamisago, M., Asahi, M., Li, G.H., Ahmad, F., Mende, U., Kranias, E.G., MacLennan, D.H., Seidman, J.G., and Seidman, C.E., 2003. Dilated Cardiomyopathy and Heart Failure caused by a mutation in Phospholamban. *Science*, 299 (5611), 1410–1413.

Schocken, D.D., Benjamin, E.J., Fonarow, G.C., Krumholz, H.M., Levy, D., Mensah, G.A., Narula, J., Shor, E.S., Young, J.B., and Hong, Y., 2008. Prevention of Heart

failure. A Scientific Statement From the American Heart Association Councils on Epidemiology and Prevention, Clinical Cardiology, Cardiovascular Nursing, and High Blood Pressure Research; Quality of Care and Outcomes Research Interdisciplinary Working Group; and Functional Genomics and Translational Biology Interdisciplinary Working Group. *Circulation*, 117 (19), 2544–2565.

Schreckenberg, R., Taimor, G., Piper, H.M., and Schlüter, K.D., 2004. Inhibition of Ca2+-dependent PKC isoforms unmasks ERK-dependent hypertrophic growth evoked by phenylephrine in adult ventricular cardiomyocytes. *Cardiovascular Research*, 63 (3), 553–560.

Schunkert, H., Jackson, B., Tang, S.S., Schoen, F.J., Smits, J.F., Apstein, C.S., and Lorell, B.H., 1993. Distribution and functional significance of cardiac angiotensin converting enzyme in hypertrophied rat hearts. *Circulation*, 87 (4), 1328–1339.

Sedej, S., Schmidt, A., Denegri, M., Walther, S., Matovina, M., Arnstein, G., Gutschi, E.M., Windhager, I., Ljubojević, S., Negri, S., Heinzel, F.R., Bisping, E., Vos, M. A., Napolitano, C., Priori, S.G., Kockskämper, J., and Pieske, B., 2014. Subclinical abnormalities in sarcoplasmic reticulum Ca^{2+} release promote eccentric myocardial remodeling and pump failure death in response to pressure overload. *Journal of the American College of Cardiology*, 63 (15), 1569–1579.

Segovia Cubero, J., Alonso-Pulpón Rivera, L., Peraira Moral, R., and Silva Melchor, L., 2004. Heart Failure: Etiology and Approach to Diagnosis. *Revista Española de Cardiología (English Edition)*, 57 (3), 250–259.

Shah, A.M. and Mann, D.L., 2011. In search of new therapeutic targets and strategies for heart failure: Recent advances in basic science. *The Lancet*, 378 (9792), 704–712.

Silswal, N., Touchberry, C.D., Daniel, D.R., McCarthy, D.L., Zhang, S., Andresen, J., Stubbs, J.R., and Wacker, M.J., 2014. FGF23 directly impairs endothelium-dependent vasorelaxation by increasing superoxide levels and reducing nitric oxide

bioavailability. *American Journal of Physiology-Endocrinology and Metabolism*, 307 (5), E426–E436.

Silver, J. and Naveh-Many, T., 2009. Phosphate and the parathyroid. *Kidney International*, 75 (9), 898–905.

Simmerman, H.K. and Jones, L.R., 1998. Phospholamban: protein structure, mechanism of action, and role in cardiac function. *Physiological Reviews*, 78 (4), 921–947.

Singh, V.P., Le, B., Bhat, V.B., Baker, K.M., and Kumar, R., 2007. High-glucose-induced regulation of intracellular ANG II synthesis and nuclear redistribution in cardiac myocytes. *American Journal of Physiology-Heart and Circulatory Physiology*, 293 (2), H939–H948.

Sipido, K.R., Bito, V., Antoons, G., Volders, P.G., and Vos, M.A., 2007. Na/Ca exchange and cardiac ventricular arrhythmias. *Annals of the New York Academy of Sciences*, 1099, 339–348.

Stehno-bittel, L., Perez-terzic, C., and Claphamt, D.E., 1995. Diffusion across the nuclear envelope inhibited by depletion of the Nuclear Ca2+ Store, *Science*, 270 (5243), 1835-1838.

Stubbs, J.R., He, N., Idiculla, A., Gillihan, R., Liu, S., David, V., Hong, Y., and Quarles, L.D., 2012. Longitudinal evaluation of FGF23 changes and mineral metabolism abnormalities in a mouse model of chronic kidney disease. *Journal of Bone and Mineral Research*, 27 (1), 38–46.

Studer, R., Reinecke, H., Müller, B., Holtz, J., Just, H., and Drexler, H., 1994. Increased angiotensin-I converting enzyme gene expression in the failing human heart. Quantification by competitive RNA polymerase chain reaction. *Journal of Clinical Investigation*, 94 (1), 301–310.

Sullivan, K.M. and Wilson, K.L., 1994. A new role for IP3 receptors: Ca2+ release during nuclear vesicle fusion. *Cell calcium*, 16 (4), 314–21.

Tadevosyan, A., Maguy, A., Villeneuve, L.R., Babin, J., Bonnefoy, A., Allen, B.G., and Nattel, S., 2010. Nuclear-delimited angiotensin receptor-mediated signaling regulates cardiomyocyte gene expression. *Journal of Biological Chemistry*, 285 (29), 22338–22349.

Tadevosyan, A., Xiao, J., Surinkaew, S., Naud, P., Merlen, C., Harada, M., Qi, X., Chatenet, D., Fournier, A., Allen, B.G., and Nattel, S., 2017. Intracellular Angiotensin-II Interacts With Nuclear Angiotensin Receptors in Cardiac Fibroblasts and Regulates RNA Synthesis, Cell Proliferation, and Collagen Secretion. *Journal of the American Heart Association*, 6 (4), e004965.

Tamura, T., Said, S., Harris, J., Lu, W., and Gerdes, A. M., 2000. Reverse remodeling of cardiac myocyte hypertrophy in hypertension and failure by targeting of the renin-angiotensin system. *Circulation*, 102, 253–259.

Taylor, C.W. and Tovey, S.C., 2010. IP3 Receptors: Toward Understanding Their Activation. *Cold Spring Harbour Perspectives in Biology*, 2 (12), a004010.

Thienpont, B., Aronsen, J.M., Robinson, E.L., Okkenhaug, H., Loche, E., Ferrini, A., Brien, P., Alkass, K., Tomasso, A., Agrawal, A., Bergmann, O., Sjaastad, I., Reik, W., and Roderick, H.L., 2017. The H3K9 dimethyltransferases EHMT1/2 protect against pathological cardiac hypertrophy. *Journal of Clinical Investigation*, 127 (1), 335–348.

Thum, T., Galuppo, P., Wolf, C., Fiedler, J., Kneitz, S., Van Laake, L.W., Doevendans, P.A., Mummery, C.L., Borlak, J., Haverich, A., Gross, C., Engelhardt, S., Ertl, G., and Bauersachs, J., 2007. MicroRNAs in the human heart: A clue to fetal gene reprogramming in heart failure. *Circulation*, 116 (3), 258–267.

Toischer, K., Rokita, A.G., Unsöld, B., Zhu, W., Kararigas, G., Sossalla, S., Reuter,

S.P., Becker, A., Teucher, N., Seidler, T., Grebe, C., Preu, L., Gupta, S.N., Schmidt, K., Lehnart, S.E., Krüger, M., Linke, W.A., Backs, J., Regitz-Zagrosek, V., Schäfer, K., Field, L.J., Maier, L.S., and Hasenfuss, G., 2010. Differential cardiac remodeling in preload versus afterload. *Circulation*, 122 (10), 993–1003.

Tombes, R.M., Faison, M.O., and Turbeville, J.M., 2003. Organization and evolution of multifunctional Ca2+/CaM-dependent protein kinase genes. *Gene*, 322 (1–2), 17–31.

Touchberry, C.D., Green, T.M., Tchikrizov, V., Mannix, J.E., Mao, T.F., Carney, B.W., Girgis, M., Vincent, R.J., Wetmore, L. A., Dawn, B., Bonewald, L.F., Stubbs, J.R., and Wacker, M.J., 2013. FGF23 is a novel regulator of intracellular calcium and cardiac contractility in addition to cardiac hypertrophy. *American Journal of Physiology-Endocrinology and Metabolism*, 304 (8), E863-E873.

van Berlo, J.H., Maillet, M., and Molkentin, J.D., 2013. Signaling effectors underlying pathologic growth and remodeling of the heart. *Journal of Clinical Investigation*, 123 (1), 37–45.

Vega, R.B., Harrison, B.C., Meadows, E., Charles, R. C., Papst, P.J., Olson, E.N., and Mckinsey, T.A., 2004. Protein Kinases C and D Mediate Agonist-Dependent Cardiac Hypertrophy through Nuclear Export of Histone Deacetylase 5. *Molecular and Cellular Biology*, 24 (19), 8374–8385.

Viaene, L., Bammens, B., Meijers, B.K.I., Vanrenterghem, Y., Vanderschueren, D., and Evenepoel, P., 2012. Residual renal function is an independent determinant of serum FGF-23 levels in dialysis patients. *Nephrology, Dialysis, Transplantation*, 27 (5), 2017–2022.

Viero, C., Wegener, S., Scholz, A., Ruppenthal, S., Tian, Q., Tabellion, W., Kreinest, M., Laschke, M.W., Kaestner, L., and Lipp, P., 2016. Endothelin-1-induced remodelling of murine adult ventricular myocytes. *Cell Calcium*, 59 (1), 41–53.

Wagner, M., Mascareno, E., and Siddiqui, M.A.Q., 1999. Cardiac hypertrophy: Signal transduction, transcriptional adaptation, and altered growth control. *Annals of the New York Academy of Sciences*, 874, 1–10.

Wang, R., Wang, Y., Lin, W.K., Zhang, Y., Liu, W., Huang, K., Terrar, D.A., Solaro, R.J., Wang, X., Ke, Y., and Lei, M., 2014. Inhibition of angiotensin II-induced cardiac hypertrophy and associated ventricular arrhythmias by a p21 activated kinase 1 bioactive peptide. *PLoS ONE*, 9 (7), e101974.

Wilkins, B.J. and Molkentin, J.D., 2002. Calcineurin and cardiac hypertrophy: Where have we been? Where are we going? *Journal of Physiology*, 541 (1), 1–8.

Wisler, J.W., Harris, E.M., Raisch, M., Mao, L., Kim, J., Rockman, H.A., and Lefkowitz, R.J., 2015. The role of β-arrestin2-dependent signaling in thoracic aortic aneurysm formation in a murine model of Marfan syndrome. *American Journal of Physiology - Heart and Circulatory Physiology*, 309 (9), H1516–H1527.

Wohlfahrt, P., Melenovsky, V., Kotrc, M., Benes, J., Jabor, A., Franekova, J., Lemaire, S., Kautzner, J., and Jarolim, P., 2015. Association of Fibroblast Growth Factor-23 Levels and Angiotensin-Converting Enzyme Inhibition in Chronic Systolic Heart Failure. *Journal of the American College of Cardiology: Heart Failure*, 3 (10), 829–839.

Wu, X. and Bers, D.M., 2006. Sarcoplasmic reticulum and nuclear envelope are one highly interconnected Ca2+ store throughout cardiac myocyte. *Circulation Research*, 99 (3), 283–291.

Wu, X., Zhang, T., Bossuyt, J., Li, X., Mckinsey, T.A., Dedman, J.R., Olson, E.N., Chen, J., Brown, J.H., and Bers, D.M., 2006. Local InsP3-dependent perinuclear Ca2+ signaling in cardiac myocyte excitation-transcription coupling. *Journal of Clinical Investigation,* 116 (3), 675–682.

Yanochko, G.M., Vitsky, A., Heyen, J.R., Hirakawa, B., Lam, J.L., May, J., Nichols, T., Sace, F., Trajkovic, D., and Blasi, E., 2013. Pan-FGFR inhibition leads to blockade of FGF23 signaling, soft tissue mineralization, and cardiovascular dysfunction. *Toxicological Sciences*, 135 (2), 451–464.

Zhang, C.L., McKinsey, T.A., Chang, S., Antos, C.L., Hill, J.A., and Olson, E.N., 2002. Class II histone deacetylases act as signal-responsive repressors of cardiac hypertrophy. *Cell*, 110 (4), 479–488.

Zhang, S.J., Zou, M., Lu, L., Lau, D., Ditzel, D.A.W., Delucinge-Vivier, C., Aso, Y., Descombes, P., and Bading, H., 2009. Nuclear calcium signaling controls expression of a large gene pool: Identification of a gene program for acquired neuroprotection induced by synaptic activity. *PLoS Genetics*, 5 (8), e1000604.

Zhang, T. and Brown, J.H., 2004. Role of Ca2+/calmodulin-dependent protein kinase II in cardiac hypertrophy and heart failure. *Cardiovascular Research*, 63 (3), 476–486.

Zhang, W., Qi, F., Chen, D.Q., Xiao, W., Wang, J., and Zhu, W., 2010. Ca2+/calmodulin-dependent protein kinase II delta orchestrates G-protein-coupled receptor and electric field stimulation-induced cardiomyocyte hypertrophy. *Clinical and Experimental Pharmacology and Physiology*, 37 (8), 795–802.

Zima, A. V., Bare, D.J., Mignery, G.A., and Blatter, L.A., 2007. IP3-dependent nuclear Ca2+ signalling in the mammalian heart. *Journal of Physiology*, 584 (2), 601–611.